EVALUATION OF CONDITIONS AND MECHANISMS OF ALPHAHERPESVIRUS SUPERINFECTION EXCLUSION

by

James Patrick Cwick

A dissertation submitted in partial fulfillment
of the requirements for the degree

of

Doctor of Philosophy

in

Immunology and Infectious Disease

MONTANA STATE UNIVERSITY
Bozeman, Montana

May 2022

DEDICATION

The completion of this dissertation and degree is dedicated to my family. First and foremost, I would like to thank my family, especially my parents and brothers. They have taught me that anything worthwhile needs time and dedication. The love and support molded me to take the decisions that push me academically and in anything I do.

Next, I would like to thank my friends Jenny and Aston. They have taught me that having fun and new experiences are just as important for living life. Experiencing something is better than not trying it at all.

ACKNOWLEDGEMENTS

I would like to acknowledge and thank two important mentors during my time at MSU: Dr. Jovanka Voyich and Dr. Matt Taylor. Jovanka initiated my passion for research as an undergraduate with knowledge and advice to influence my desire to pursue graduate school. Her expertise and support were always felt, even during graduate school. As my graduate advisor, Matt's encouragement and support not only helped me academically through new information about viruses but also emotionally supported me during failed experiments and low points. His mentorship made graduate school a pleasant experience, and I hope to emulate his positive traits of knowledge and resilience in my future career.

Next, I would like to acknowledge the Taylor lab during my time there: Irina, Kyle, Gary, Luke, Jonathan, and Gabby. The lab banter and camaraderie are things that I will miss.

Next, I would like to thank Dr. Kari Cargill for her continual guidance and support that lead me into my acceptance of the PhD program. She assisted in my desire to pursue research, since the start of my freshman year in college and made my dreams come true for graduate school. Her friendship and assistance are greatly appreciated.

Finally, I would like to acknowledge my committee members of Dr. Quinn, Dr. Aga, and Dr. Jovanka Voyich. I thank you for the time each of you invested in me and the comments that made me a better scientist.

TABLE OF CONTENTS

TABLE OF CONTENTS CONTINUED

LIST OF FIGURES

Figure Page

Common List of Abbreviations

BAC	bacterial artificial chromosome
CFP	cyan fluorescent protein
DMSO	dimethyl sulfate
DRG	dorsal root ganglion
eYFP	enhanced yellow fluorescent protein
GFP	green fluorescent protein
HPI	hours post inoculation
HSV-1	Herpes Simplex Virus Type 1
MOI	Multiplicity of infection
NLS	nuclear localized signal
PRV	Pseudorabies virus
RFP	red fluorescent protein
SIE	Superinfection exclusion
U_L	unique long region
U_S	unique short region
VP	viral protein
WT	wild type
YFP	yellow fluorescent protein

VIRUSES FEATURED IN EXPERIMENTAL MODELS

HSV-OK14	RFP fusion to VP26
PRV 443	GFP fusion to VP26
PRV 287	NLS eYFP expression cassette inserted between UL37 and UL38
PRV 289	NLS Turq2 expression cassette inserted between UL37 and UL 38
PRV137	eGFP fusion to gM and mRFP fusion to VP26
PRV Becker	Wild type
HSV-1 Strain 17	Wild type
HSV-1 mScarlet	RFP-NLS
HSV-1 MT01	Turq2-NLS

ABSTRACT

Superinfection exclusion (SIE) is a natural phenomenon where one virus prevents subsequent entry of another virus. Studies have shown its impact on viral replication and reproduction of many different viruses, where exclusion targets specific parts of the virus' lifecycle. Alphaherpesviruses, specifically pseudorabies virus (PRV) and Herpes Simplex virus type 1 (HSV-1), have demonstrated at least two forms of SIE. However, the form of SIE that occurs early in viral replication remains of interest due to both its timing and unknown mechanisms of regulation. Research on this topic will stimulate development of vaccines in global health by providing targets for disruption of alphaherpesvirus infection and information on unknown aspects of alphaherpesvirus infection. We have developed two models for assessing early SIE for alphaherpesviruses: a fluorescent reporter model to quantify virions within the cell. Both models contributed to data that determined our early SIE is influenced by multiplicity of infection (MOI) for both the primary and secondary virions. Imaging flow cytometry was utilized in conjunction with fluorescent microscopy as a possible means to study early SIE in large population samples. Subsequent data from my experiments indicates that cellular factors like cellular receptors, clathrin, and actin arrangement had minimal influence on early SIE of alphaherpesviruses. However, the results from capsid trafficking model in combination with experiments involving heparin and bortezomib indicate that early SIE differs in PRV and HSV-1. Data indicates that PRV SIE inhibits the step of viral entry/fusion, while HSV-1 SIE disrupts in a post-entry manner. Data obtained from this dissertation indicates that early SIE influences alphaherpesviruses differently and presents possible means to study antiviral techniques and methods.

CHAPTER ONE

INTRODUCTION TO ALPHAHERPESVIRUSES, REGULATION OF COINFECTION, AND SIE OF ALPHAHERPESVIRUSES

A Brief History and Overview of Alphaherpesviruses

Herpesviridae are categorically classified as a large, double-stranded DNA genome virus that exhibit a complex viral cycle of infection (Campadelli-fiume & Roizman, 2022; Davison, 2007). Before 1971, these viruses were named according to their host, the presentable pathology associated with infection, or to their discoverers (Group, 1973). To better classify herpesviruses in the future, a system was established based upon the following criteria: the primary categorization according to biological hosts and then secondarily assortment according to traits like genome size and structure (Davison, 2007). This became the organization of how herpesviruses are currently classified into three subfamilies: *Alphaherpesvirinae*, *Betaherpesvirinae,* and *Gammaherpesvirinae*.

Of the three subfamilies, alphaherpesviruses exhibit an expanded host range that pathologically affect the central nervous systems of many mammals (Gabriella Campadelli-Fiume et al., 2000b; Spear et al., 2000). Their easy-to-disseminate nature and ability to establish latent infections in sensory ganglions permit a myriad of neurological symptoms. These symptoms can vary in severity and result in neurological deficiencies depending upon the site of their trafficking and reactivation. Symptoms can present as discomforting nodules on the body's surface of skin and epithelial layers or promote severe inflammation in immune-deficient organs like the brain and eyes (Arduino & Porter, 2006; Kollias et al., 2014; Kukhanova et al., 2014;

Tsatsos et al., 2016; Whitley & Roizman, 2001). Despite genetic differences between species of alphaherpesviruses, most viral processes including virion trafficking and genome replication are conserved, permitting a model alphaherpesvirus for understanding general alphaherpesvirus biology and replication (Gabriella Campadelli-Fiume et al., 2000a; Pomeranz et al., 2005; Szpara et al., 2011). Of the many types of alphaherpesviruses, Herpes Simplex Virus type 1 and type 2 (HSV-1 and HSV-2), varicella zoster virus (VZV), and Pseudorabies virus (PRV) are among the most utilized for examining impactful pathogens (Kramer & Enquist, 2013a). Typically, HSV-1 and HSV-2 are used as models of human alphaherpesviruses pathogenesis, while PRV is utilized as the model of animal alphaherpesvirus pathogenesis. The defining feature of alphaherpesviruses is their ability to establish latent infection in the ganglia of the nervous system (C. Jones & Perng, 2010; Madavaraju et al., 2021; Maroui et al., 2016; Roizman & Whitley, 2013; G. Smith, 2012; Thellman & Triezenberg, 2017). Alphaherpesvirus are able to efficiently evade the immune system due to the immune-privileged sites where they persistently infect, the general lack of gene production during latency except the latency (LAT) gene, and the many genes produced during their lytic phase that specifically target many functions of the immune system like cytokines (Kramer & Enquist, 2013a).

The interplay between infection and the reactivation cycles for alphaherpesviruses can lead to several neurological pathologies depending upon the site of trafficking and reactivation, the strain of virus, and the host (Jiang et al., 2016). After initial establishment of the virus in the sensory ganglion, stressors like UV radiation, illness, and emotional distress promote lytic replication and viral production (Bonneau et al., 1991; Cliffe et al., 2015; Cuddy et al., 2020; De Chiara et al., 2019; Doll et al., 2019; W. Huang et al., 2011; Rooney et al., 2019; Suzich &

Cliffe, 2018). Details of this can be found later in this chapter. Then, viral progeny travel in an anterograde fashion back towards their initial site of inoculation, causing inflammation and presentation of symptoms. In most instances, reactivation typically presents as cold sores or nodules that cause only minor discomfort. In more severe cases, these viruses can traffic to other immune-privileged sites like the mucosal regions of the eyes and oral cavity, resulting in periodontitis and keratitis. In extremely rare cases, the virus can also traverse the blood-brain barrier and cause neurologically devastating cases of encephalitis in both neonates and adults (Biswas & Rouse, 2005; Bradshaw & Venkatesan, 2016; Brandt, 2005; Kidokoro et al., 2017; Mitterreiter et al., 2016; Tsatsos et al., 2016). Although there are strains of alphaherpesviruses with more severe pathological presentation, the exact cause and origin for these severe neurological symptoms is still an ongoing investigation in this field and further demonstrates the complex nature associated between infection and disease of alphaherpesviruses.

Important Pathogens of Alphaherpesviruses

Herpes Simplex Virus type-1

Herpes Simplex virus is a neuroinvasive alphaherpesvirus that is commonly referred to as HSV. Although they have been shown to infect animal models at a reduced capacity, humans are the primary host of both HSV-1 and HSV-2 (Kollias et al., 2014; Madavaraju et al., 2021). Although there were many instances in history about the mention of lesions in various anecdotes, Vidal in the late 1800s discovered person-person transmission of HSV-1 and its isolation in culture (Whitley et al., 1998). However, it would not be about until the mid-1900s that HSV-1 reactivation events were connected back to the virus (Escobedo-Bonilla, 2021).

Currently, the global infection rates of HSV type 1 and 2 are collectively upwards of 80%, with approximately 40% seroprevalence in the United States (Loncoman et al., 2017; Looker, Magaret, May, et al., 2015). Current studies lack the comprehensive global burden of HSV-1 associated costs in healthcare. However, very conservative estimates predict an annual healthcare cost of $109 million US dollars for treatment of only 30% of US patients (S. W. H. Lee et al., 2022). Most of these costs derive from acutely treating with Acyclovir for episodic events of HSV, and marketing for these treatments has been a very lucrative industry. Other studies estimate that patients contracted with HSV-2 accrue $540 million US dollars in their life, excluding hospitalization charges for sequential sequelae, complications arising from susceptibility to HIV infection, and neonatal herpes (Johnston et al., 2016). Currently, no effective vaccines against HSV-1 or 2 exist. The antiviral Acyclovir is effective at treating active HSV-1 infections but fails to eliminate latent virus. The rise of acyclovir-resistant HSV-1 strains further underscores the limitations of available treatments or prophylactics for HSV-1 (Fujii et al., 2019; Mitterreiter et al., 2016; van Velzen et al., 2013).

Pseudorabies virus

PRV is a veterinary alphaherpesvirus that can infect many animal hosts and is neuroinvasive like HSV-1. Despite its natural host of adult swine, this virus has been shown to infect a broad range of small rodents, large cattle, livestock including chicken and goats (Pomeranz et al., 2005). This pathogen has a high rate of mortality and causes severe neurological symptoms that resemble rabies virus infection, including ataxia, pruritus, and muscle control (Kramer & Enquist, 2013b). The current economic impact of PRV agriculture is estimated to exceed $500 million within the US alone. These costs account for vaccination,

disease surveillance, and livestock eradication (Meurens et al., 2004).

HSV and PRV are two of the best understood alphaherpesviruses and often serve as models for studying alphaherpesvirus infection. Although there is remarkably similar genome representation shared across different alphaherpesviruses, studies have shown that there are still variations for species differentiation. For instance, the short sequencing repeats (SSRs) within the repeating sections of the genome can vary across viral species, which could possibly explain more neurovirulent strains (Szpara et al., 2011). Even between HSV-1 and HSV-2, there is only 83% homology between their genomic sequences. Current circulating strains of clinical alphaherpesviruses isolates exhibited had higher levels recombination and virulent properties than parent strains. These same studies hypothesized that frequent encounters in the form of both homologous and heterologous species recombination contributes to the variety of geographical strains (Bowden et al., 2004a; Loncoman et al., 2017; Szpara et al., 2014). There exist many forms of polymorphisms due to base substitutions at key cleavage sites and even random mutations caused from divergent events based on geography (Renner & Szpara, 2017). These forms of viral genome variation need to be examined through both the lens of human and non-human hosts.

Virion Structure of Alphaherpesviruses

The virion structure for alphaherpesviruses is similar for both HSV-1 and PRV. A mature virion contains 4 elements: an icosahedral capsid, a protein layer called the tegument, an outer lipid bilayer containing glycosylated viral proteins, and the core containing the linear, double-stranded DNA genome (Roizman & Furlong, 1974). A representation of this virion is

shown in Figure 1.1. However, the genome between alphaherpesviruses differs slightly. The PRV genome contains a unique long (U_L) and a unique short (U_s) sequence, with tandem repeats only flanking the short sequence. The HSV-1 genome also consists of unique segments that are named unique long (U_L) and unique short (U_S); yet both segments are flanked by inverted tandem repeats (Roizman & Furlong, 1974). The U_s region has been observed to be a distinct alphaherpesvirus feature that aids in viral spread and neurovirulence (Brunovskis & Velicer, 1995).

The diameter of alphaherpesviruses is approximately 200 nm in diameter with a T=16 icosahedral core containing the linear DNA genome (Roizman & Furlong, 1974). This core is composed of VP5, VP26, VP23, and VP19 that tightly packages and coils the genome (Vallbracht et al., 2018; Yuan et al., 2018). The tegument proteins are classified as either an "inner" or "outer" leaflet. The inner tegument layer associates with the capsid, while the outer tegument layer is associated with viral glycoproteins (Dai & Hong Zhou, 2018; Zhou et al., 1999). There are at least 18 tegument proteins contributing to the formation of the tegument layers (Scholtes & Baines, 2009). Envelope of alphaherpesviruses utilize host cell membranes to form a matrix of viral glycoproteins and non-glycosylated proteins (Scholtes & Baines, 2009).

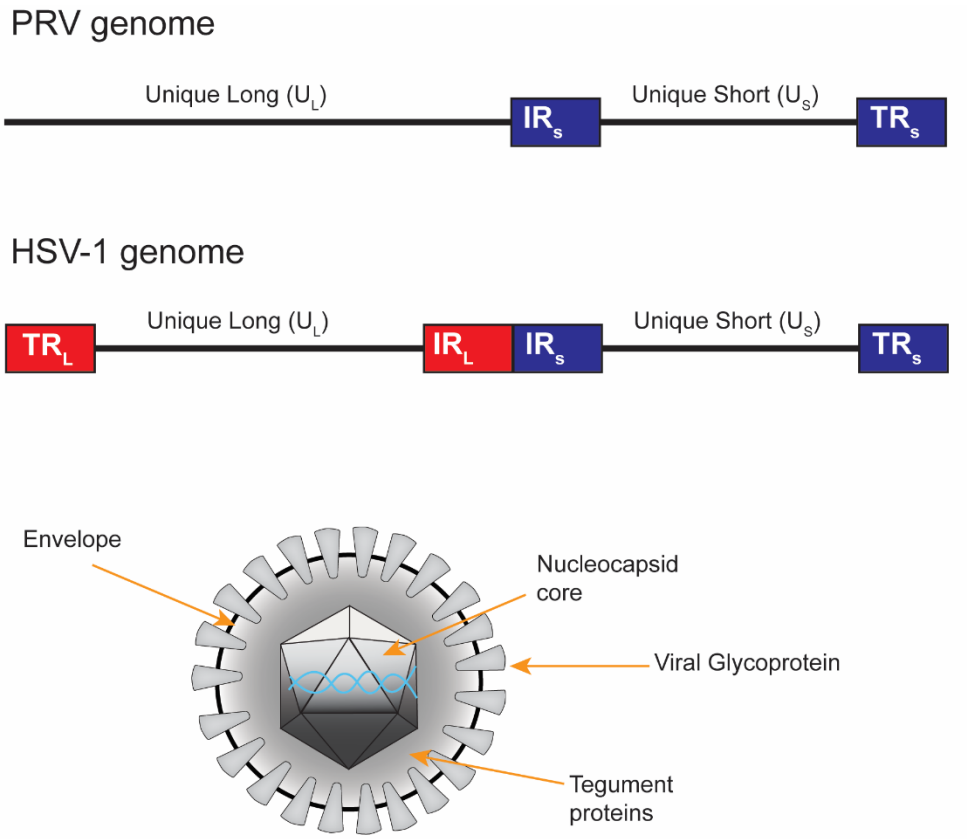

Figure 1.1 Representation of alphaherpesvirus genome and virus.
A) A schematic of linear double stranded DNA. PRV does not have repeat codons on the end of its unique long sequence while HSV-1 does.
B) Model of alphaherpesvirus virion

Viral Replication of alphaherpesviruses

The initial step of viral replication for alphaherpesviruses begins with the step of viral attachment and entry. This step involves the attachment of viral proteins that cognately bind cellular surface glycoproteins. Initially, attachment of viral glycoproteins B and C retain surface attraction between viral protein D and cellular receptors like herpesvirus entry mediator (HVEM), 3-O sulfated heparan sulfate (3-O HS) and nectin-like receptors (Akhtar et al., 2008; Clement et al., 2006a; Connolly et al., 2001; Shukla et al., 2009). This binding is then facilitated

through the fusion of a viral complex comprised of glycoproteins B, H, and L to permit virion uptake into the cell (Cooper & Heldwein, 2015). However, this process is not only dependent upon cellular receptors but also can be dependent upon cell-lines. In addition to the aforementioned form of entry via fusion, studies have shown that both PRV and HSV-1 can utilize an endocytic pathway for entry in cells that lack the corresponding receptors (Miller et al., 2019; Tebaldi et al., 2020). Both modes for alphaherpesvirus entry demonstrate the wide host range and infectivity for these pathogens.

After viral attachment and entry, processes of immune evasion, viral transcription, and regulation of cellular proteins are controlled through the release of tegument proteins. The proteins in this tegument layer are typified as either "inner" or "outer" regions. Tegument proteins that are part of this "outer" leaflet like U_L46, U_L47, and U_L48 disassociate from the capsid to promote more global functions that aid viral replication. Meanwhile, proteins of the "inner" leaflet like U_L14 and U_L16 continually to associate with the capsid and aid in its trafficking to the nucleus through interactions with microtubule motor proteins (Bohannon et al., 2013; Owen et al., 2015; Pomeranz et al., 2005; G. Smith, 2012). In conjunction with U_L36, U_L25 assists in capsid docking on the nuclear pore of the host cell and the release of viral genome into the nucleus (G. et al., 2008).

For the step of viral genome replication, transcription of the viral genome occurs after the double-stranded, linear DNA genome circularizes and recruits host RNA polymerase II with the assistance of viral factors ICP4, ICP0, ICP27, and ICP22 (Birkenheuer et al., 2018; Birkenheuer & Baines, 2019). Viral proteins of alphaherpesviruses are classified by three main groups of immediate-early, early, and late. Nearly all immediate-early viral proteins are

delivered with the viral genome to facilitate genome replication, produce early and late proteins, and counteract host immune responses in the cell. ICP4 initiates cellular complexes that enhance transcription and repress viral genes. ICP0 acts as an E3 ubiquitin ligase and functions to counteract immune responses by the host. ICP27 facilitates nuclear export of mRNA into the cytosol for translation of viral proteins by ribosomes, while ICP22 promotes late gene transcription (L. et al., 2022). Typically, transcription of viral genes occurs in a serial cascade of proteins that are also grouped in three waves: immediate-early, early, and late genes. However, recent studies have suggested that this strict delineation of protein groups occurs more as a continuous timeline rather than discrete time points (Rutkowski et al., 2015). Immediate-early mRNA of genes like ICP0 and ICP4 are produced via the transcription factor of VP16 tegument protein with cellular protein HCF-1. Then, certain transcription factors like TATA-binding protein (TBP) form a complex to begin transcription. Early genes utilize ICP4 as a transcription factor and produce early proteins like viral DNA polymerase and the helicase/primase complex for genome replication. After undergoing rolling circle formation, the late genes are transcribed, which typically represent structural proteins and tegument proteins. Ultimately, translated late proteins are set up to be incorporated into the step of viral assembly.

For viral assembly, synthesis of new capsids occurs within the nucleus. $U_L26.5$ and U_L26 viral proteins complex with scaffolding proteins to form the U_L6 portal for DNA encapsulation. The viral genome is spooled through the UL6 portal, which is wedged between vertices of major and minor capsid proteins. To escape the nucleus, the now mature nucleocapsids undergo a complex process of multiple envelopment and de-envelopment steps before finally egressing from the cell. In the step of primary envelopment, a nuclear egress

complex (NEC) is formed with viral proteins U_L31 and U_L46. NEC disrupts the nuclear lamina through direct binding of viral proteins U_L31 and U_L46. Through the assistance of U_S3 viral kinase and cellular protein kinase-C (PKC), the nucleocapsid fuses and traverses the intracellular space of the nuclear lamina. The virus then de-envelopes in the outer nuclear space, where it prepares for secondary envelopment (Crump, 2018c).

During the step of secondary envelopment and viral egress, tegument proteins from translation are attached to the capsid according to the localized structure of the "inner" or "outer" regions. These tegument proteins assist in the stabilization of virion and interaction between surface glycoproteins and the nucleocapsid. Then, these virions undergo a secondary envelopment through the endoplasmic reticulum and the trans-Golgi network. The vesicles formed from secondary envelopment contain mature virions that utilize kinesin motors to migrate to the cell periphery for cell egress. The virus uses viral proteins U_S9 and gE/gI to interact with kinesin-1 to traffic to the cell periphery, where the vesicle interacts with cellular fusion proteins to be released from the cell (Crump, 2018c). In some cases, the viruses can utilize junctions to directly infect other cells. An illustration of this process is shown in Figure 1.2.

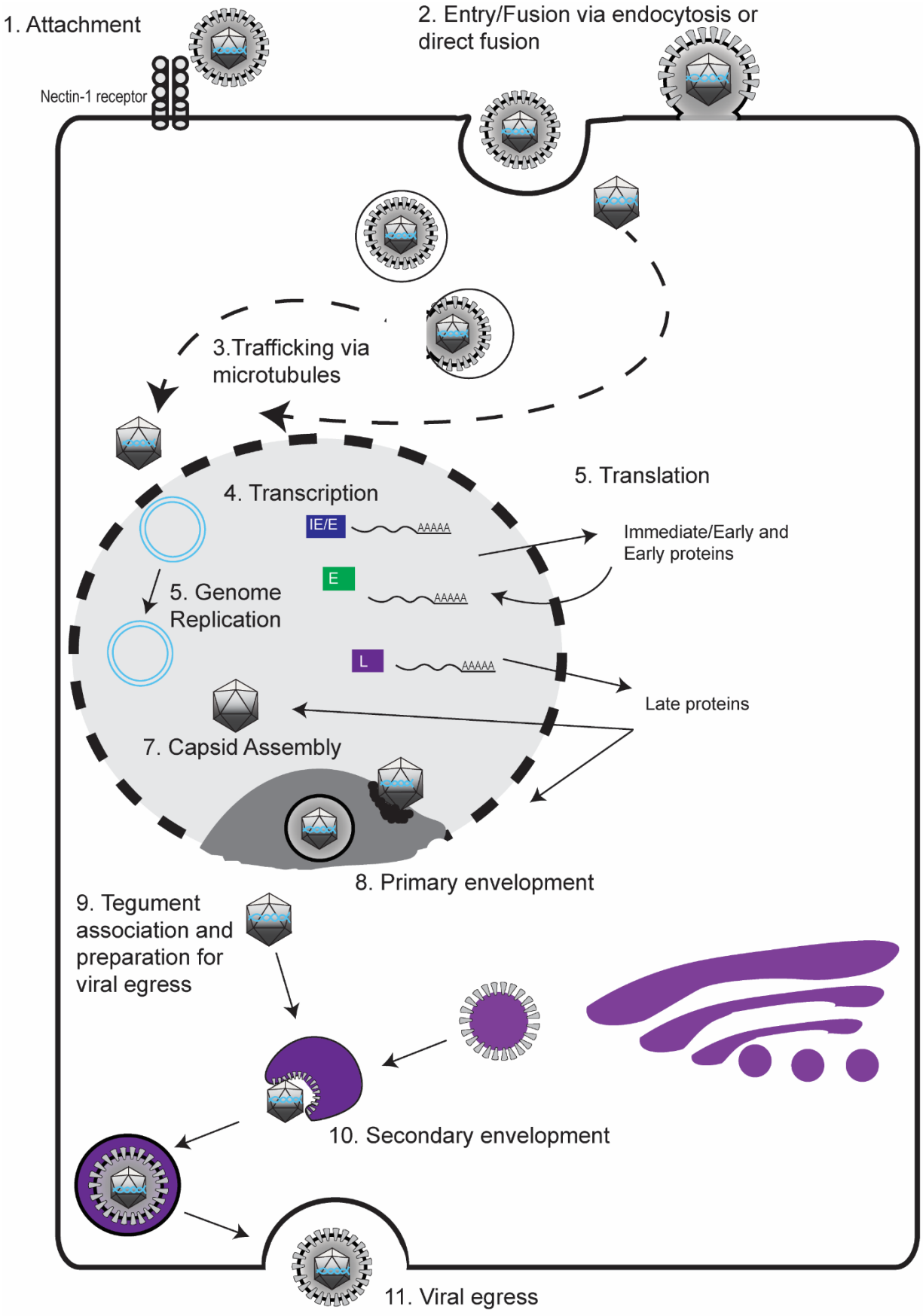
1. Attachment
Nectin-1 receptor
2. Entry/Fusion via endocytosis or direct fusion
3.Trafficking via microtubules
4. Transcription
IE/E
AAAAA
E
AAAAA
L
AAAAA
5. Translation
Immediate/Early and Early proteins
Late proteins
5. Genome Replication
7. Capsid Assembly
8. Primary envelopment
9. Tegument association and preparation for viral egress
10. Secondary envelopment
11. Viral egress

Figure 1.2 Model of alphaherpesvirus life cycle. Virus binds and attaches to cellular surface proteins (1) and then facilitates entry via endocytic pathway or direct fusion (2). Then, the virus travels to the nucleus via microtubules and inserts viral genome into the nucleus (3). Here, the virus undergoes viral transcription (4) and genome replication (5). Viral mRNAs are exported to ribosomes for protein translation in a serial cascade of immediate/early, early, and late proteins (6). The capsid is assembled in the nucleus and DNA is spooled through the portal protein (7). Viral proteins allow the virus to cross the nuclear lamina in a process called primary envelopment and fuses through to the cytosolic space (8). Then, tegument proteins associate with the virus (9), when then fuses with a vesicle from the trans Golgi network in a process called secondary envelopment (10). Then, the virus fuses with the cellular membrane and is secreted from the cell (11).

Lytic and Latent Infection of alphaherpesviruses

One of the defining traits of alphaherpesviruses is its ability to persistently establish latency in the sensory neurons of their hosts. Alphaherpesviruses infect the epithelial cells at the primary site of inoculation, which is symptomatically represented as cold sores. The virus travels through the infected neuron in a retrograde manner to the nearest ganglion nerve center to start the process of latency.

Upon entry of the viral genome, the virus undergoes latency through the transcription of the latency associated transcript (LAT) gene. This gene suppresses production of lytic genes like ICP4 and represses promotors of miRNA involving the encoding of lytic activity. Conditions of reactivation occur during disruption of neuron homeostasis and the promotion of stressors like UV radiation and fever (Cuddy et al., 2020; Roizman & Whitley, 2013; Suzich & Cliffe, 2018). These reactivation events cause the promotion of serially cascading lytic genes that promote the synthesis of new virions.

These newly synthesized virions travel down the neuron in an anterograde manner back to the initial site of infection for the dissemination of the virus to other hosts. Viral glycoproteins

gE/gI and Us9 promote transmission in a tightly regulated manner that deposits a single viral capsid at axonal termini. This interplay between lytic and latent activation results a dynamic process that contributes to understanding infection and coinfection of alphaherpesviruses.

Viral Infection of Alphaherpesviruses

Viral infection of alphaherpesviruses is a tightly regulated process that promotes the generation of new infectious viral particles and establishes conditions for coinfection to occur. The infection cycle of alphaherpesviruses begins in primary cells found within the epithelial layer of the host and then disseminated to the site of sensory neurons. Of importance to this dissertation, the primary cells infected for HSV-1 and PRV are the urogenital or oral mucosae of the host. Upon reaching the sensory neuron, the virus then either undergoes lytic or latent activation upon certain signals.

Models from previous studies have attempted to demonstrate the mode of virion transport and its regulation in coinfection. To travel the length of an axon, kinesin-motor proteins along microtubules are needed to assist in the transport of virions from the terminus to the cell body within the neuron. For alphaherpesviruses, differences between PRV and HSV-1 exist in terms of how viral egress and transport occur. In the case of PRV, viral proteins Us9 and heterodimer gE/gI recruit kinesin-3 to transport the secreted vesicles containing virions (Crump, 2018b). For HSV-1, kinesin-1 has been shown to interact with Us9 and Us11 (Crump, 2018b). Without either of these viral proteins, viral egress becomes attenuated in neuronal cells for HSV-1. However, the exact viral proteins and the cellular components contributing to this mechanism are still largely unknown (Crump, 2018a). It is due to this uncertainty where two proposed

models arise for viral transport. These viruses with their assembly proteins can either travel separately or together for eventual egress and are respectively called the separate or married model. Currently, more evidence for herpesviruses seems to be representative for the married model, since the assembly proteins of PRV are heavily dependent upon the coupled kinesin motor proteins. In this way, these virion-containing vesicles need to travel together due to their dependency upon the cytoskeletal pathways within the neuron. Since HSV-1 is similar to transportation of the viral proteins, HSV-1 might be dependent upon this married model, albeit in a slightly alternative means (Crump, 2018b). In either case, studies have demonstrated that this highly regulated process ultimately delivers approximately only one viral genome to the neuronal cell body for infection (Kobiler et al., 2010; M. P. Taylor et al., 2012). This small delivery despite the multitude of virions produced seems to indicate that alphaherpesviruses evolved the means to regulate coinfection of other virions within their infection cycle.

The regulation of coinfection seems to be dependent upon several factors for the outcome of alphaherpesvirus progeny. In most cases, there seems to be a dominant virus that produces a singular population upon infection if given enough time to establish replication (Kim et al., 1999; Koyuncu et al., 2015; Schmid, 2019; M. P. Taylor et al., 2012). In these cases, MOI and the neuroinvasive capability of the virus seem to be the predominant cause in favoring the selection of incoming genomes. Analysis of clinical strains demonstrated increased neurovirulence in progeny strains when compared to parental strains (Frank, 2001; Wojaczynski et al., 2015). However, when different alphaherpesviruses compete with similar MOI and neuroinvasive, unexpected recombination occurs that does not evenly develop ratios of parental strains and new progeny. Although hard to track in nature, a study analyzed ratios of progeny

and compared them to the original parental strains in both *in vivo* and *in vitro* modeling. This study compared direct and indirect competition of fluorescently labeled HSV-1 viruses and studied the ratios for 3 generations. Although initial passages revealed roughly equal percentage for fluorescence, sequential passages revealed an increasing discrepancy of progeny produced, with non-fluorescent progeny overcoming the percentage of fluorescent coinfection of the primary viruses (Law et al., 2018). This percentage greatly changed as well when comparing if infection occurred in the neuron or in cell culture. Although a mechanism was not elucidated, these differences have a strong impact on how alphaherpesvirus infections are impacted when considering healthcare cases of HSV-1 or the coinfection between vaccines and wild PRV strains. In fact, despite this limited transmission of only one viral genome, current studies on the strains in nature of alphaherpesviruses seem to indicate a high recombination rate unusual for DNA viruses (Bowden et al., 2004b; Casto et al., 2019, 2020; Schmid, 2019). Alphaherpesviruses could have multiple times of recombination events due to their latency, asymptomatic shedding, and specific polymorphisms (Brunnemann et al., 2016; Mertz, 2008; Muylkens et al., 2009). Although there are many factors that influence coinfection, my dissertation focuses on the viral process of superinfection exclusion.

History of Superinfection Exclusion

Superinfection exclusion (SIE) is a unique phenomenon where a cell infected with a primary virus excludes infection by a secondary virus. Although this event theoretically could involve species of different viruses, most observable SIE phenotypes are typically restricted to viruses of similar species (Folimonova, 2012; Sloutskin et al., 2014; Zhang et al., 2018). Superinfection exclusion has been observed across a myriad of different viruses including West

Nile virus (WNV), human immunodeficiency virus (HIV), poxvirus, hepatitis C virus, and vesicular stomatitis virus (VSV) (Karpf et al., 1997a; Koyuncu et al., 2015; Y.-M. Lee et al., 2005; Shearer et al., 2003; Tscherne et al., 2007; Walters et al., 2004; Zhang et al., 2018). SIE involves interference at specific steps of the viral life cycle including attachment, entry, genome replication and translation, and viral egress (Adams & Brown, 1985; Bratt & Rubin, 1968; Breiner et al., 2001; Ellenberg et al., 2007; Karpf et al., 1997b; Kathie-Anne et al., 2004; Nethe et al., 2005; Schneider-Schaulies et al., 1995; Simon et al., 1990; Singh et al., 1997; Steck & Rubin, 1966; Stevenson et al., 1988; Till et al., 2003; Volker et al., 2003).

The earliest case of viruses interfering with one another could be attributed to vaccination for smallpox. Reports of superinfection exclusion were first made in 1929 for the tobacco mosaic virus and two strains of herpesvirus in rabbit exhibiting different tissue tropism (Isaacs & Burke, 1959; Lennette, 1951; Lennette & Koprowski, 1946; Schlesinger, 1959). In both these cases, observable outcomes were used to delineate outcomes that demonstrated SIE occurred: the crops for the tobacco mosaic virus survived, while surviving rabbits exhibited no encephalitis symptoms (Isaacs & Burke, 1959; Lennette & Koprowski, 1946). Since these studies did not discriminate antibody or other immune interference of infection, studies have attempted to focus less on the more organismal level and more on the cellular level to elucidate mechanisms of SIE directly for viruses.

SIE has been described as an inherently “selfish” means to out compete viruses for limited cellular resources (Anna et al., 2014; Frank, 2001; Nowak & May, 1994). The obvious benefits for SIE include increased viral transmission within other uninfected individuals in a population and the maintenance of viral genes that increase the fitness of the virus.

Current literature has detailed a couple of SIE mechanisms of alphaherpesviruses that are hinge on the use of glycoprotein D (gD). Canonically, as described earlier, glycoprotein D is an important viral protein responsible for the entry and fusion of alphaherpesviruses into cells. As a part of this process, interaction of cellular proteins like nectin, heparan sulfate, and HVEM is required to facilitate entry. Since newly synthesized glycoprotein D from viral replication can also facilitate cellular protein interactions, newly synthesized glycoprotein D can directly interfere with these cellular proteins or endocytose these cellular receptors and prevent subsequent entry of other alphaherpesviruses (G Campadelli-Fiume et al., 1988; Johnson & Spear, 1989; Stiles & Krummenacher, 2010). This was not limited to viruses of the same species, since these interactions were observed between HSV-1 and VSV and alphaherpesviruses of other species (Dasika & Letchworth, 2000; Meurens et al., 2004; Muylkens et al., 2009; Sloutskin et al., 2014). Since this SIE is dependent upon gD expression, this SIE occurs approximately 4-6 hours post-infection.

However, another form of SIE was discovered that occurred early during infection and was independent of gD. Previous studies lacked direct evidence for this early SIE, although it was served as a possible explanation for the limited amount of viral transport to newly infected neurons (E. et al., 2010; Meurens et al., 2004). This early SIE occurred as soon as 2 hpi and operated independently of gD (Criddle et al., 2016). In this study, both PRV and HSV-1 were tested and demonstrated to have similar outcomes of SIE. Chemical treatment with cycloheximide (CHX) and phosphonoacetic acid (PAA) indicated that the viral proteins most likely affecting this early SIE were viral genes occurring during IE/E or E phase of viral replication and translation. However, the viral genes, the part of the viral life cycle that this early

SIE impacts, nor the mechanism of this gD-independent SIE was identified.

It is the objective of this dissertation to better elucidate the conditions surrounding this early SIE. Chapter 2 defines a means to quantify and compare virion conditions between alphaherpesviruses, while Chapter 3 attempts a means to utilize alternative means to visually study samples in population dynamics. Chapter 4 describes the effect of cellular processes with the greatest effect on early SIE through chemical and genetic intervention.

Hypothesis

The diversity of alphaherpesviruses results in the factors that contribute to coinfection and its regulation. Despite experimental data exhibiting low virion transmission in both *in vivo* and *ex vivo* cultures, wild alphaherpesviruses exhibit diverse and stable populations that do not necessarily coincide with the limited mutation that is usually typified by a DNA virus. Efforts to understand regulation of this coinfection do not incorporate population dynamics and the factors that regulate it at that level. A possible means of explanation for the regulation of coinfection is superinfection exclusion. However, the study of SIE is severely understudied as to the conditions that contribute to it and the effects it has on population studies. Thus, the overarching hypothesis for this dissertation is that early SIE is conserved across pathogenic alphaherpesviruses and greatly impacts early steps of the viral infection cycle.

To address this hypothesis, a new means to quantify early SIE needed to be developed. To address early SIE, two models were developed: a fluorescent reporter model and capsid trafficking model. Oftentimes, the fluorescent reporter model was used to distinguish viral infection and outcome of intervention in assays. This was useful for experiments involving

factors like MOI or chemical intervention, as shown in chapters 2 and 5 respectively. The capsid trafficking model was more useful for factors affecting early viral infection process like trafficking, which were heavily evaluated in chapter 2. In Chapter 2, early SIE used both models to discuss the *differences between direct infection and early SIE at a quantifiable level*. Data from this study demonstrated that early SIE occurs in an MOI-dependent manner that is unaffected by cellular surface proteins. Additionally, the data demonstrates that early SIE limits virion trafficking and localization. Chapter 2 also focuses on the part of the hypothesis to determine if *SIE is conserved across different alphaherpesviruses.* Data from this study identified that early SIE has statistical differences between virion localization between conditions of SIE and direct infection for PRV and HSV-1.

Data from chapter 3 discusses attempts to create population studies in conjunction with representative visuals using an imaging flow cytometer. Data from the comparison between the imaging flow cytometer and fluorescent microscopy could serve as an alternative means to study virion localization differences.

Data from chapter 4 demonstrates the use of chemical and genetic intervention assays to determine *if cellular processes affect early SIE of alphaherpesviruses.* Assays specifically targeting heparan sulfate receptors, Rho proteins, clathrin, proteosome, and actin formation were used as specific cellular process with the highest influence upon early SIE.

Collectively, my dissertation research presents novel findings in defining factors that affect early SIE for alphaherpesviruses. In summary, early SIE involves viral genes that affects the steps of entry and fusion for PRV and a post-entry regulation for HSV-1.

CHAPTER TWO

SUPERINFECTION EXCLUSION OF ALPHAHERPESVIRUSES INTERFERES WITH VIRION TRAFFICKING

Contribution of Authors and Co-Authors

Author: James P Cwick

Contributions: wrote, edited, and prepared manuscript

Co-Author: Jonathan E. Owen

Contributions: data collection and minor editing

Co-Author: Irina Kochetkova

Contributions: data collection and production

Co-Author: Kyle S. Hain

Contributions: data collection and production

Co-Author: Nick Van Horssen

Contributions: data collection

Co-Author: Matthew P. Taylor

Contributions: project oversight, manuscript editing and preparation

Manuscript Information

James P. Cwick, Jonathan E. Owen, Irina Kochetkova, Kyle S. Hain, Nick Van Horssen, and Matthew P. Taylor

Microbiology Spectrum

Status of Manuscript: [Put an x in one of the options below, delete this]
_____ Prepared for submission to a peer-reviewed journal
_____ Officially submitted to a peer-reviewed journal
__X__ Accepted by a peer-reviewed journal
_____ Published in a peer-reviewed journal

Microbiology Spectrum
Submitted 24 February 2022

Superinfection Exclusion of Alphaherpesviruses Interferes with Virion Trafficking

Authors: James P. Cwick, Jonathan E. Owen, Irina Kochetkova, Kyle S. Hain, Nick Van Horssen, and Matthew P. Taylor

Affiliations: Dept. of Microbiology & Cell Biology, Montana State University

Corresponding Author:
Matthew P. Taylor
Email: mptaylor@montana.edu
Phone: 406-994-7467
Keywords: alphaherpesvirus, Pseudorabies virus, Herpes simplex virus type 1, Superinfection exclusion, fluorescent protein, entry

Abstract

Superinfection exclusion (SIE) is a phenomenon in which a primary viral infection interferes with secondary viral infections within that same cell. Although SIE has been observed across many viruses, it has remained relatively understudied. A recently characterized glycoprotein D (gD) -independent SIE of alphaherpesviruses presents a novel mechanism of co-infection restriction for Herpes Simplex Virus Type 1 (HSV-1) and Pseudorabies virus (PRV). In this study, we evaluated the role of multiplicity of infection (MOI), receptor expression, and trafficking of virions to gain greater insight into potential mechanisms of alphaherpesvirus SIE. We observed that high MOI secondary viral infections were able to overcome SIE in a manner that was independent of receptor availability. We next assessed virion localization during SIE through live microscopy of fluorescently labeled virions and capsid assemblies. Analysis of these fluorescent assemblies identified changes in the distribution of capsids during SIE. These results indicate that SIE during PRV infection inhibits viral entry or fusion while HSV-1 SIE inhibits infection through a post-entry mechanism. Although the timing and phenotype of SIE is similar between alphaherpesviruses, the related viruses implement different mechanisms to restrict coinfection.

Importance

Most viruses utilize a form of superinfection exclusion to conserve resources and control population dynamics. gD-dependent superinfection exclusion in alphaherpesviruses is well-documented. However, the under-characterized gD-independent SIE provides new insight into how alphaherpesviruses limit sequential infection. The observations described here demonstrate

that gD-independent SIE differs between PRV and HSV-1. Comparing these differences provide new insights into the underlying mechanisms of SIE implemented by two related viruses.

Introduction

Alphaherpesviruses are a family of neurotropic viruses with the ability to establish latency in neurons and have a broad impact on human health and agriculture. Herpes Simplex Virus type 1 (HSV-1) has achieved a global infection rate of 80% with approximately 40% of individuals seropositive within the United States (Loncoman et al., 2017; Looker, Magaret, Turner, et al., 2015). Documented cases of both symptomatic and asymptomatic shedding within infected individuals promote high circulating populations of HSV-1 and the increased probability for sequential exposure (Bowden et al., 2004a; Casto et al., 2019; Mertz, 2008; Rooney et al., 2019). These conditions of viral prevalence and transmission increase the probability of superinfection within an individual that can lead to the development of recombinant genomes with novel phenotypes (Bowen et al., 2016; Schmid, 2019; Song et al., 2016). These novel recombinant genomes can present with varying degrees of virulence depending upon a wide range of factors. Recombinant viruses generated from superinfection have been observed in many alphaherpesviruses including Varicella Zoster virus (VZV) and between Herpes Simplex Virus type 1 and 2 (Casto et al., 2020; Dasika & Letchworth, 2000; Koelle et al., 2017; Meurens et al., 2004; Sloutskin et al., 2014). Pseudorabies virus (PRV) is an alphaherpesvirus of pigs that greatly impacts agricultural practices and production. An estimated $500 million is spent annually in the United States for vaccination, disease surveillance, and livestock eradication (Meurens et al., 2004). The prevalent use of glycoprotein-E negative vaccines has allowed

possible recombination with circulating strains of PRV (Bo et al., 2021). Despite concerns about novel recombinant genomes, we still do not know much about the mechanisms that HSV-1 and PRV employ to either limit coinfection or interfere with superinfecting virions.

Superinfection exclusion (SIE) is a process by which an infecting virus prevents subsequent infection of the same cell. Typically, SIE only occurs between identical or closely related viruses, a characteristic that distinguishes this virally mediated process from cellular antiviral responses. First discovered for Tobacco Mosaic Virus in the 1920s, SIE has been utilized by plant virologists to generate "cross-protection" in crops, whereby inoculation with a mildly pathogenic virus can exclude disease-causing strains (McKinney, 1926). Interest in mammalian SIE picked up in the 1970s when it was discovered that the endogenous proviral mouse gene FV1 (genetically comparable to the retrovirus gag gene) was able to confer resistance to various strains of Murine Leukemia Virus (Hull, 2002). SIE has since been observed for several viral species, all of which employ unique mechanisms for inhibiting different aspects of secondary virus infection. For example, Influenza and HIV prevent the attachment and entry of secondary virions by occluding, internalizing, or downregulating cellular co-receptors (I.-C. Huang et al., 2008; Jolicoeur, 1979; Michel et al., 2005). In certain persistent viral infections, like Duck Hepatitis B virus and Bornaviruses, the stoichiometry of late-stage viral replication elements generates unfavorable conditions for incoming viruses, preventing the transcription of secondary virus genes (Geib et al., 2003; Kathie-Anne et al., 2004). The mechanism of SIE also influences the timing of exclusion, which can have important implications on both its pathological and therapeutic relevance. Such is the case for Alphaherpesviruses, which employ mechanistically independent early and late forms of SIE

(Criddle et al., 2016). Research into SIE for alphaherpesviruses have focused on the role and effect of glycoprotein D expression (gD) (Centifanto-Fitzgerald et al., 1982; Fuller & Spear, 1987). However, another mechanism for alphaherpesvirus SIE has been observed that is independent of gD expression (Criddle et al., 2016). This gD-independent SIE is potentially a departure from the canonical mechanism of occlusion or internalization of cellular receptor proteins like nectin-1 (Akhtar et al., 2008; Linehan et al., 2004). Additionally, gD-independent SIE was dependent upon active viral replication and protein synthesis during the first 2 hours of primary viral infection to exclude secondary viral inoculum. However, these results could neither isolate the step of viral infection inhibited nor the mechanism contributing to gD-independent SIE (Criddle et al., 2016). To better characterize and understand SIE for both HSV-1 and PRV, we applied a combination of live fluorescent microscopy with fluorescent protein expressing recombinant viruses to understand inhibition of secondary infection. We investigated the roles of multiplicity of infection (MOI), receptor internalization, and virion distribution to understand PRV and HSV-1 SIE. Together, results from this work will demonstrate that SIE interferes with early steps of viral infection to suppress the replication of superinfecting viruses.

Materials and Methods

Cells and viruses

Porcine kidney epithelial cells (PK15), G5 cells, and green African monkey kidney (Vero) cell lines were obtained from the Enquist laboratory. Human keratinocyte cells (HaCat) were obtained from ATCC. All cells were maintained in Dulbecco's modified Eagle's medium (DMEM) supplemented with 10% (vol/vol) fetal bovine serum (FBS) and 1% (vol/vol)

penicillin-streptomycin. PRV stocks and plaque assays were performed on PK15 cells as previously described (del Rio et al., 2002). PRV isolates containing glycoprotein D deletion were propagated on PK15 cells that stably express glycoprotein D (G5 cells) needed for supporting virion infectivity (G Campadelli-Fiume et al., 1990; Criddle et al., 2016; G. A. Smith & Enquist, 2000). These cells were cultured as above but supplemented with histidinol (50 µg/mL) to maintain glycoprotein D expression. HSV-1 stocks were propagated and tittered on Vero cells (Huber et al., 2001).

All fluorescent PRV recombinants were derived from a PRV Becker background. PRV 287 and 289 express either an enhanced yellow fluorescent protein (eYFP) or cyan fluorescent protein (Turq2) fused to a 3xNLS signal peptide as described previously (Criddle et al., 2016; Huber et al., 2001). PRV 180 contains an mRFP fusion to the minor capsid protein VP26 as previously characterized (del Rio et al., 2005). PRV 137 expresses both an eGFP in-frame fusion to gM and an mRFP fusion to VP26 as previously described (Hogue et al., 2014). PRV GS442 is a kind gift from Dr. Greg Smith and the Enquist Lab. PRV GS442 is a viral mutant lacking glycoprotein D expression. A PRV BAC was utilized to excise the gD gene via homologous recombination inserting a diffusible green fluorescent protein (eGFP). Originally, stocks of PRV GS442 were maintained in a mixture of G5 and PK15 cells in a ratio of approximately 3:1. Viral titers of PRV GS442 were determined with PK15 cells (G Campadelli-Fiume et al., 1990; Criddle et al., 2016; G. A. Smith & Enquist, 2000). Fluorescent HSV-1 recombinants were derived from HSV-1 strain 17. HSV-1 OK14 expresses an mRFP fusion to the capsid protein VP26 (del Rio et al., 2005).

All stocks of fluorescent viruses were confirmed by fluorescence microscopy of plaques

to ensure maintenance and fidelity of the associated fluorescent profiles. Experiments requiring fluorescent virions utilized fresh viral supernatants. Stocks were initiated with an MOI 10 infection of a 10 cm dish of support cells. At 24 hours post-infection, media was collected and subjected to low-speed centrifugation to remove cells and debris. Media was supplemented with 20mM HEPES pH 7.0. Cell-free viral stocks of PRV 180 and HSV-1 OK14 were stored in 500 µL aliquots to maximize virion associated fluorescence.

Microscopy

Images were acquired on a Nikon Ti-Eclipse (Nikon Instruments, Melville, NY) inverted microscope equipped with a SpectraX LED (Lumencor, Beaverton, OR) excitation module and fast-switching emission filter wheels (Prior Scientific, Rockland, MA). Fluorescence imaging used paired excitation/emission filters and dichroic mirrors for cyan fluorescent protein (CFP), YFP, and RFP (Chroma Technology Corp., Bellow Falls, VT). Brightfield images utilized a Plan Fluor 20 phase contrast (Ph) objective and an iXon 896 EM-CCD (Andor Technology Ltd., Belfast, Northern Ireland) camera using NIS Elements software. Acquisition of fluorescent virions utilized a CFI Plan Apochromat Lambda 60x and 100x oil immersion objective to visualize individual virion localization within infected cells. Infected cells were imaged at the time post-infection indicated in each figure legend, dependent on experimental design. Experiments were tested at least twice with multiple fields acquired for each condition of the experiment.

Live imaging was performed on the microscope in conjunction with a stage-top incubation system [Quorum Scientific, Puslinch, ON, CA]. PK15 cells were cultured on Lab-Tek II chambered coverglass. Prior to imaging, a nonfluorescent primary virus was used to establish

primary infection, washed, and then feed with media for 2 hours before the secondary infection was applied. Cells were maintained at 37 °C in a 5% (vol/vol) CO2 enriched atmosphere using a stage top incubator system. Imaging began directly after application of fluorescent viral inoculum, as described. Images were acquired every 2.5 minutes and fluorescent illumination intensity was set to 35% power with less than 100 milliseconds exposure for each channel to avoid photobleaching.

Flow cytometry

Detection of extracellular nectin-1 in infected cells was performed using a BD LSR II or BD LSR Fortessa cytometer (BD Biosciences, San Jose, CA). Infected cells were harvested by 5mM EDTA supplemented with Dulbecco's PBS (D-PBS) and washed once with Ca2+ and Mg2+ -free D-PBS with 0.1% BSA (flow cytometry buffer). Cells were then fixed 2% PFA, washed with 1x PBS solution, and resuspended in 200 µl of flow cytometry buffer. Fixed cells were incubated with mouse IgG monoclonal nectin-1-specific antibody (CK8) [ThermoFisher, Waltham, MA] at 2.5 µg/ml for 1 hour at room temperature. Cells were washed again and subsequently incubated with secondary goat anti-mouse IgG conjugated to Alexa Fluor 488 [ThermoFisher, Waltham, MA]. After 1 hour of incubation, cells were washed with 1x PBS solution and resuspended in flow cytometry buffer for analysis. Acquisition and gating were set on mock-infected and non-specific, secondary antibody-stained infected cell populations. All cytometry data were analyzed using the FlowJo data analysis software (FlowJo, LLC, Ashland, OR).

MOI dependency for superinfected cells

FP expression in infected cells was assessed through fluorescent microscopy. The day before experiments, $1.0x10^5$ PK15 cells per well were seeded in 12-well plates. The next day, at time T=-1 hours, initial inoculations across four MOI conditions (10, 25, 50, and 100) were performed with PRV 289. One-hour post-inoculation, inoculum was aspirated, and cells were washed with 2 mL PBS per well. Then, 1 mL of viral media (DMEM, 2% FBS, 1% Pen-Strep) was supplemented into each well. This time point, T=0 hours, was taken to be the time of initial infection. At T=2 hours, media was aspirated, cells were again washed with 2 mL PBS per well, and secondary inoculations were performed with PRV 287. These infections were also performed across four MOI conditions (10, 25, 50, and 100), such that a 4x4 matrix was generated whereby every initial infection condition was subjected to every superinfection condition. At T=3 hours, superinfecting inoculum was aspirated, cells were washed with PBS, and cells were again overlaid with 1 mL viral media per well. Finally, at T=6 hours, cells were imaged on brightfield, CFP, and YFP channels using paired fluorescent filters. In certain experiments, cycloheximide (CHX) was used to inhibit protein synthesis in the initial inoculation. In these cases, after the wash of the initial inoculum at T=0, cells were overlaid with 1 mL viral media per well supplemented with 100 μg/mL cycloheximide (CHX). Consequently, at T=2 hours cells were subjected to two washes with PBS prior to application of the second inoculum, to ensure removal of any CHX during subsequent incubations.

Virion localization.

Fluorescent virion assemblies were imaged on an epifluorescent microscope and photomicrographs were acquired with 60x and 100x magnification objectives. Sequential photos

of infected cells through the z-axis (z-stacks) were acquired and used to generate a 3-D reconstruction with NIS-Elements software to facilitate analysis of capsid localization on a per cell basis. Individual capsid assemblies were then counted in a single-cell analysis based upon their localization in the cell: perinuclear (adjacent to nuclear region of cell), intracellular virions (inside cellular membrane), and external virions (virions attached but unentered). Average counts of virions were then compared across all conditions and represented out of total virions.

The following conditions were used for experimental procedures: direct infection (DI), SIE, and SIE with CHX. Direct infections were established by the inoculation of mRFP-VP26 virions (HSV-1 OK14 and PRV 180) onto Vero or PK15 cells, respectively, for a 1-hour duration in a 37˚C incubator. For SIE, cells were initially inoculated for 1 hour at 37˚C with a non-fluorescent HSV-1 or PRV wild-type virus. Cells were then washed and maintained for 3 hours at 37˚C. Afterward, they were subsequently infected with mRFP-VP26 labeled virions as described for direct infection. For SIE with CHX, cells were initially inoculated for 1 hour at 37˚C with a non-fluorescent HSV-1 or PRV wild-type virus, then washed and supplemented with media containing CHX at 100 µg/mL during the 3-hour incubation at 37˚C. After incubation, cells were subsequently infected with mRFP-VP26 labeled virions as described for direct infection. One hour after application of fluorescent virions, cells were washed and supplemented with fresh cellular media.

Statistical analysis of virion localization

To compare the statistical differences between conditions of the virion localization experiments, statistical analysis was performed through GraphPad Prism (GraphPad Software, San Diego, California USA). To process the data derived from capsid localization, descriptive

statistics was used in Prism to determine basic statistical parameters of quartiles, mean, and 95% confidence interval. D'Agostino & Pearson tests were applied to confirm that the data sets did not follow parameters of normal standardization due to the presence of outliers. Statistical comparisons were done with Kruskal Wallis tests, with Dunn's multiple comparisons test as a means for comparing differences between conditions (SIE, DI, and SIE with CHX). One-Way ANOVA graphs depicting statistical significance and single cell analysis comparing the localization of viral capsids among conditions are shown in Figures 2.4-2.6.

Results

PRV SIE is dependent upon MOI

SIE is a virally induced process that can directly or indirectly inhibit or block secondary virion infection (Folimonova, 2012). However, the timing and extent of SIE for any virus is dependent on several variables of infection, including the inoculating dose. The number of virions infecting a single cell, the multiplicity of infection (MOI), has an immense effect on outcomes of viral replication. In previously published data, we established the timing of HSV-1 and PRV SIE under equivalent inoculation conditions of MOI 10. We hypothesized that SIE established by the initial MOI of the primary virus might be overcome with varying MOIs of the secondary virus.

To test the effect of MOI on SIE, we evaluated the effect of different doses for the primary and secondary inoculations. For all infections, application of the secondary viral inoculum occurred 2 hours after removal of the primary inoculum. To detect infection by both primary and secondary viruses, we evaluated fluorescent protein expression from recombinant

viruses. Fluorescent protein expression correlating with either primary (CFP) or secondary (YFP) infection was evaluated by fluorescent microscopy at 7-9 hours post inoculation (Figure 1.1a). The extent of primary infection is determined by CFP expression, with representative images of CFP expression at each MOI for the given row. Secondary infection was determined by the extent of YFP expression, with representative images shown across different MOIs. The extent of YFP expression inversely reflects the degree of SIE. Fewer YFP positive nuclei indicate greater SIE, while more YFP positive nuclei indicate less SIE. In line with our previous report, we observe extensive SIE when primary and secondary inoculations are an equal MOI (Figure 1.1b).

Conditions where the secondary MOI was lower than the initial infection resulted in reduced YFP positive nuclei, indicative of greater or more effective SIE. In line with our hypothesis, higher MOIs for the secondary inoculation were able to overcome SIE, resulting in greater numbers of YFP expressing cells. The greatest difference of YFP expression occurred with a low primary inoculation and a high secondary MOI (MOI 10 primary, 100 secondary). The extent of FP expression under these conditions was nearly equivalent to that observed with simultaneous inoculation of the two viruses, suggesting no exclusion of the secondary virus.

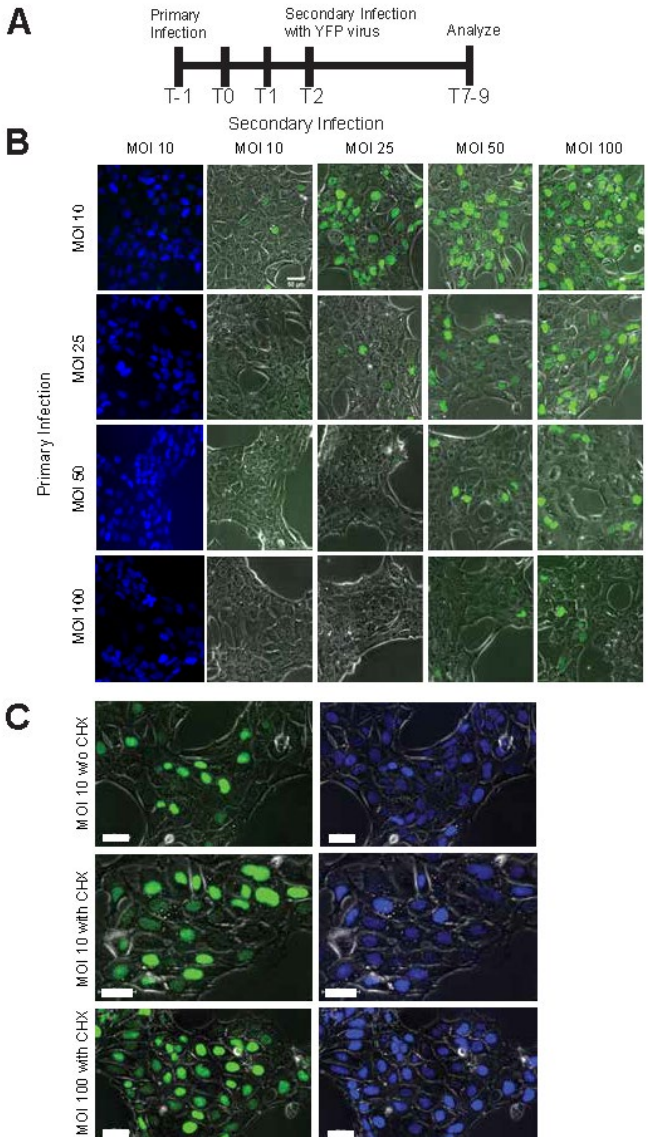

Figure 2.1 SIE dependence on primary and secondary MOIs**.** Experiments done in triplicate on PK15 cells. A) Diagram of the timeline of experimentation. B) Comparison of SIE across a 4x4 matrix of primary and secondary infections. Top row corresponds to the MOI of the secondary virus (YFP labeled), while the vertical column corresponds to the MOI of the primary virus. Images were acquired and analyzed 7-9 hours after initial infection (or 4-6 hours after superinfection). Column with CFP fluorescent expression represents confluent infection with primary virus and is representative for all conditions in the row. C) Analysis of SIE with CHX treatment. Experiments were repeated with previously described SIE conditions. CHX treatment occurred between the application of the primary and secondary inoculum. Top row depicts fluorescent protein expression without CHX (MOI 10), while the middle (MOI 10) and the bottom (MOI 100) depict fluorescent protein expression with CHX treatment.

In previous work, it was observed that alphaherpesvirus SIE could be disrupted using the protein synthesis inhibitor cycloheximide (CHX) (Criddle et al., 2016). To determine if protein synthesis is necessary for SIE at the different inoculating doses, we utilized CHX treatment to alleviate SIE at the extremes of our inoculating doses of MOI 10 and 100. Fluorescent protein detection during SIE was repeated with CHX treatment during the 2-hour window between primary and secondary inoculation. CHX treatment during both MOI 10 and 100 infections alleviated SIE, with an increase of YFP expressing cells (Figure 1.1c). Importantly, there are relatively similar extents of YFP positive nuclei at both conditions, consistent with a similar mechanism of exclusion independent of MOI.

The data supports that PRV SIE is dependent upon MOI of both the primary and secondary virus. Alleviation of SIE occurred by either an overwhelming inoculating dose of secondary virus or through inhibition of protein synthesis by CHX treatment. In both cases, protein production by either cellular or viral origins still plays an important role in the dynamics contributing to SIE establishment.

SIE is independent of surface receptor modulation

Since other forms of SIE disrupt receptor-mediated entry of virions, a possible explanation for SIE disruption of alphaherpesviruses could be dependent upon modulation of available surface receptors. In fact, alphaherpesviruses like HSV-1 have shown cell-dependent entry mechanisms of both direct fusion with the cell membrane and low pH endocytic processes that later release virions (Tebaldi et al., 2020). In both cases, cell entry is primarily mediated by gD engagement with cellular receptors: Herpes Virus Entry Mediator (HVEM), Nectin-1 and Nectin-2, and heparan sulfate (Spear, 2004). During infection, modulation of receptor

availability occurs through internalization of surface expression for cellular entry receptors like nectin-1 (Deschamps et al., 2017a; Nagel et al., 2012). A decrease in the availability of cellular receptors following primary infection would thus decrease the capacity for secondary virion entry. We hypothesized that reduction of cellular receptors on the surface of cells could mediate SIE.

To address this hypothesis, nectin-1 surface expression was evaluated during PRV infection. We chose Nectin-1 as a model receptor due to the ubiquity of cellular expression and its use by multiple alphaherpesvirus. PK15 cells were either mock-infected or infected with wild-type PRV. Following infection, cells were then either mock treated or treated with CHX. At the indicated times post-infection, cells were fixed, stained, and assessed by flow cytometry for surface expressed nectin-1.

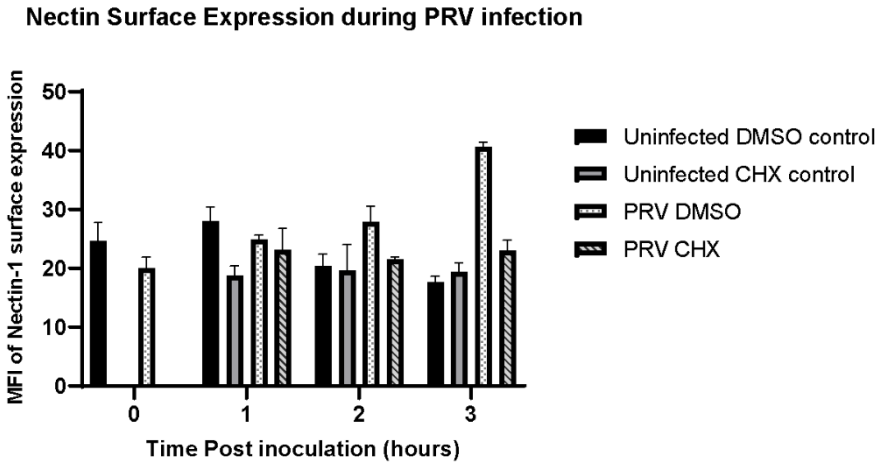

Figure 2.2. Cell surface nectin expression does not correlate with SIE during PRV infection. Depicted is the percentage of nectin-1 expression on the surface of the PK15 cells during PRV infection (MOI 50) at hours after inoculum removal. CHX treatment occurred 1 hour before the application of infection and then removed. Cells were gated for being positive of stained fluorescence as compared to unstained controls.

For these experiments, changes in surface nectin-1 detection were compared at 0-, 1-, and 2-hours post-inoculum removal during the time of SIE induction. At T0, there was a significant drop in the surface of nectin-1 expression during PRV infection. This outcome supports past literature that observable internalization of nectin-1 occurs following alphaherpesvirus infection (Geraghty et al., 2000; Stiles & Krummenacher, 2010). However, T1 observes no notable difference regarding surface expression of nectin-1 for PRV infection with or without CHX treatment (Figure 2.2). Overall, the data demonstrates that relative expression of nectin-1 for CHX treated and untreated conditions remains the same. Although CHX inhibits SIE, it does reduce surface nectin-1 levels. This supports a model that reduced nectin-1 expression following primary virion entry is still sufficient for effective entry of a secondary virus. These results surmise that any potential SIE mechanism is not mediated by changes in nectin-1 surface expression.

SIE impacts entry of secondary virions

Our previous experiments using fluorescent viruses indicate that glycoprotein D independent SIE interferes with secondary viral infection. However, it could not isolate the step(s) of infection that were inhibited (23). Inhibition of one or several steps of infection– including attachment, entry, capsid trafficking, or transcription–could result in inhibition of secondary virus associated FP expression (Geraghty et al., 2000; Jarosinski, 2012). To understand the extent of secondary virion inhibition during SIE, we developed a method to monitor virion entry and trafficking using direct FP fusions to virion components.

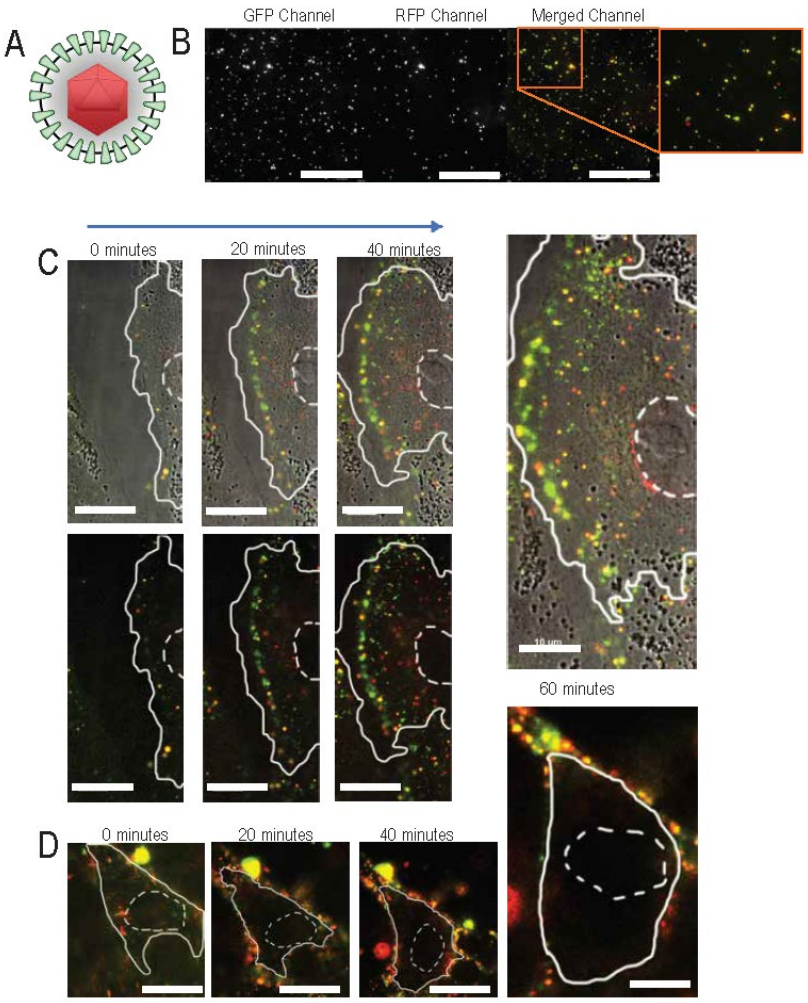

Figure 2.3 Live fluorescent microscopy observes absence of nuclear localized capsids during SIE. A) Model of PRV 137 virion containing a mRFP-VP26 fusion (red capsid) and a gM-eGFP fusion (green envelope protein). B) Distribution of PRV 137 fluorescent assemblies from a viral supernatant preparation. Images split into designated fluorescent channels and composite image. C) Select images from a time course of direct infection with PRV 137 on PK15 cells. Images taken every 20 minutes. Top row corresponds to brightfield and fluorescent composite images, while the bottom row demonstrates only fluorescent merged images. Nucleus is outlined with dashed lines while the cell boundary is outlined with a solid line. D) Select images from a time course of PRV 137 during SIE. Images were taken every 20 minutes after application of PRV 137. Cell boundaries as depicted above.

To determine how SIE impacts early steps of viral entry, time-lapse microscopy was performed with a dual fluorescently labeled virion (PRV 137). As modeled in Figure 2.3a,

PRV137 produces virions that incorporate a GFP fusion to viral protein gM and a mRFP fusion to the capsid associated protein VP26 (Nagel et al., 2012). Colocalization of both fluorophores indicates an intact virion, while dissociation of the two fluorescent signals occurs following entry of the capsid into the cell. The gM protein should remain at the plasma membrane, while the VP26 viral capsid protein will traffic towards the nucleus for insertion of the viral genome and subsequent viral replication. Microscopic examination of secreted PRV 137 virions used for experimental inoculation observed approximately 75% of fluorescent capsid assemblies (red puncta) contain detectable amounts of GFP (Figure 2.3b). Therefore, these co-labeled virions provide an excellent means to evaluate the distribution and structure of virions during entry.

To evaluate virion entry under SIE conditions, sequential micrographs of cells were acquired using a live-imaging approach after inoculation (Hogue et al., 2014). For our live-imaging experiment, we evaluated virion localization and fluorescence during conditions of direct infection (DI) and SIE. For DI, PRV 137 at an MOI 100 was applied to uninfected cells. In parallel for SIE, cells were first inoculated with a non-fluorescent PRV followed by application of PRV 137 two hours later. Image acquisition for both conditions began immediately after application of the PRV 137 inoculum and every 2.5 minutes for a period of one and a half hours. Representative images at 20 minutes intervals from the resulting time-lapse movies (Supplemental Movies 1 and 2) are depicted for both DI and SIE. Under conditions of DI (Figure 2.3c), we observed separation of fluorescence, with an increased number of red punctate structures within the cell. Capsid internalization and subsequent trafficking towards the nucleus are evidenced by red puncta near the nucleus. In contrast, cells superinfected with PRV 137 (SIE condition) exhibit no internalized or nuclear-associated capsid assemblies (Figure 2.3d). In fact,

most of the fluorescent structures remain at or near the cellular boundary.

These observations are consistent with our expectations that internalization or trafficking of secondary virions is strongly suppressed during SIE. The lack of separation between the two fluorescent labels suggests an impairment of virion fusion, while the absence of internalized red fluorescent capsids is evidence of impaired capsid trafficking. To further evaluate the impact of SIE on secondary virion entry, we sought to develop more quantitative approaches to understand virion trafficking.

SIE in PRV reduces capsid entry

To quantify the extent of virion entry and trafficking, we evaluated the distribution of fluorescent capsids within a 3-dimensional reconstruction of infected cells. Cells were inoculated with mRFP-VP26 labeled capsids (PRV 180 or HSV-1 OK14) under conditions of direct infection, SIE, and SIE with treatment of CHX. Following infection, cells were sequentially imaged through their z-axis to acquire a full imaging volume. After image acquisition, cells were rendered into 3-D models and individual fluorescent puncta were counted and categorized by relative location in each cell: capsids near the nuclear region (nuclear), within the cellular boundary (intracellular), and capsids at the cellular boundary (peripheral). Analysis of infected cells from each condition excluded cells with extensive fluorescence aggregation or those that contained overlapping cellular boundaries. Representative images of infections under the different conditions are depicted in Figure 2.4, 2.5 and 2.6.

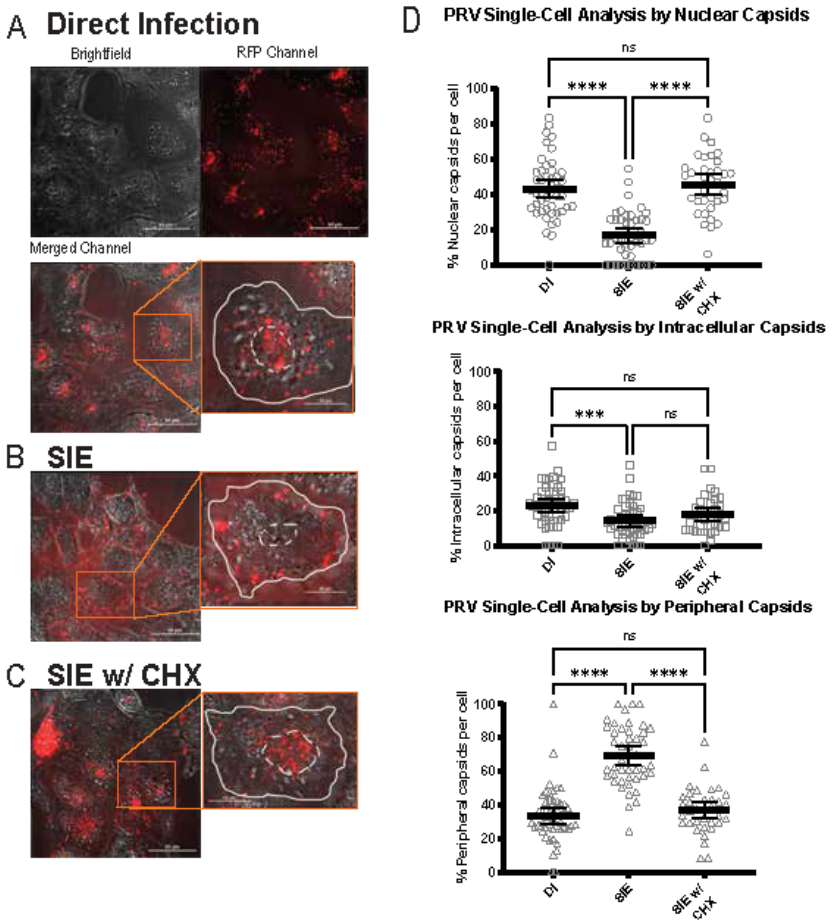

Figure 2.4. PRV SIE exhibits a strong reduction in nuclear associated capsids. PK15 cells under indicated conditions. Depicted channels are brightfield, red fluorescence channel, and merged. Inset shows magnified image of a representative single cell from the field. The white dotted line corresponds to the nuclear region of the cell, while a solid line depicts the periphery of the cell. For each condition, a minimum of 3 fields were analyzed and depicted as percent of total capsids per cell for each category. Quantitative results from single-cell analysis were statistically compared by One-Way ANOVA analysis. A) Direct infection with PRV 180 (MOI 100). B) SIE infection with primary infection of PRV Becker (MOI 100) with secondary infection of PRV 180. C) SIE with CHX treatment. CHX treatment occurred between infection of primary and secondary. D) Dunn's multiple comparison test (One Way ANOVA) comparing capsid localization between conditions. * represents a p-value of 0.0129. ** represents a p-value of 0.0016. *** represents a p-value of 0.0004. **** represents a p-value of <0.0001.

The counts and categorizations of fluorescent capsid assemblies for PRV are presented in Figure 2.4. We were able to quantify an average of 45 virions per cell, with a total of 35 to 48

cells within each condition. Plotted are the numbers of capsids categorized for each condition out of the total observed capsids on a per cell basis. We also compared capsid localization across different conditions to determine the statistical significance between infection conditions.

Comparisons between capsid distributions by condition reveal that there was a strong statistical difference between SIE and direct infection (DI) for all capsid categorizations (Figure 2.4a-c). Comparisons of capsid distribution between SIE and DI revealed that there was a significant difference between the nuclear and peripheral distribution of capsids but not any statistical difference for capsids localized to the intracellular region of the cell. For the DI condition, an average of 47% of cell-associated capsids were localized near the nucleus. For the condition of SIE only 14% of capsids localized near the nucleus. For the condition of SIE with CHX treatment, capsid distributions more closely matched DI conditions, with 47% of capsids at the nucleus. It is important to note that the values are averaged across multiple cells observed for each condition. As a result, most average values under-represent the most observed state of capsid distribution. For SIE, many cells contain no nuclear capsids with 100% of capsids retained at the periphery. The overall reduction of nuclear capsids and the accumulation of peripheral capsids during SIE correlates with our live fluorescent microscopy observations. Together, the difference in capsid distribution is consistent with our prior interpretation that PRV-induced SIE inhibits secondary virion entry.

HSV-1 SIE does not alter intracellular capsid accumulation

To compare how SIE alters secondary capsid uptake between different alphaherpesviruses, we performed a parallel experiment with HSV-1 expressing an mRFP fusion to VP26 (HSV-1 OK14) under similar conditions. We quantified an average of 40 capsids per

cell, analyzing between 39 and 46 cells per condition.

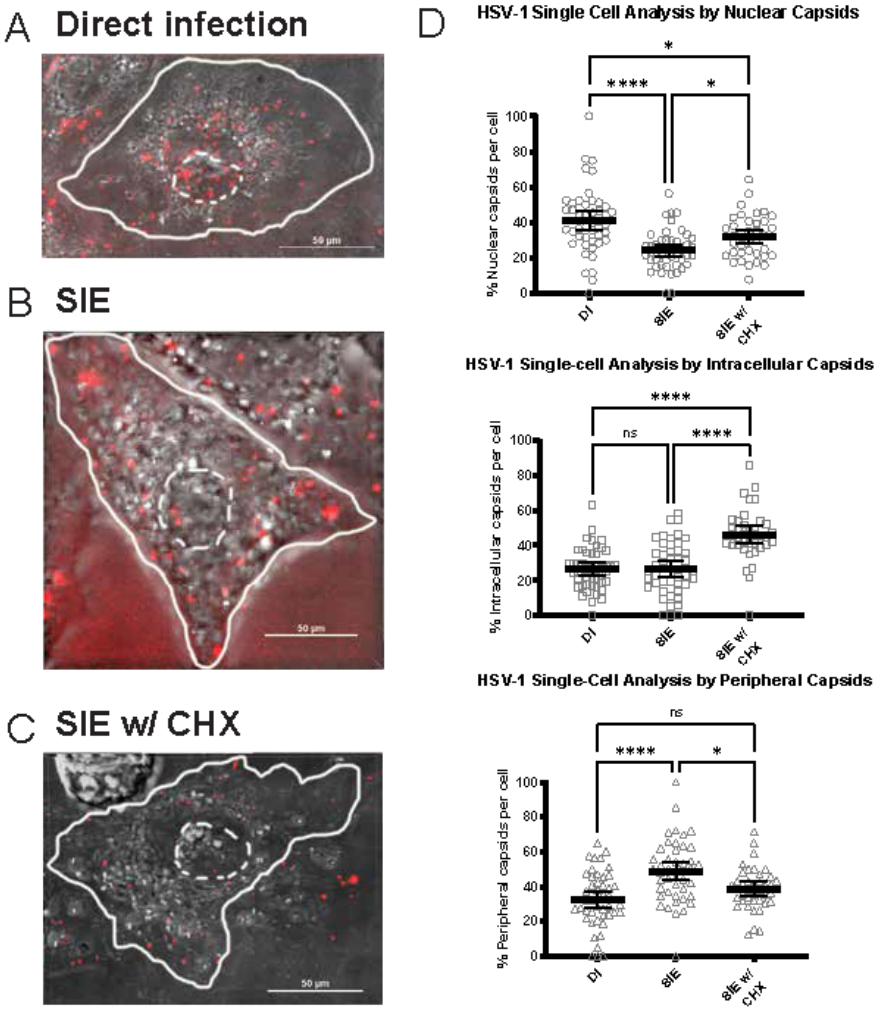

Figure 2.5. HSV SIE exhibits a modest reduction in nuclear capsids. Representative images of an infected Vero cell with capsid distributions from three conditions of infection. The white dotted line indicates the nuclear region of the cell, while a solid line depicts the periphery of the cell. For each condition, a minimum of 3 fields were analyzed and depicted as percent of total capsids per cell for each category. Quantitative results from single-cell analysis were statistically compared by One-Way ANOVA analysis. A) Direct infection with HSV OK14 (MOI 100). B) SIE infection with primary infection of HSV-1 17 (MOI 100) and secondary infection of HSV OK14. C) SIE with CHX treatment. CHX treatment occurred between infection of primary and secondary. D) Dunn's multiple comparison test (One Way ANOVA) comparing capsid localization between conditions. * represents a p-value of 0.0264. **** represents a p-value of <0.0001.

Results from the quantification of mRFP-labeled HSV-1 capsids revealed a surprising difference of capsid distribution compared to PRV. As shown in Figure 2.5d, there was a reduction of nuclear capsids and an increase in peripheral capsids between HSV SIE and HSV-1 DI. However, most cells in the SIE condition did have detectable capsids localized to the nuclear boundary. This differs from PRV, where most cells under SIE lacked any nuclear localized capsids. Moreover, treatment with CHX in HSV-1 SIE elicited a strong increase in intracellular capsids but did fully match distributions seen for DI conditions. These differences in capsid distribution seem to indicate that HSV-1 does not interfere with superinfecting virion entry to the same extent as PRV.

PRV gD-expression is not necessary to reduce capsid trafficking

We previously determined that SIE for PRV occurred independently of gD expression (Criddle et al., 2016). However, it does not eliminate the possibility that gD-expression could be interfering with the entry of the superinfecting virion. To test if gD expression is necessary for the observed reduction in capsid entry during PRV SIE, a gD-null virus (PRV GS442) was utilized as a primary inoculum.

Using the same conditions as already defined in figure 2.4, an average number of 58 fluorescent capsids were quantified for 30 to 55 cells for each condition. Although this is a greater average count per cell in comparison to the prior analyses, aggregates of fluorescent capsids were more extensive during superinfection of gD-null infected cells. Cells with excessive capsid aggregation were excluded from quantification with our analysis focusing on cells with individual capsid assemblies.

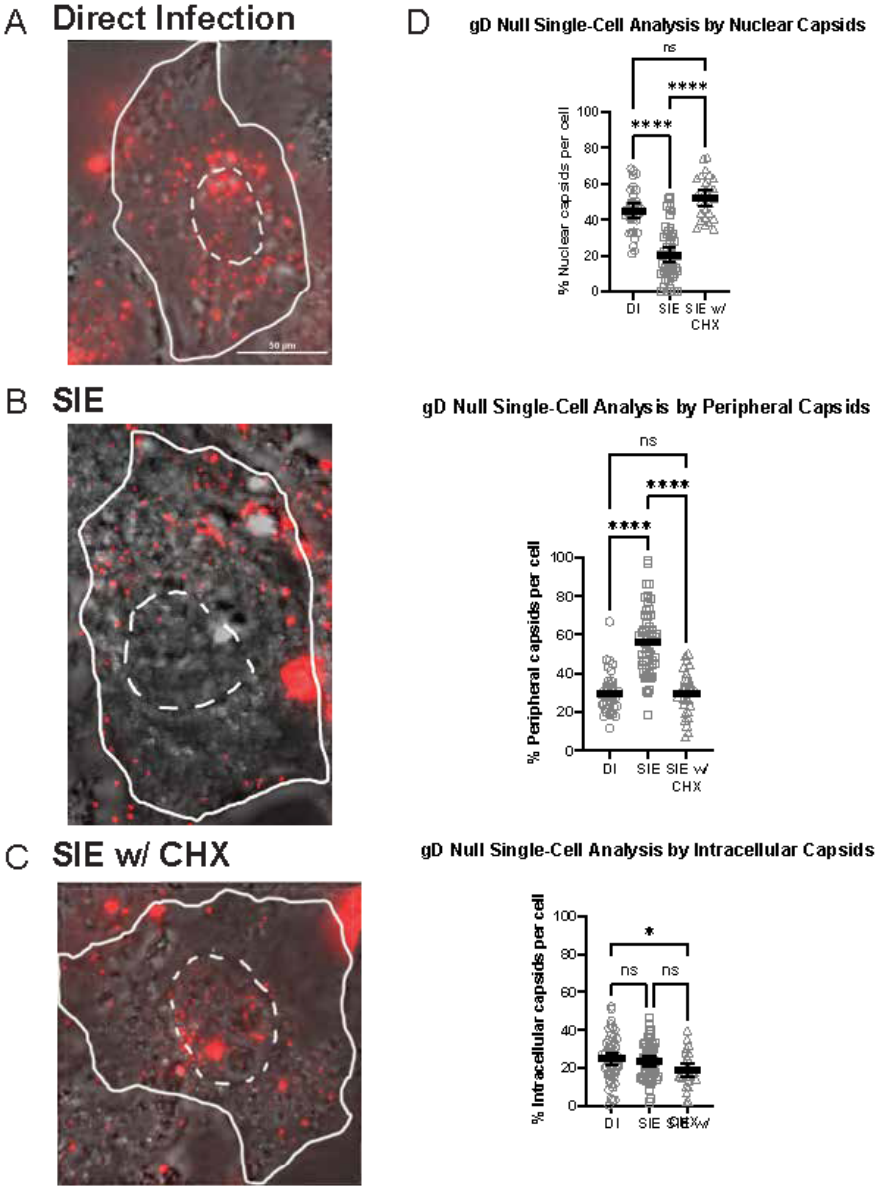

Figure 2.6. SIE during gD-null infection also reduces nuclear-associated capsids. Representative images of capsid distribution under three conditions of infection. The dotted white line indicates the nuclear region of the cell, while a solid line depicts the periphery of the PK15 cell. For each condition, a minimum of 3 fields were analyzed and depicted as percent of total capsids per cell for each category. Quantitative results from single-cell analysis were statistically compared by One-Way ANOVA analysis. A) Direct infection with PRV 180 (MOI 100). B) SIE infection with primary infection of PRV GS442 (gD null) with secondary infection of PRV 180. C) SIE infection with CHX treatment. CHX treatment occurred between infection of primary and secondary. D) Dunn's multiple comparison Test (One Way ANOVA) comparing capsid localization between conditions. * represents a p-value of 0.0292. **** represents a p-value of <0.0001.

As shown in figure 2.6, SIE following gD-null primary inoculation was very similar to our previous observation of decreased capsid association with the nucleus and accumulation of capsids at the periphery. Comparing the capsid distributions demonstrated a significant reduction (approximately 50%) for nuclear internalization between DI and SIE with no difference between DI and SIE with CHX treatment. There is an increase of capsids on the periphery of the cell for SIE only with no differences between DI and SIE with CHX treatment. The only distinct difference between wild-type SIE and gD null SIE is the percent of intracellular capsids not associated with the nucleus. This lack of difference in internalized capsids may be related to the accumulation of fluorescent capsid assemblies at the periphery or to changes in secondary virion fusion compared to wild-type PRV primary infection. Despite the subtle changes in capsid uptake, the reduction in nuclear capsid association following gD-null primary infection is consistent with a mechanism inhibiting virion entry that is independent of gD expression.

Discussion

This study probed the effect of glycoprotein-D independent SIE during secondary entry of the alphaherpesviruses PRV and HSV-1. We observed that the MOI for both the primary and secondary inoculum played a significant role in the establishment and extent of exclusion. A higher MOI secondary inoculum was able to overcome SIE, while lower MOIs of secondary challenge are more efficiently excluded. One possible explanation for these observations is that higher MOI primary infections exhibit expedited viral gene expression and implementation of SIE. For example, an MOI of 10 for the initial virus completely failed to exclude a superinfecting MOI of 25, while an initial MOI of 25 required a superinfecting MOI of 100 to achieve a similar

expression of SIE. Additionally, conditions with a higher initial MOI are more capable of excluding the secondary virus (as shown in the columns when comparing conditions like MOI 50 and 100 with a lower secondary viral infection). Our experiments have demonstrated that infection of the primary virus was extensive (as shown through CFP expression), indicating that the observable phenomenon is not misrepresented by lack of infection of the primary virus. This suggests that the kinetics of viral replication and genome production likely play roles in regulating implementation of SIE. The importance of primary viral genome number and subsequent protein production was further confirmed using CHX to inhibit protein production by the primary viral infection. High or low inoculation with similar MOIs and CHX treatment alleviated SIE. This indicates that it is not just the presence of a high inoculating virus, but also its amount relative to the secondary virus.

Although concurrent results indicate viral factors can influence the extent of SIE, nonviral factors could not be excluded. To this end, we evaluated surface expression of nectin-1 during infection. Although there is a drop in nectin-1 following initial infection at 0 hours post-infection, the level of surface nectin-1 is similar when treated with CHX. Since CHX has been previously shown to alleviate SIE, the limited nectin-1 present on the surface is still capable of mediating superinfection. This observation strongly suggests that interference with cell surface presentation of entry receptors is not important for the mechanism of alphaherpesvirus SIE.
To identify the step of viral infection impacted by gD-independent SIE, we visualized capsid entry with live fluorescent microscopy. Dual-labeled virions allowed the observation of distinct fluorescent profiles for virion distribution between SIE and direct infection conditions. Accumulation of dual fluorescent PRV virions at the plasma membrane of cells during SIE

suggests an inhibition of virion fusion and confirms prevention of entry. This is further supported by the quantitative analysis of fluorescent capsids which revealed strong reductions in nuclear association following entry. These results raise the possibility that gD-independent SIE might inhibit virion entry or subsequent trafficking.

Initially, it was expected that effect of SIE on entry would be similar between alphaherpesviruses due to observations of SIE for HSV-1 and PRV in Criddle et al. Although the outcome of SIE suppression remains similar across alphaherpesviruses, experiments from this paper demonstrated that the mechanism of how HSV-1 and PRV SIE operate may differ. PRV-mediated SIE results in reduced capsid internalization, with most accumulating on the periphery. This could be a result in which the PRV mechanism of SIE inhibits both direct fusion and low endocytic processes, allowing the strong accumulation of virions on the surface of the cell. HSV-1 SIE, however, doesn't exhibit reduced capsid internalization while still resulting in accumulation on the periphery. This result indicates that HSV-1 SIE might employ a combination of post-entry factors to suppress expression of a superinfecting virus, while PRV SIE likely targets only virion fusion (Figure 2.7). This difference strongly suggests there are multiple mechanisms employed by alphaherpesviruses to suppress superinfection. The single-cell analysis of capsid distribution is one potential means for continued study into the differences of SIE between related viruses.

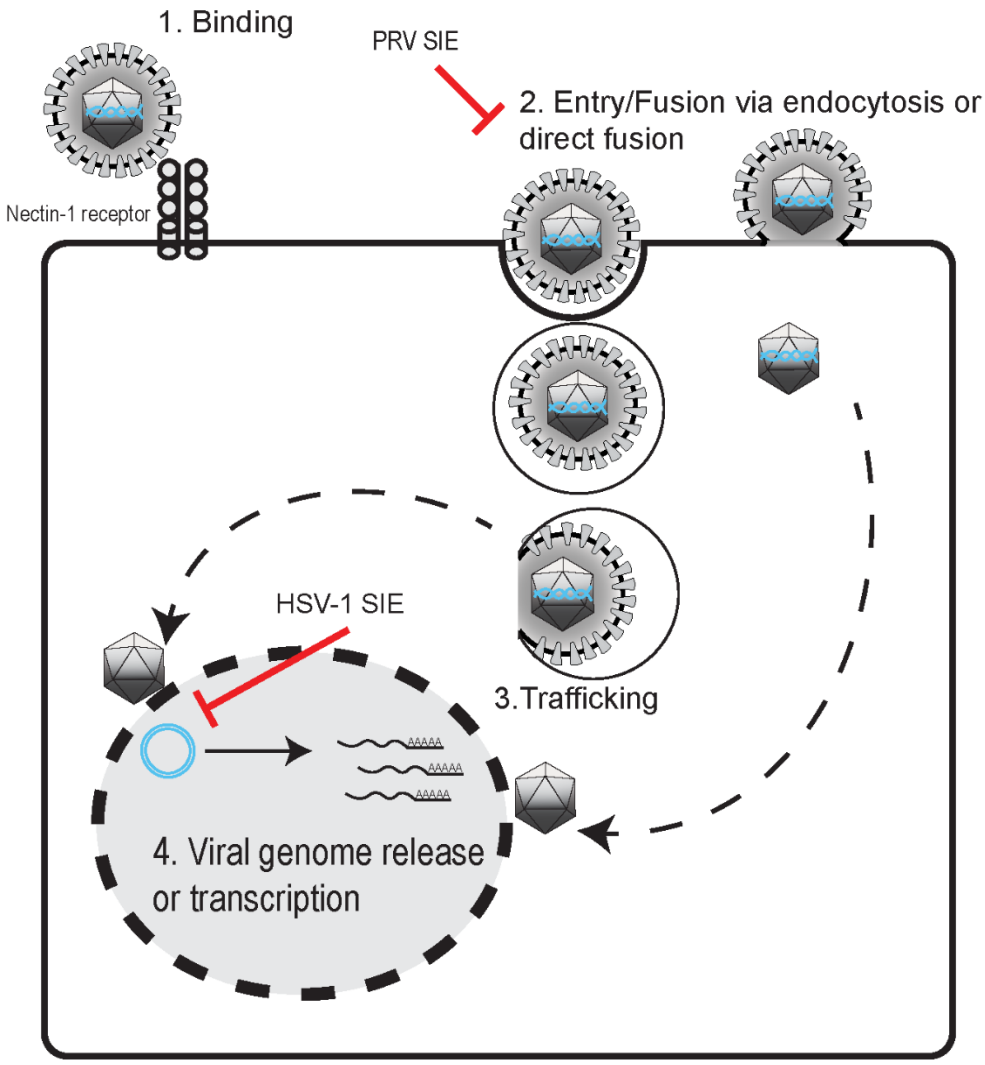

Figure 2.7. Model of SIE inhibition of alphaherpesviruses. A schematic representation of the proposed points of inhibition of secondary virion infection during SIE. PRV SIE suppresses entry/fusion, while HSV-1 possibly inhibits viral genome release or transcription.

Taken together, work from this study provides new insights into the properties of alphaherpesvirus SIE. This work supports our previous finding that SIE is a virally induced, gD-independent phenotype but differs in the mechanism of exclusion between PRV and HSV-1. PRV mediated SIE appears to inhibit entry of secondary virions in a gD-independent manner,

while HSV-1 SIE impacts a post-entry step. Further work will further characterize the differences between PRV and HSV-1 SIE, as well identify the viral mechanism(s) which mediate exclusion. Most likely, this will address the kinetics of viral protein between primary and secondary challenge of viruses. This data about gD-independent SIE will provide valuable insight regarding alphaherpesvirus population dynamics, disease kinetics for neuronal pathologies, and development of antiviral therapies.

Acknowledgements

The authors appreciate the sharing of reagents by the Smith and Enquist labs. We also thank Kyle Hain for providing critical reading and commentary of the manuscript. This work was supported by National Institutes of Health R21 Exploratory/Development Award Grants [R21AI139935] and [R21AI146952].

Supplemental Movie legends

Supplemental Movie 1. Live fluorescent microscopy of direct infection. Movie of direct infection with PRV 137 on PK15 cells. Images taken every 2.5 minutes for 1 hour. Playback speed is 5 frames per second. Scale is equal to 10 μm.

Supplemental Movie 2. Live fluorescent microscopy of SIE. Movie of SIE with secondary inoculation of PRV 137, primary with nonfluorescent PRV Becker. Images taken every 2.5 minutes for 1 hour. Playback speed is 5 frames per second. Scale is equal to 10 μm. Infection occurred on PK15 cells.

REFERENCES CITED

Akhtar, J., Tiwari, V., Oh, M. J., Kovacs, M., Jani, A., Kovacs, S. K., Valyi-Nagy, T., & Shukla, D. (2008). HVEM and nectin-1 are the major mediators of herpes simplex virus 1 (HSV-1) entry into human conjunctival epithelium. *Investigative Ophthalmology and Visual Science*, *49*(9), 4026–4035. https://doi.org/10.1167/iovs.08-1807

Bo, Z., Miao, Y., Xi, R., Gao, X., Miao, D., Chen, H., Jung, Y. S., Qian, Y., & Dai, J. (2021). Emergence of a novel pathogenic recombinant virus from Bartha vaccine and variant pseudorabies virus in China. *Transboundary and Emerging Diseases*, *68*(3), 1454–1464. https://doi.org/10.1111/TBED.13813

Bowden, R., Sakaoka, H., Donnelly, P., & Ward, R. (2004). High recombination rate in herpes simplex virus type 1 natural populations suggests significant co-infection. *Infection, Genetics and Evolution : Journal of Molecular Epidemiology and Evolutionary Genetics in Infectious Diseases*, *4*(2), 115–123. https://doi.org/10.1016/j.meegid.2004.01.009

Bowen, C. D., Renner, D. W., Shreve, J. T., Tafuri, Y., Payne, K. M., Dix, R. D., Kinchington, P. R., Gatherer, D., & Szpara, M. L. (2016). Viral forensic genomics reveals the relatedness of classic herpes simplex virus strains KOS, KOS63, and KOS79. *Virology*, *492*, 179–186. https://doi.org/10.1016/j.virol.2016.02.013

Campadelli-Fiume, G., Qi, S., Avitabile, E., Foà-Tomasi, L., Brandimarti, R., & Roizman, B. (1990). Glycoprotein D of herpes simplex virus encodes a domain which precludes penetration of cells expressing the glycoprotein by superinfecting herpes simplex virus. *Journal of Virology*, *64*(12), 6070–6079. http://www.ncbi.nlm.nih.gov/pubmed/2173780

Casto, A. M., Huang, M. L. W., Xie, H., Jerome, K. R., Wald, A., Johnston, C. M., & Greninger, A. L. (2020). Herpes simplex virus mistyping due to HSV-1 × HSV-2 interspecies recombination in viral gene encoding glycoprotein B. *Viruses*, *12*(8), 1–8. https://doi.org/10.3390/v12080860

Casto, A. M., Roychoudhury, P., Xie, H., Selke, S., Perchetti, G. A., Wofford, H., Huang, M.-L., Verjans, G. M. G. M., Gottlieb, G. S., Wald, A., Jerome, K. R., Koelle, D. M., Johnston, C., & Greninger, A. L. (2019). Large, Stable, Contemporary Interspecies Recombination Events in Circulating Human Herpes Simplex Viruses. *The Journal of Infectious Diseases*, *Xx Xxxx*, 1–9. https://doi.org/10.1093/infdis/jiz199

Centifanto-Fitzgerald, Y. M., Varnell, E. D., & Kaufman, H. E. (1982). Initial herpes simplex virus type 1 infection prevents ganglionic superinfection by other strains. *Infection and Immunity*, *35*(3), 1125–1132. http://www.ncbi.nlm.nih.gov/pubmed/6279513

Criddle, A., Thornburg, T., Kochetkova, I., DePartee, M., & Taylor, M. P. (2016). gD-Independent Superinfection Exclusion of Alphaherpesviruses. *Journal of Virology*, *90*(8), 4049–4058. https://doi.org/10.1128/JVI.00089-16

Dasika, G. K., & Letchworth, G. J. (2000). Homologous and heterologous interference requires bovine herpesvirus-1 glycoprotein D at the cell surface during virus entry. *Journal of General Virology*, *81*(4), 1041–1049. https://doi.org/10.1099/0022-1317-81-4-1041

del Rio, T., Ch'ng, T. H., Flood, E. A., Gross, S. P., & Enquist, L. W. (2005). Heterogeneity of a Fluorescent Tegument Component in Single Pseudorabies Virus Virions and Enveloped Axonal Assemblies. *Journal of Virology*, *79*(7), 3903–3919. https://doi.org/10.1128/jvi.79.7.3903-3919.2005

del Rio, T., Werner, H. C., & Enquist, L. W. (2002). The Pseudorabies Virus VP22 Homologue (UL49) Is Dispensable for Virus Growth In Vitro and Has No Effect on Virulence and Neuronal Spread in Rodents. *Journal of Virology*, *76*(2), 774–782. https://doi.org/10.1128/jvi.76.2.774-782.2002

Deschamps, T., Dogrammatzis, C., Mullick, R., & Kalamvoki, M. (2017). Cbl E3 Ligase Mediates the Removal of Nectin-1 from the Surface of Herpes Simplex Virus 1-Infected Cells. *Journal of Virology*, *91*(12). https://doi.org/10.1128/jvi.00393-17

Folimonova, S. Y. (2012). Superinfection Exclusion Is an Active Virus-Controlled Function That Requires a Specific Viral Protein. *Journal of Virology*, *86*(10), 5554 LP – 5561. http://jvi.asm.org/content/86/10/5554.abstract

Fuller, A. O., & Spear, P. G. (1987). Anti-glycoprotein D antibodies that permit adsorption but block infection by herpes simplex virus 1 prevent virion-cell fusion at the cell surface (neutralizing antibodies/membrane fusion/glycoproteins/viral penetration) (Vol. 84). http://www.pnas.org/content/pnas/84/15/5454.full.pdf

Geib, T., Sauder, C., Venturelli, S., Hässler, C., Staeheli, P., & Schwemmle, M. (2003). Selective Virus Resistance Conferred by Expression of Borna Disease Virus Nucleocapsid Components. *Journal of Virology*, *77*(7). https://doi.org/10.1128/jvi.77.7.4283-4290.2003

Geraghty, R. J., Jogger, C. R., & Spear, P. G. (2000). Cellular expression of alphaherpesvirus gD interferes with entry of homologous and heterologous alphaherpesviruses by blocking access to a shared gD receptor. *Virology*, *268*(1), 147–158. https://doi.org/10.1006/viro.1999.0157

Hogue, I. B., Bosse, J. B., Hu, J. R., Thiberge, S. Y., & Enquist, L. W. (2014). Cellular Mechanisms of Alpha Herpesvirus Egress: Live Cell Fluorescence Microscopy of Pseudorabies Virus Exocytosis. *PLoS Pathogens*, *10*(12). https://doi.org/10.1371/journal.ppat.1004535

Huang, I.-C., Li, W., Sui, J., Marasco, W., Choe, H., & Farzan, M. (2008). Influenza A Virus Neuraminidase Limits Viral Superinfection. *Journal of Virology*, *82*(10). https://doi.org/10.1128/jvi.00079-08

Huber, M. T., Wisner, T. W., Hegde, N. R., Goldsmith, K. A., Rauch, D. A., Roller, R. J., Krummenacher, C., Eisenberg, R. J., Cohen, G. H., & Johnson, D. C. (2001). Herpes Simplex Virus with Highly Reduced gD Levels Can Efficiently Enter and Spread between Human Keratinocytes. *Journal of Virology*, *75*(21), 10309–10318. https://doi.org/10.1128/jvi.75.21.10309-10318.2001

Hull, R. (2002). *Matthews' Plant Virology*. Academic Press New York.

Jarosinski, K. W. (2012). Dual Infection and Superinfection Inhibition of Epithelial Skin Cells by Two Alphaherpesviruses Co-Occur in the Natural Host. *PLoS ONE*, *7*(5), e37428. https://doi.org/10.1371/journal.pone.0037428

Jolicoeur, P. (1979). The Fv-1 gene of the mouse and its control of murine leukemia virus replication. In *Current topics in microbiology and immunology* (Vol. 86). https://doi.org/10.1007/978-3-642-67341-2_3

Kathie-Anne, W., A., J. M., R., A. W., P., F. K., & J., T. D. L. (2004). Superinfection Exclusion in Duck Hepatitis B Virus Infection Is Mediated by the Large Surface Antigen. *Journal of Virology*, *78*(15), 7925–7937. https://doi.org/10.1128/JVI.78.15.7925-7937.2004

Koelle, D. M., Norberg, P., Fitzgibbon, M. P., Russell, R. M., Greninger, A. L., Huang, M. L., Stensland, L., Jing, L., Magaret, A. S., Diem, K., Selke, S., Xie, H., Celum, C., Lingappa, J. R., Jerome, K. R., Wald, A., & Johnston, C. (2017). Worldwide circulation of HSV-2 × HSV-1 recombinant strains. *Scientific Reports*, *7*(March), 1–12. https://doi.org/10.1038/srep44084

Linehan, M. M., Richman, S., Krummenacher, C., Eisenberg, R. J., Cohen, G. H., & Iwasaki, A. (2004). In vivo role of nectin-1 in entry of herpes simplex virus type 1 (HSV-1) and HSV-2 through the vaginal mucosa. *Journal of Virology*, *78*(5), 2530–2536. https://doi.org/10.1128/JVI.78.5.2530-2536.2004

Loncoman, C. A., Vaz, P. K., Coppo, M. J., Hartley, C. A., Morera, F. J., Browning, G. F., & Devlin, J. M. (2017). Natural recombination in alphaherpesviruses: Insights into viral evolution through full genome sequencing and sequence analysis. In *Infection, Genetics and Evolution* (Vol. 49, pp. 174–185). Elsevier. https://doi.org/10.1016/j.meegid.2016.12.022

Looker, K. J., Magaret, A. S., Turner, K. M. E., Vickerman, P., Gottlieb, S. L., Newman, L. M., May, M. T., Turner, K. M. E., Vickerman, P., Gottlieb, S. L., & Newman, L. M. (2015). Global estimates of prevalent and incident herpes simplex virus type 2 infections in 2012. *PLoS ONE*, *10*(1). https://doi.org/10.1371/journal.pone.0114989

McKinney, H. H. (1926). Virus mixtures that may not be detected in young tobacco plants. *Phytopathology*, *16*(89).

Mertz, G. J. (2008). Asymptomatic shedding of herpes simplex virus 1 and 2: Implications for prevention of transmission. *Journal of Infectious Diseases*, *198*(8), 1098–1100. https://doi.org/10.1086/591914

Meurens, F., Schynts, F., Keil, G. M., Muylkens, B., Vanderplasschen, A., Gallego, P., & Thiry, E. (2004). Superinfection prevents recombination of the alphaherpesvirus bovine herpesvirus 1. *Journal of Virology*, *78*(8), 3872–3879. https://doi.org/10.1128/JVI.78.8.3872-3879.2004

Michel, N., Allespach, I., Venzke, S., Fackler, O. T., & Keppler, O. T. (2005). The nef protein of human immunodeficiency virus establishes superinfection immunity by a dual strategy to downregulate cell-surface CCR5 and CD4. *Current Biology*, *15*(8). https://doi.org/10.1016/j.cub.2005.02.058

Nagel, C. H., Döhner, K., Binz, A., Bauerfeind, R., & Sodeik, B. (2012). Improper Tagging of the Non-Essential Small Capsid Protein VP26 Impairs Nuclear Capsid Egress of Herpes Simplex Virus. *PLoS ONE*, *7*(8). https://doi.org/10.1371/journal.pone.0044177

Rooney, B. V., Crucian, B. E., Pierson, D. L., Laudenslager, M. L., & Mehta, S. K. (2019). Herpes virus reactivation in astronauts during spaceflight and its application on earth. In *Frontiers in Microbiology* (Vol. 10, Issue feburay). https://doi.org/10.3389/fmicb.2019.00016

Schmid, D. S. (2019). Mixing It Up: New Insights Into Interspecies Recombination Between Herpes Simplex Virus Type 1 and 2. *The Journal of Infectious Diseases*, *18*(Xx), 1–2. https://doi.org/10.1093/infdis/jiz200

Sloutskin, A., Yee, M. B., Kinchington, P. R., & Goldstein, R. S. (2014). Varicella-Zoster Virus and Herpes Simplex Virus 1 Can Infect and Replicate in the Same Neurons whether Co- or Superinfected. *Journal of Virology*, *88*(9), 5079–5086. https://doi.org/10.1128/JVI.00252-14

Smith, G. A., & Enquist, L. W. (2000). A self-recombining bacterial artificial chromosome and its application for analysis of herpesvirus pathogenesis. *Proceedings of the National Academy of Sciences of the United States of America*, *97*(9), 4873–4878. https://doi.org/10.1073/pnas.080502497

Song, R., Koyuncu, O. O., Greco, T. M., Diner, B. A., Cristea, I. M., & Enquist, L. W. (2016). Two modes of the axonal interferon response limit alphaherpesvirus neuroinvasion. *MBio*, *7*(1). https://doi.org/10.1128/mBio.02145-15

Spear, P. G. (2004). Herpes simplex virus: Receptors and ligands for cell entry. *Cellular Microbiology*, *6*(5), 401–410. https://doi.org/10.1111/j.1462-5822.2004.00389.x

Stiles, K. M., & Krummenacher, C. (2010). Glycoprotein D actively induces rapid internalization of two nectin-1 isoforms during herpes simplex virus entry. *Virology*, *399*(1), 109–119. https://doi.org/10.1016/j.virol.2009.12.034

Tebaldi, G., Pritchard, S. M., & Nicola, A. V. (2020). Herpes Simplex Virus Entry by a Nonconventional Endocytic Pathway. *Journal of Virology*, *94*(24). https://doi.org/10.1128/jvi.01910-20

CHAPTER THREE

EVALUATION OF VIRION DETECTION METHOD FOR ALPHAHERPESVIRUS ENTRY

Contribution of Authors and Co-Authors

Author: James P Cwick

Contributions: data collection and analysis, wrote manuscript, figure presentation

Co-Author: Matthew P Taylor

Contributions: oversight, figure presentation, manuscript editing and writing

Manuscript Information

James P Cwick, Matthew P Taylor

Journal of Infectious Diseases

Status of Manuscript: [Put an x in one of the options below, delete this]
__X__ Prepared for submission to a peer-reviewed journal
_____ Officially submitted to a peer-reviewed journal
_____ Accepted by a peer-reviewed journal
____ Published in a peer-reviewed journal

Development of virion entry assay with an Imaging flow cytometer

Authors: James P. Cwick and Matthew P. Taylor

Affiliations: Dept. of Microbiology & Cell Biology, Montana State University

Corresponding Author:
Matthew P. Taylor
mptaylor@montana.edu
406-994-7467

Keywords: Pseudorabies virus, imaging flow cytometer, Superinfection exclusion, fluorescent protein, fixation

Abstract

The development of viral entry assays is an important means to study a vital aspect of the virus life cycle. Although there are many viral entry assays, few assays fail to combine both aspects of visual acuity of the sample and high output for population studies. Although a flow cytometer and microscopy have separately contributed to the development of various viral entry assays, the imaging flow cytometer has the means to greatly impact the field of viral entry. In this article, we evaluated virion entry of pseudorabies virus (PRV) through direct comparison of images between an imaging flow cytometer and direct microscopic examination. Our method utilized a superinfection exclusion model, since SIE events can have rare representation in population studies and need to be visually confirmed. Results from this present possible alternative means of studying viral superinfection and entry events.

We observed that internalized virion particles are more difficult to detect than surface associated virions due to reduced fluorescence. Additionally, an imaging flow cytometer has similar images for a microscope given similar conditions of infection, with the improved bonus of quantitative data for whole cell population studies. These results demonstrate that an imaging flow cytometer demonstrates the capability to provide an alternative means of population studies.

Introduction

A viral infection typically involves the steps of attachment, entry and/or fusion, trafficking, viral genome transcription and translation, and egress of virions. Knowing these steps of a virus' life cycle remain paramount for understanding the course of infection and the development of antiviral compounds that inhibit those steps. To this end, it is important to develop assays that measure and analyze these steps. Arguably, the steps of viral attachment and entry are of upmost importance since failure of entry precludes establishment of viral infection. Due to both the complexity and variety of virus life cycles, many types of viral entry assays have been developed that typically utilize either biochemical or visual aspects of quantification.

Biochemical assays for viral entry detect components of virions to quantify the extent of entry. These assays typically utilized forms of radio-labeling, biochemical reactions, or western blot detection. Radiolabeling has been used both to directly label virion parts as a proxy for entry or as a reporter for viral activity (Bray et al., 2010). Although there is still research that employs it as a means of treating or tracking infection, it is rarely used due to enhanced health and safety risks when compared to other biochemical entry assays (Neumaier et al., 2020). As a result, other forms of biochemical assays have been developed to analyze specific viral products. In the case of viral attachment and entry, most assays rely on some sort of reporter that can be them assessed via fluorescence or luminescence detection. One possible means is analysis through enzymatic activity like in the beta-lactamase assay. Originally developed to study bacteria fission, this has been adopted for viral fusion protocols (Da Silva Santos et al., 2016; D. M. Jones & Padilla-Parra, 2016; Tscherne et al., 2010). In this method, a virus containing the beta-lactamase enzyme is delivered into a cell loaded with a reporter substrate, CCF2-AM. Successful delivery can be

measured through a shift in internal FRET fluorescence from the dual-fluorophore compound. However, several caveats must be considered for the implementation of this assay. Usually, viruses must be primed for entry on the cell surface, often by reduced temperature and concentration steps for maximal detection of fluorescence output. This step reduces the random stochastic means of virus attachment and fusion, achieving maximal viral entry and change of fluorescence. Modification of any of these steps results in decreased efficiency and detection of BLAM (D. M. Jones & Padilla-Parra, 2016). Application of additional chemicals like probenecid can further assist in the detection of fluorescence changes associated with virion entry.

Another biochemical assay utilizes antibody conjugate binding with the use of fluorescein isothiocyanate (FITC). FITC is an excellent indicator due to its low nonspecific binding of biological tissues and relatively high fluorescence with small quantities. However, its properties of photo-instability, overlap of cell autofluorescence, and sensitivity to pH changes can present challenges to interpretation and limitations in some biological studies (Clark Brelje et al., 2002; J. W. Harvey, 2012). Its use in flow cytometry has established many conventional uses for biological applications of immunology and cellular component interactions. However, it has also been implemented for many types of viruses for viral entry assays (K.-J. Huang et al., 2006; Nichols et al., 1993; van Iwaarden et al., 1991). In nearly all these assays, the FITC is conjugated onto external virion proteins. Fusion causes a signal quench that results in the loss of resonance energy transfer (Nichols et al., 1993). Although this represents a great way to study large events (ie population studies), it lacks the visual confirmation for individual events and usually represents endpoint results. Another variation of this is fluorescence-assisted sorting

(FACS) that outputs change in fluorescence. To represent biological samples in real time tracking with visual cues, microscopy remains the best means to evaluate changes in localization of sub-cellular structures.

The best representation for viral entry assays utilizes fluorescent proteins that associate with specific viral proteins. In the case of alphaherpesviruses, this has been immensely helpful in models studying virion trafficking and entry in neurons and cell culture (Antinone et al., 2006; Banfield et al., 2003; de Oliveira et al., 2008; del Rio et al., 2005; Lynn W. Enquist & Card, 2003; Etienne, L.; Poorval, J.; Dingle, L.; Huang, E.; Grzesik, P.; Desai, 2017; Gallagher et al., 2014; Hamilton, 2009; Hogue et al., 2015; Ian B. Hogue, Jolie Jean, Andrew D. Esteves, Nikhila S. Tanneti, Julian Scherer, 2018; Law et al., 2018; Lyman et al., 2009; Nishi & Saigo, 2007; Sanfilippo et al., 2004; Sloutskin et al., 2014; Sugimoto et al., 2008). In each study, virions incorporate a fluorescent protein(s) to track virions during specific phases of their infection. Most of the fusions genes replace or insert in non-essential viral genes like gG in pseudorabies virus (PRV) (Hogue et al., 2015). However, a wide library now exists for both PRV and Herpes Simplex Virus type 1 with varying fluorescent tags of important viral proteins (Pomeranz et al., 2005). Although this is great for studying live processes of viral infection, microscopic images focus on single cell/neuron dynamics that lack the whole picture for population dynamics. Although multiple images could be compared for a representative population of results, this may contain inherent biases based upon sampling.

The means of studying virus entry and fusion makes studying conditions like superinfection exclusion (SIE) difficult. Studies involving SIE note the complexity that surrounds it. SIE can affect different steps of viral infection that are unique to each virus.

Additionally, some of these SIE events were rare and hard to define without given large population samples (Folimonova, 2012). Without the combination of visual confirmation of SIE exclusion and high output of events, wildly biased interpretations may arise due to selection bias of microscopy samples or incorrect assumptions about population dynamics.

PRV has long been shown as an excellent model for both *in vitro* and *in vivo* experiments involving *Alphaherpesvirinae* (Brittle et al., 2004; Ch'ng & Enquist, 2005; Chen et al., 2019; L. W. Enquist, 2002; Osorio & Rock, 1992; Pomeranz et al., 2005; Ren et al., 2021). Typically, PRV tagged with fluorescent proteins utilize its neurological tracing properties to better analyze pathology associated with its viral replication and transmission. Experiments involving cell chamber cultures with fluorescent microscopy have underlined processes associated with the rate of transmission during infection and spread, while *in vivo* cultures of murine models demonstrate its pathological presentation (Brittle et al., 2004; Pomeranz et al., 2005; M. P. Taylor et al., 2012; Matthew P. Taylor & Enquist, 2015). However, superinfection exclusion is still understudied in this field.

Although some research exists in literature of SIE in alphaherpesviruses, most examples almost exclusively study under conditions of single cell analysis and not through population (G Campadelli-Fiume et al., 1990; Criddle et al., 2016). Few technologies originally existed to have the discriminatory power to not only sort and count cells but also concordantly group represented images. For example, flow cytometry has been utilized in past experiments to detect internalized virions of *alphaherpesvirinae* through fluorescence shifts. This provided an excellent means of studying a large sample size but lacked the visual representation of each sample within a given group. However, virion entry in microscopy readily depicts internalized virions within a

localized field. Although multiple fields could be utilized as a means of possibly studying the whole population, it still lacks the large sample size that could be collected from technologies like a flow cytometer (Loret et al., 2012; Matthew P. Taylor & Enquist, 2015). Although many assays exist to discriminate by fluorescence like FISH and fusion proteins, having both a large sample size and representative visual images within the same methodology would standardize data collection and provide a powerful means of study.

The recent technological invention of an imaging flow cytometer has to potential to overcome these deficiencies. The imaging flow cytometer has the unique capabilities to combine aspects of traditional flow cytometry with microscopic visualization. Although many people have utilized it in studying microorganisms the size of bacteria and whole cell studies, few people have attempted to utilize it in experiments studying viral entry (Doan et al., 2018). The closest uses of this technology for viral studies involve the use of nanoparticles for vaccine development (van der Pol et al., 2018; Vlasak et al., 2016). Due to the relative size of alphaherpesviruses, it is theoretically possible to examine viral entry, now in the context of a large population.

This article will directly compare results of the imaging flow cytometer and fluorescent microscopy to study alphaherpesvirus virion entry using the model system of PRV. The data from this study indicates the effect of fixation on internalized virions and the conditions of SIE and direct infection for visualization of virion entry assays. In this way, we provide novel means to study SIE through our PRV model of using imaging flow cytometer.

Materials and Methods

Cells and viruses

Porcine kidney epithelial cells (PK15), human keratinocyte cells (HaCat), and green African kidney Vero cell lines were maintained in Dulbecco's modified Eagle's medium (DMEM) supplemented with 10% (vol/vol) fetal bovine serum (FBS) and 1% (vol/vol) penicillin-streptomycin. PRV stocks and plaque assays were performed on PK15 cells as previously described (del Rio et al., 2002).

All fluorescent PRV recombinants were derived from a PRV Becker background. PRV GS443 is a kind gift from Dr. Greg Smith and the Enquist Lab. PRV GS443 contains an insertion of eGFP fusion at VP26 (Antinone et al., 2006).

All stocks of fluorescent viruses were confirmed by fluorescence microscopy of plaques to ensure maintenance and fidelity of their fluorescent profiles. Experiments requiring fluorescent virions utilized fresh viral supernatants. Stocks were initiated with an MOI 10 infection of a 10 cm dish of support cells. At 24 hours post-infection, media was collected and subjected to low-speed centrifugation to remove cell debris and cells. Media was supplemented with 20mM HEPES pH 7.0 (1:50 from a 1M stock). These cell-free viral stocks of PRVGS442 were stored in 500 mL aliquots to avoid degradation of fluorescence caused from freeze/thaw cycles. These stocks were used in virion counting experiments.

Microscopy

Images were acquired on a Nikon Ti-Eclipse (Nikon Instruments, Melville, NY) inverted microscope equipped with a SpectraX LED (Lumencor, Beaverton, OR) excitation

module and fast-switching emission filter wheels (Prior Scientific, Rockland, MA). Fluorescence imaging used paired excitation/emission filters and dichroic mirrors for eGFP (Chroma Technology Corp., Bellow Falls, VT). Brightfield images utilized a Plan Fluor 20 phase contrast (Ph) objective and an iXon 896 EM-CCD (Andor Technology Ltd., Belfast, Northern Ireland) camera using NIS Elements software. Acquisition of fluorescent virions utilized a CFI Plan Apochromat Lambda 60x and 100x oil immersion objective to visualize individual virion localization within infected cells. Infected cells were imaged at the time post-infection indicated in each figure legend, dependent on experimental design. Experiments were tested at least twice with multiple fields acquired for each condition of the experiment.

Samples run on the Imaging flow cytometer were imaged on the Lab-Tek II chambered coverglass. After acquisition on the imaging flow cytometer, samples were immediately run on the fluorescent microscope and acquired with less than 100 milliseconds exposure for each channel to avoid photobleaching.

Imaging flow cytometry

Imaging flow cytometry was taken using an ISX Mark II (MilliporeSigma, Seattle, WA) dual CCD camera system equipped with the MultiMag option (20x, 40x, and 60x magnification) and lasers of 405, 488, 561, 592, 642 nm. Channel 1 was set to capture brightfield images of cells, while channel 2 was set to excitation with the 488 nm laser. Other channels were disabled to avoid overexposure of samples. Samples were collected with scatter, brightfield, and 488 nm laser. For all samples, a total of 10,000 events were collected at 60x magnification using the program INSPIRE (MilliporeSigma, Seattle, WA) offered for data acquisition with the machine.

Initial samples were collected with DRAQ5 for nuclear staining with the 642 nm laser (as shown in Figure 3.2) to represent the nuclear region of the captured cell. Later, DRAQ5 staining was forgone for direct comparisons between fluorescent microscopy and imaging flow cytometry. Data was saved as raw image files and then analyzed with IDEAS software version 6.2.

Virion visualization

Fluorescent virion assemblies were imaged by epifluorescent microscope and photomicrographs were taken with 60x magnification objectives. Images were acquired to demonstrate representative images of conditions described in the experiments for infected cells. The following conditions were used for experimental procedures: direct infection and SIE. Direct infections were established by the inoculation of gFP-VP26 virions (PRVGS443) PK15 cells, respectively, for a 1-hour duration in a 37˚C incubator. For SIE, cells were initially inoculated for 1 hour at 37˚C with a non-fluorescent PRV wild-type virus. Cells were then washed and maintained for 2 hours at 37˚C. Afterward, they were subsequently infected with GFP-VP26 labeled virions as described for direct infection. After incubation, cells were subsequently infected with GFP-VP26 labeled virions as described for direct infection. One hour after application of fluorescent virions, cells were washed and supplemented with fresh media. Cells were fixed with 2% paraformaldehyde (PFA) to ensure conditions during imaging on either the fluorescent microscope or the imaging flow cytometry.

Results

Fixation affects detectability of internalized capsids

Nearly all samples for flow cytometry require fixation to examine samples. Since

fixation has been known to affect fluorescence (Hogue et al., 2015), various levels of fixation were tested to determine minimal disruption for fluorescence detection of internalized capsids. As shown in Figure 3.1a, fixation does affect the level of fluorescence, which is to be expected due to the changed state caused from cross-linking of fusion protein. However, figure 3.1b compares the relative fluorescence per condition based upon the unfixed infection condition. Although there is a notable decrease in fluorescence, there is still easily discernible capsid structures at the 2-minute mark that became less pronounced at other times points. Therefore, the 2-minute fixation time was utilized as a standard in comparing conditions of direct infection and SIE for future experiments.

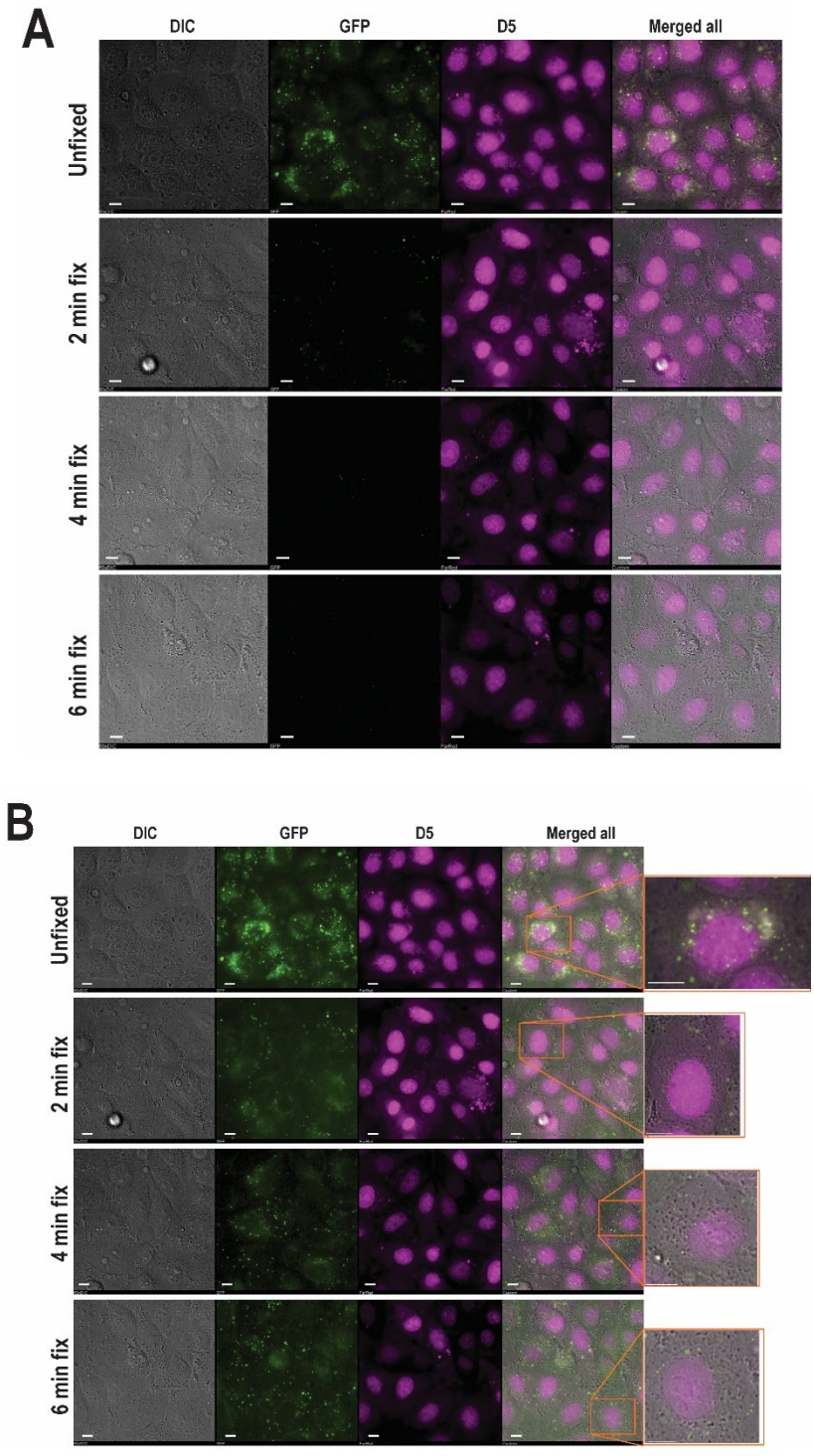
A
DIC
GFP
D5
Merged all
Unfixed
2 min fix
4 min fix
6 min fix
B
DIC
GFP
D5
Merged all
Unfixed
2 min fix
4 min fix
6 min fix

Figure 3.1. Increased fixation time causes decrease in detectability of internalized capsids. In the figure above, fixation with 2% PFA was applied to cells infected with PRV443. The top row indicates the unfixed condition, whereas each consecutive row demonstrates 2 minutes of fixation until 6 minutes. A) Fluorescence of GFP set to unfixed condition. B) Fluorescence of GFP set to view capsids. The insets demonstrated enhanced visualization of single cell. Bar corresponds to 10 microns.

Detecting capsids in whole cell populations for viral infection and SIE of PRVGS443

Although conditions of fixation exhibited a detrimental decrease of fluorescence detection for internalized capsids, quantitative analysis of whole cell populations needed to be coupled with micrograph images to demonstrate the circumstances surrounding SIE. To determine how, an imaging flow cytometer was utilized to couple SIE events with representative images for whole cell population analysis.

To develop a reliable and reproducible method of discerning virion internalization during samples, a mask for the GFP channel was developed for virion collection. A fluorescence threshold was set to limit ambient fluorescence and accurately depict virion particles, as shown in Figure 3.2a. A total of 10,000 events were sampled with three channels to represent images: a brightfield for cell images, a GFP channel to determine virion particles, and a 642 nm laser for nuclear staining of the cell with DRAQ5. Figure 3.2b depicts the imaging flow cytometer data for direct infection of PRVGS443. In this, micrographs of low, medium, and high fluorescence were categorized to demonstrate representative images of the population. Multiple steps of gating occurred to accurately depict representative images for direct infection of PRVGS443. Initial gating for data collection excluded cell debris but included cells based upon molecular size. After data collection, individual samples were then gated based upon their fluorescent levels to represent the population. This took the form of a histogram as represented in figure

3.2b. Results from this process indicated that the “middle” fluorescent profile represents approximately 89% of the given events. The “low” fluorescent profile (undetectable infection) corresponds to about 10%, while the “high” fluorescent profile corresponds to about 1.5% of the events. Given our mask for virion particles, the “middle” fluorescent profile contains images that would be commonly viewed on a microscope, with the other fluorescent profiles corresponding to outliers in microscopy. Although this represents the capability to have fluorescent images of viral entry, a direct comparison between images of an imaging flow cytometer and fluorescent microscope needed to be performed for fidelity of viral representation.

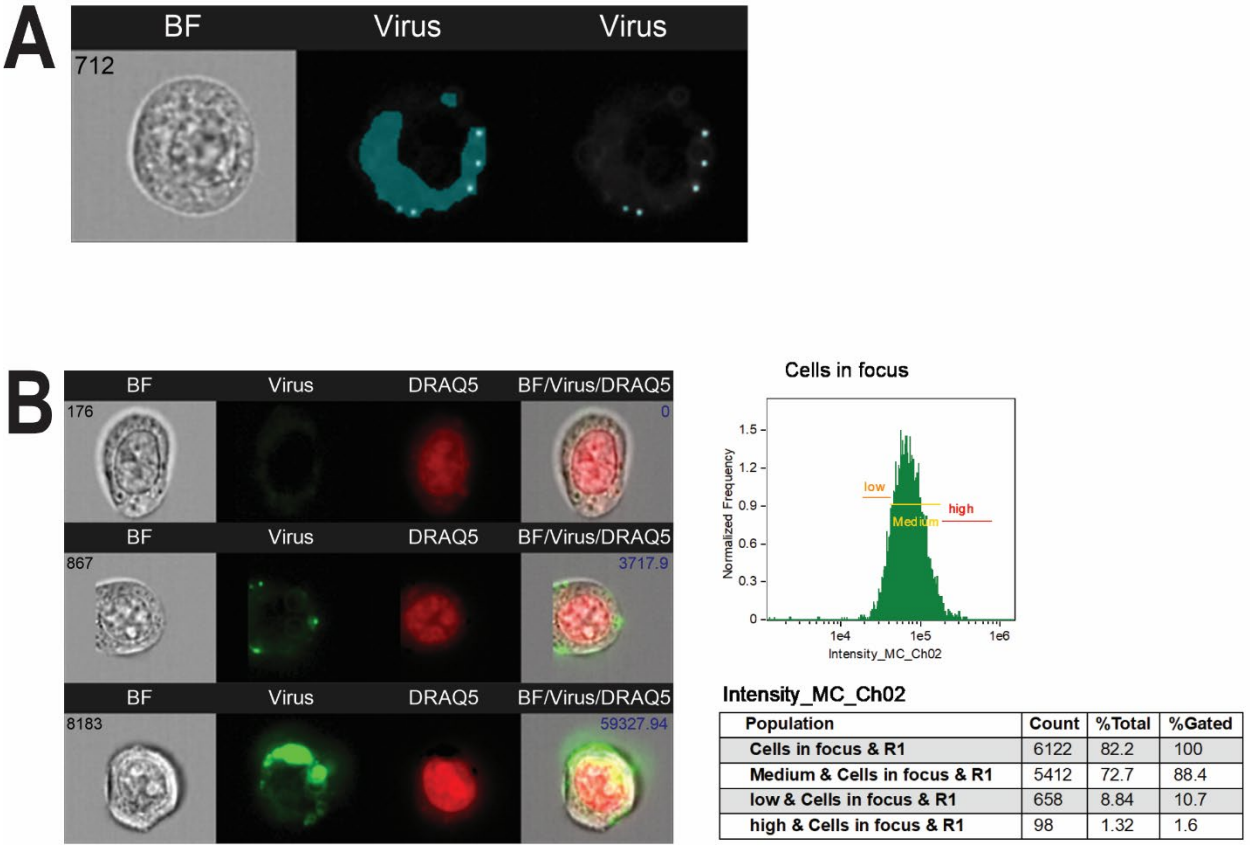

Intensity_MC_Ch02

Population	Count	%Total	%Gated
Cells in focus & R1	6122	82.2	100
Medium & Cells in focus & R1	5412	72.7	88.4
low & Cells in focus & R1	658	8.84	10.7
high & Cells in focus & R1	98	1.32	1.6

Figure 3.2. Image stream depiction of viral infection of PRVGS443. The figure above depicts the process for acquiring data on the Image Stream. A) Depiction of mask utilized to represent virions in direct infection. Fluorescence was set to a minimal for puncta (GFP capsids). B) Images representing gates infection of PRVGS443. Left are the qualitative images representing low (top), medium (middle), and high (bottom) fluorescence for the cell populations. Right is the histogram depicting the gated population with quantitative representation below.

We followed up on this with a direct comparison between micrograph data obtained from a fluorescent microscopy and an imaging flow cytometer. Histogram data corresponds to imaging flow cytometry data only. The micrograph obtained from fluorescent microscope was taken immediately after imaging flow cytometry data collection and is representative of micrographs obtained in that process. Figures 3.3 shows this direct comparison featuring conditions of direct infection (figure 3.3a) and superinfection exclusion (figure 3.3b). In the case

of the imaging flow cytometer, virion particles were similar in the number to fluorescent microscopy without as high of resolution. However, in terms of both the representation, both images seemed similar in terms of virion localization and relative representation of virion particles. However, it is important to note that micrographs obtained from the imaging flow cytometer did not display as many virion particles in comparison to the micrographs from fluorescent microscopy. Although several factors could contribute to this discrepancy, the most likely cause could be the resolving power. Although both images utilized 60x for image acquisition, the fluorescent microscope has a much higher resolving power due to the components of spectra display and cameras present in its hardware. Despite their similar representation of virion particles, the imaging flow cytometer may not have the capacity to measure all virion particles within the sample.

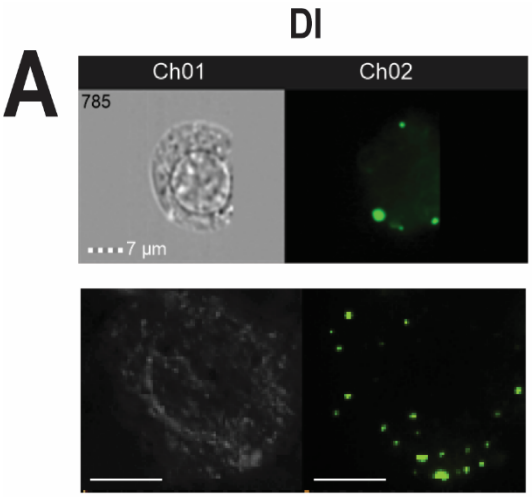

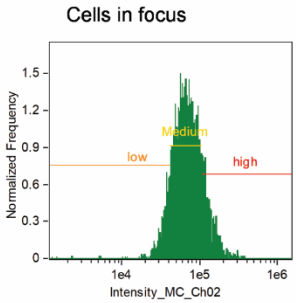

Intensity_MC_Ch02

Population	Count	%Total	%Gated	Median
Cells in focus & R1	6122	82.2	100	68783.88
Medium & Cells in focus & R1	4447	59.7	72.6	65990.62
low & Cells in focus & R1	673	9.04	11	35973.84
high & Cells in focus & R1	980	13.2	16	129286.13

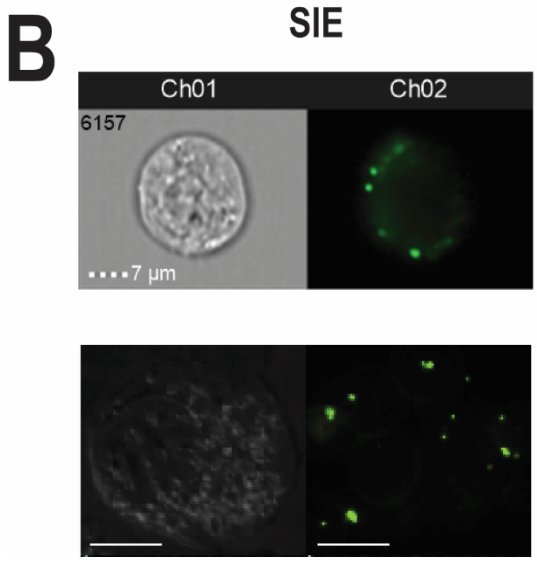

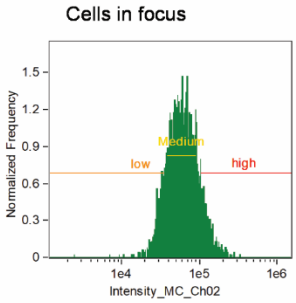

Intensity_MC_Ch02

Population	Count	%Total	%Gated	Median
Cells in focus & R1	4838	80.5	100	59723.35
Medium & Cells in focus & R1	3235	53.8	66.9	58606.18
low & Cells in focus & R1	579	9.64	12	30921.87
high & Cells in focus & R1	593	9.87	12.3	120706.83

Figure 3.3. Image stream comparison to fluorescent microscopy of SIE and DI. The figure above depicts representative images for Imaging flow cytometry and fluorescent microscopy. A) Depiction of direct infection. Top image shows the representative image (medium in the histogram) for flow cytometry while the bottom shows a single cell from fluorescent microscopy. Histogram represents cells in focus sorted by fluorescence intensity. B) Depiction of SIE. Top image shows the representative image (medium in the histogram) for flow cytometry while the bottom shows a single cell from fluorescent microscopy. Histogram represents cells in focus sorted by fluorescence intensity.

Discussion

This study analyzed a means to study viral entry in whole cell populations using PRV as a model. We observed that fixation was able to affect internalized virion particles, resulting in reduced fluorescence. Although reduced fluorescence was to be expected, internalized virions were not expected to have reduction of fluorescence. Past literature has demonstrated that virion particles are susceptible under fixation conditions due to cross-linked protein bridges (Hogue et al., 2015; Joosen et al., 2014). However, this was usually connected to overall fluorescence and not the actual detection of internalized virion particles.

Additionally, this study presents a novel means of studying viral entry in the context of population. This was shown through a PRV model of virion entry under conditions of direct infection and SIE. As shown in Figure 3.3, the images between the imaging flow cytometer and the fluorescent microscope demonstrate similar depictions of virion particle presentation.

Although the representation and localization virion particles were similar for both conditions, the number of virion particles differed between the imaging flow cytometer and fluorescent microscope. Although this could mostly be due to relative sampling received during the microscope, it is important to note that this could also be due to the higher discriminatory power of camera offered through the fluorescent microscope. As such, the imaging flow cytometer could provide a powerful means of population studies; however, it should be further validated with additional experiments.

Overall, this study provides new insights not only into SIE conditions using PRV as a model but also demonstrates the novel used of imaging flow cytometry for population studies. Further work will be needed to develop secondary support of population studies of SIE not only

for *alphaherpesvirinae* but also other studies involving SIE.

CHAPTER FOUR

CELLULAR FACTORS AND CHEMICAL INTERVENTION TO UNDERSTAND ALPHAHERPESVIRUS SIE

Nearly all documented cases of SIE for viruses are understood through the action of viral effector proteins. Viral mechanisms of intervention include RNA interference, protein occlusion of viral attachment and entry, or secondary viral products that trigger host antiviral responses (Biryukov & Meyers, 2018; Folimonova, 2012; Remeijer et al., 2002; Zou et al., 2009). While SIE is dependent upon viral factors, these mechanisms often rely on cellular responses that are equally necessary. Most of the documented cases of SIE for viruses heavily interact with cellular process for entry and trafficking of the virus to the nucleus. In the case of alphaherpesviruses, potentially strong targets that could involve cellular factors include surface cellular proteins for virion attachment and binding, proteins responsible for virion fusion and entry, proteasomal activity on endosomal compartments formed after endocytosis of virions, and microtubule trafficking of the virus to the nucleus. To understand the role or importance of these disparate pathways, we utilized chemical or genetic interventions to determine their effect on early SIE of alphaherpesviruses.

Cellular Factors

Heparin

It is well documented that alphaherpesviruses can alter the surface presentation of cellular receptors. Exposure of nectin-1 at the cell surface decreases after infection of alphaherpesviruses, while the other viral receptors can become occluded through this process

(Deschamps et al., 2017b; Kopp et al., 2014; Thier et al., 2017; Wang et al., 2019). Although the mechanism for this occlusion is not completely defined, interference with surface receptors prevent subsequent virion entry and antiviral signaling within the host cell. To understand the role of surface receptor presentation on virion attachment during SIE, we introduced heparin as an intervention in our experimental model for early SIE. Although heparin was originally identified as an anticoagulant for thrombosis, it has since been demonstrated to have many anti-inflammatory and antiviral properties through its interaction with cytokines and receptors (Seffer et al., 2021). In the case of alphaherpesviruses, heparin was discovered to inhibit viral infection without inactivating the virions (J. & Sidney, 1964). Since this discovery, experiments detailing this mechanism have determined that heparin mimics the active domain of heparan sulfate receptors (3-OS HS) on the cellular surface to occlude entry of virions (Copeland et al., 2008; Seffer et al., 2021). However, there is mixed results as what specific viral protein is responsible for this interaction (Foster et al., 2001; Rux et al., 2002). Additionally, heparin experiments have demonstrated that HSV-1 infection is more susceptible to heparin than PRV infection, with decreased plaques and titers (Copeland et al., 2008; Sawitzky et al., 1990). Taking this into consideration, we applied heparin to our early fluorescent reporter model to evaluate whether heparin can influence early SIE. As shown in figure 4.1, our PRV model utilized a primary infection of PRV289 expressing a Turq2-NLS fluorescent protein, which was then removed and washed 1 hour post inoculation. Then, wells were treated with heparin at concentrations of 5-50 µg/mL. Subsequently, infected cells were washed and subjected to secondary infection with PRV287 expressing an eYFP-NLS fluorescent protein at 2 hours post initial inoculation. This method was similarly applied to our HSV model with the utilization of HSV-1 MT01 featuring a

Turq2-NLS fluorescent protein as the primary virus and HSV-1 OK12 with an eYFP-NLS fluorescent protein as the secondary virus.

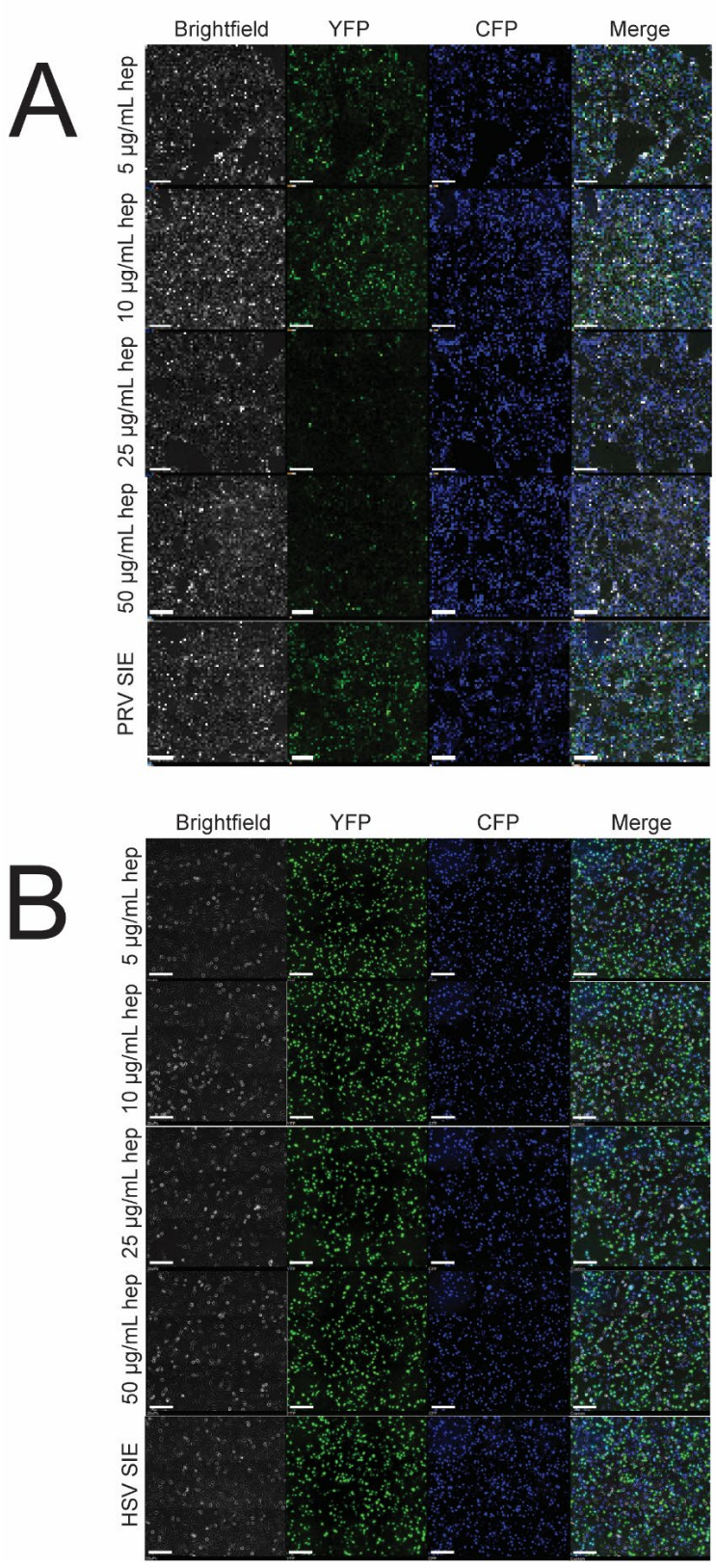
A
Brightfield
YFP
CFP
Merge
5 µg/mL hep
10 µg/mL hep
25 µg/mL hep
50 µg/mL hep
PRV SIE
B
Brightfield
YFP
CFP
Merge
5 µg/mL hep
10 µg/mL hep
25 µg/mL hep
50 µg/mL hep
HSV SIE

Figure 4.1. Heparin affects SIE for PRV but not HSV. This model used a blue, fluorescent virus as the primary virus and a yfp (green) fluorescent virus as a secondary. Conditions were set up as the reporter SIE model both the control and heparin (hep) treatment. Heparin treatment occurred between application of the primary virus and application of the secondary virus in doses of 5-50 micrograms per mL. A represents results for PRV SIE and B represents results for HSV SIE. The scale bars correspond to 200 micrometers.

As shown in Figure 4.1, treatment with heparin at high concentrations of greater than 25 μg/mL seemed to enhance PRV SIE, as shown with the further decrease of secondary virus in comparison with the PRV SIE control. Low concentrations seem to suppress SIE, nearly restoring fluorescence as if were a direct infection. However, such results were not mirrored in the case of HSV-1. No matter the concentration, heparin seemed to have little effect on HSV-1 SIE with neither suppression nor enhancement. In the context of data from chapter 2, heparin with its mimicry of cellular receptors causes occlusion of virions in the supernatant not engaged with cellular receptors. For PRV SIE, this would have synergistic effect and prevent further entry of viruses, which would explain why there was an enhanced exclusion for secondary viruses. This further validates our model that PRV SIE inhibits the step of virion fusion and entry. For HSV-1 SIE, one possible explanation for a lack of effect from heparin is that heparin's efficacy occurs too late within the process of HSV-1 SIE. Since heparin mimics cellular receptors for virion occlusion, the post-entry regulation of SIE by HSV-1 would avoid the influence of heparin.

Overall, data from heparin seems to further validate that PRV SIE operates at virion entry/fusion step, while HSV-1 SIE operates in a post-entry manner.

Fusion Proteins and Proteasomes

Alphaherpesviruses use different pathways for virion entry depending upon environmental stimuli and the host cell. One pathway involves the virion triggering fusion at the plasma membrane, allowing capsid delivery directly into the cytosol. In contrast, an endocytic pathway uses a pH-independent method of fusion of the viral envelope inside the endosome and capsid release into the cytosol. The direct fusion method follows the conventional means of viral attachment and entry for alphaherpesviruses. As described earlier in chapter 1 for the life cycle of alphaherpesviruses, alphaherpesviruses utilize gB and gC for initial attachment and binding of the virion to the cell. Then, gD binds to a cellular receptor like necin-1, heparan sulfate, or HVEM and initiates a fusion complex of gB, gH, and gL to facilitate entry (Agelidis & Shukla, 2015; Clarke, 2016; Connolly et al., 2011; Linehan et al., 2004). Direct fusion is commonly used in many cells types including neurons and Vero cells, while the endocytic pathway is not (Nicola & Straus, 2004; Nicola et al., 2005; Rahn et al., 2011; Tatiana et al., 2004). Direct fusion utilizes specific viral proteins (aforementioned in the section of alphaherpesvirus life cycle) to directly bind and deposit the capsid in the cytosol. However, the endocytosis pathway is different with a few key aspects. This pathway is mediated by clathrin pits and may occur in a pH-dependent manner. The uptake of the virion utilizes massive cytoskeletal rearrangement and Rho proteins in conjunction with these pits to phagocytose the virion. After sequestration in the endosomal compartment, pH acidification occurs and allows the virion to fuse with the endosome and release into the cytosol for viral trafficking to the nucleus (Agelidis & Shukla, 2015; Clement et al., 2006b; Copeland et al., 2008; Madavaraju et al., 2021; Nicola & Straus, 2004; Nicola et al.,

2005; Rahn et al., 2011; Tatiana et al., 2004). In terms of studying important cellular processes of entry involved in early SIE, some of the key factors between both pathways of entry include the clathrin-pits during direct fusion and the Rho proteins and endosomal compartment during the endocytosis pathway. As such, a variety of chemical molecules were used to target these key players: ATP-gamma S for inhibiting Rho function, clathrin-deficient cells, and bortezomib to inhibit endosomal release.

ATP-gamma S is a unique chemical that serves as an analogue of ATP. Upon its introduction, ATP-gamma S competes with ATP but is unable to be hydrolyzed. ATP binding proteins become "locked" and lose function (Allen et al., 2005). Application of ATP-gamma S occurred before application of the secondary virus in our SIE model to maximally arrest Rho protein functions or other ATP-hydrolysis dependent processes.

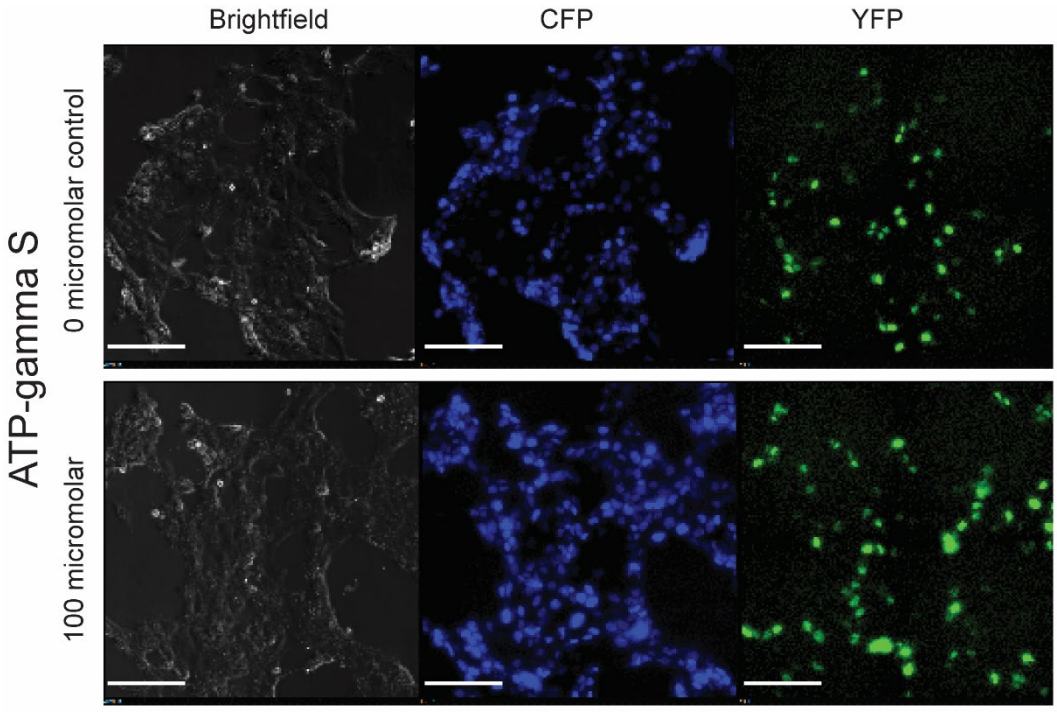

Figure 4.2. ATP-gamma S affects PRV SIE. This model used a blue, fluorescent virus as the primary virus and a yfp (green) fluorescent virus as a secondary. Conditions were set up as the reporter SIE model both the control and ATP-gamma S treatment. ATP-gamma S treatment with a 100 micromolar concentration occurred between application of the primary virus and application of the secondary. The scale bars correspond to 200 micrometers.

As shown in figure 4.2, PRV SIE with ATP-gamma S exhibits a minor increase of fluorescence but does not seem to significantly affect the condition of SIE. Since direct fusion and possible endocytic pathways could be present in this experimental model, data from that is inconclusive about which pathway PRV SIE could affect. Since ATP-gamma S is a chemical that will affect a broad range of cellular activities, other G proteins would be affected in addition to Rho proteins. As such, data from this is inconclusive about the role (if any) of Rho protein involvement in PRV SIE.

For clathrin-inhibition, our lab utilized a CRISPR-knockout cell line called AP1G2 that truncated functional clathrin protein formation. When applied to our PRV SIE model, results indicated a minor effect of PRV SIE when compared to its parental cell line. As shown in figure 4.3, the mutated cell line exhibited an overall decrease in viral infection of both primary and secondary infection of PRV.

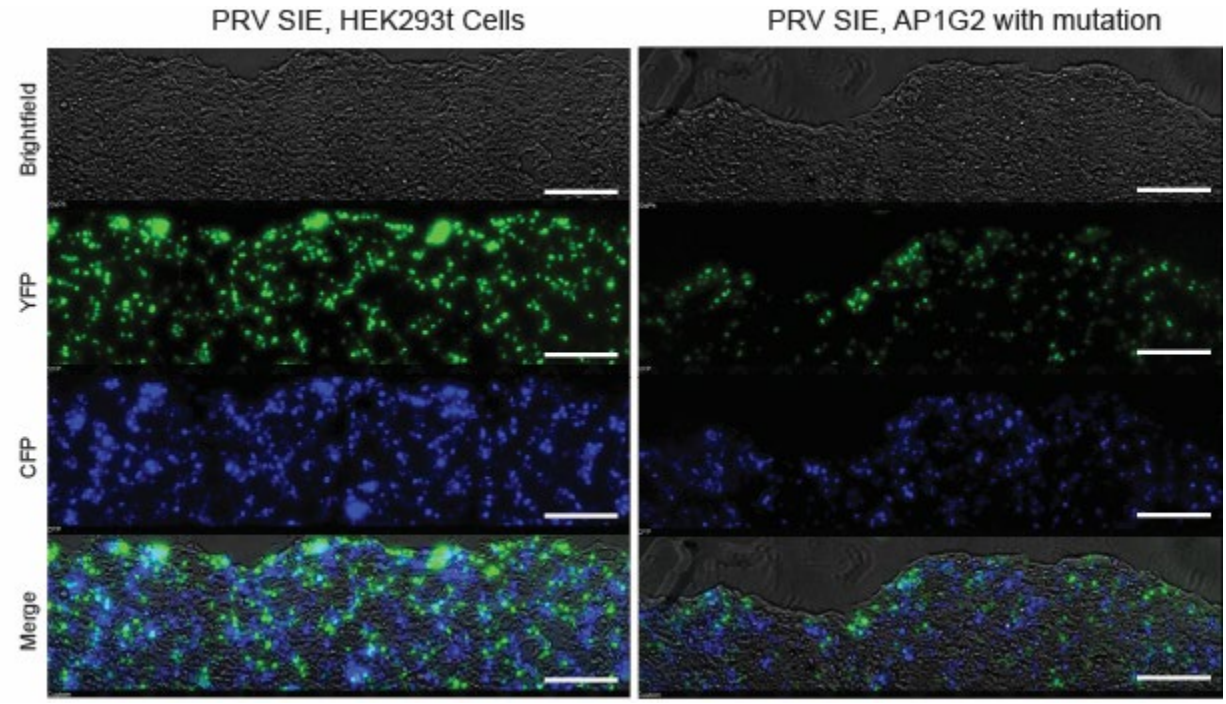

Figure 4.3. Clathrin inhibition causes a decrease in both infection and fluorescence for secondary infection. Conditions were set up as the reporter SIE model both the control and cell lines. HEK293T cells is the parental cell line of the AP1G2 knockout cell line, which features a mutation that causes disruption of clathrin pit formation. The scale bars correspond to 200 micrometers.

This is to be expected since PRV direct infusion pathway would be inhibited, mainly relying upon alternative means of entry. However, there was a significant decrease in fluorescence and infection of the secondary virus, indicating that clathrin could influence secondary infection. It is important to note that Hek293T cell lines are one of the cell lines that seem to be more likely to utilize the endocytosis pathway rather than direct fusion of alphaherpesviruses due to the lack of cellular surface receptors primarily responsible for direct fusion. As such, this data seems to exemplify the fact that PRV SIE might be dependent upon endocytic processes, although future tests would be needed to confirm this.

For endosomal compartments, our lab utilized chemical intervention from bortezomib.

Bortezomib is a proteosome inhibitor like MG132, which are designed to block the degradative activity of cellular proteosomes (Schneider et al., 2019). In addition to its primary function of blocking degradation, these class of drugs are also able to impair HSV-1 transport to the nucleus, stabilize nuclear domain 10 protein complexes, prevent promyelocytic leukemia (PML) protein degradation, and prevent lytic replication (Delboy et al., 2008; Everett et al., 1998; Everett & Maul, 1994; Maul et al., 1993; Schneider et al., 2019). However, its use for this experiment will be dependent upon its anti-degradative properties. In this experiment, we applied bortezomib at 500 nM concentration continuously with the secondary inoculation of HSV mScarlet protein-NLS. Using this fluorescent reporter model, we would determine if a post-entry process like bortezomib would affect HSV SIE.

As shown in figure 4.4, there was a decrease in fluorescence for the primary virus of HSV MT01 (Turq-2 NLS) and an increase in fluorescence for the secondary virus of HSV mScarlet (RFP-NLS) during application of bortezomib. This is interesting to note, since blocking proteasome activity allows cellular proteins like PML to repress HSV replication and infection. This explains the decrease in fluorescence for the primary virus but not necessarily the increase in fluorescence for the secondary virus. It appears that inhibition of proteasome activity causes suppression of HSV SIE, as shown with the increase of fluorescence for the secondary virus. This could be some sort of interplay between viral proteins that allows more progeny to be produced without degradation caused from cellular proteins. However, without protein confirmation or a targeted viral protein, this is hard to follow up on.

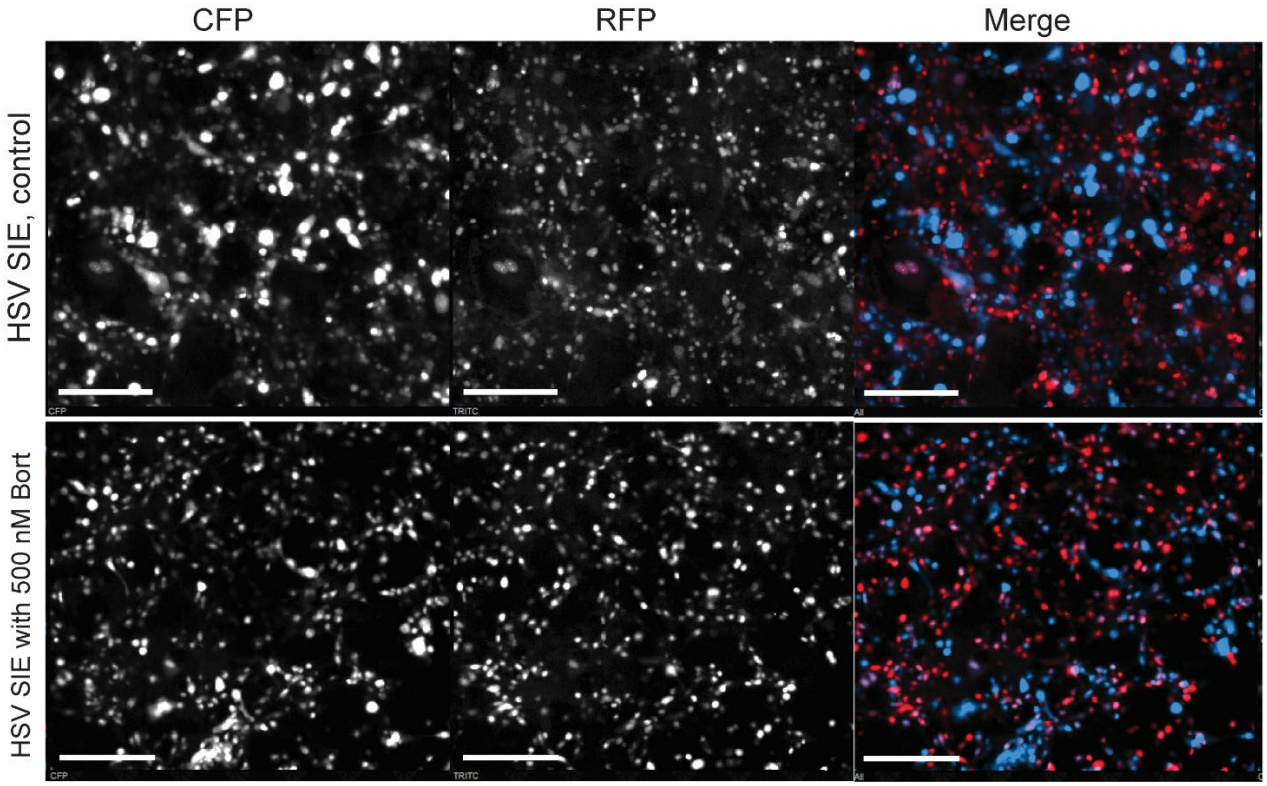

Figure 4.4. Bortezomib suppresses HSV SIE. Conditions were set up as the reporter SIE model using a Turq-2 NLS (CFP) as a primary virus while a secondary virus used a mScarlet (RFP). The scale bars correspond to 200 micrometers.
Bortezomib treatment occurred after primary virus inoculation and continuously through the rest of the experiment. Coinfection control taken 1 hpi, while other conditions were taken 6 hpi.

Overall, these results of fusion protein and proteosome disruptions with chemical intervention seem to indicate that most cellular processes had minimal effect on SIE for HSV-1 and PRV. However, heparin disruption for PRV SIE and bortezomib disruption for HSV SIE seemed to be possible targets for further exploration and support of our bifurcated modeling of SIE control for PRV and HSV-1.

Cytoskeletal Arrangement During Alphaherpesvirus SIE

Alphaherpesviruses infection induces cytoskeletal rearrangement to better support viral replication. In terms of entry and fusion, it has been previously described that microtubule formation and rearrangement assist in virus entry of the endocytosis pathway (Madavaraju et al., 2021; Rahn et al., 2011). However, additional cytoskeletal arrangement occurs that assists in virion transport to the nucleus or the penultimate step of viral egress and transmission to other cells. Viral proteins VP22, gE, gI, and U_S9 have all been implicated for direct involvement of protein association of cytoskeletal rearrangement (Everett et al., 1998; Kotsakis et al., 2001; Maul et al., 1993). In most cases, alphaherpesviruses directly bind to dynein and kinesin motors on the plus-end of microtubules for transport, while dynactin-1 assists in the initial entrapment of alphaherpesviruses (Naghavi & Walsh, 2017; Yedowitz et al., 2005). Additionally, actin filaments are typically presented in bundles or networks, as in stress fibers and filopodia. Formation of these is regulated through Rho GTPases. Alphaherpesviruses utilize U_S3 to disassembly these stress fiber bundles. Actin rearrangement also occurs inside the nucleus with actin motor myosin V, largely to support viral replication (Yedowitz et al., 2005). However, this mechanism of this is still largely unknown. With such expansive manipulation of cytoskeletal elements, we wanted to examine if there were possible cytoskeletal differences during SIE for alphaherpesviruses.

Using our capsid trafficking model, we primary infected with a non-fluorescent virus and then secondarily infected with PRV180, an RFP expressing virus for VP26. Afterwards, cells were fixed and then counterstained with Hoescht to label nuclei and phalloidin for actin

filaments. As shown in figure 4.5, infection with PRV caused disruption of the actin filaments and loss of stress fibers. With regards to differences of actin arrangement between SIE and direct infection, initial results seem to indicate there are no significant differences. Most of the actin rearrangement described in literature occurs hours past the observable time point for our early SIE condition. Without secondary tests to validate actin disruption of possible motor proteins, results from this remain inconclusive.

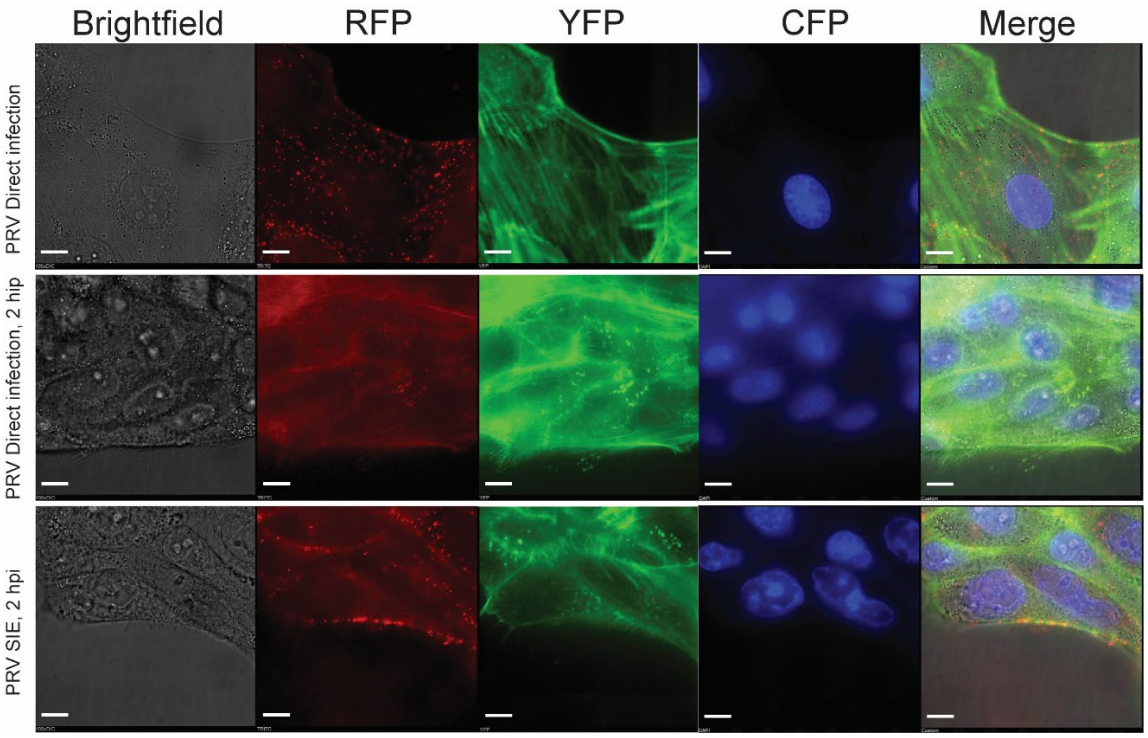

Figure 4.5. Actin arrangement during SIE of PRV infection. PK15 cells were infected with fluorescent PRV 180, fixed and then stained with HOESCHT for nuclear region and phalloidin for actin filament presentation. Experiments were done in triplicate and at an MOI of 100. PRV direct infection with PRV 180 and PRV Direct Infection at 2 hpi serve as controls. Scale bar represents 10 micrometers.

Conclusion

Overall, initial results for most cellular factors influencing early SIE for alphaherpesviruses seem to be either minor or inconclusive based on current data. Although the studies of heparin and bortezomib seem to validate the proposed current models of SIE for PRV and HSV-1, the other experiments seem to have no significant differences between SIE and direct infection for PRV in the context of disrupting Rho proteins, clathrin, and actin arrangement. However, most of these experiments were performed without the context received from Chapter 2, that alphaherpesviruses might exhibit different forms of SIE. As such, each of these experiments will need to be performed in the context of both PRV and HSV-1 as well to better determine the effect of cellular factors that could influence early SIE of alphaherpesviruses.

CHAPTER FIVE

CONCLUSIONS AND FUTURE STUDIES

Conclusions

Despite the relatively innocuous presentation for most cases, alphaherpesviruses represents a significant burden on global health and agriculture. Although alleviation of symptoms and disease can be curtailed with acyclovir, the rise of acyclovir-resistant strains and high recombination rate in circulating populations of alphaherpesviruses demands attention for the development of anti-viral therapies. Although these strains are being monitored, few studies have delved into the mechanisms contributing to the regulation of coinfection. This dissertation presents new methodologies and analysis of alphaherpesvirus entry to understand the mechanism underlying SIE and limitations to coinfection.

In chapter 2, a method was developed to quantifiably measure the differences in virion trafficking between SIE and direct infection conditions. Previous methods of SIE represented more qualitative means of SIE assessment but did not optimize to study how SIE influenced steps between entry and trafficking to the nucleus. This model utilized fluorescence to understand differences in real time for secondary infection.

Using methods described in chapter 2, we investigated how the condition of SIE impacts virion trafficking. These studies compared virion particle localization during conditions of SIE and direct infection, utilizing a 3-D construction from fluorescent z-stack micrographs. These studies quantifiably compared virion trafficking between conditions of SIE and direct infection to determine if there were differences for the disruption of virion trafficking.

As expected of all cases for our established early SIE condition, our condition of direct infection for all alphaherpesviruses exhibited increased virion particles in the nuclear region of the cell and decreased virion particles on the periphery when compared to SIE. This lines up with past experiments and expectations, since SIE excludes entry of the secondary virus and accumulates secondary virion particles on the surface of the cell. However, there was an unexpected difference comparing SIE and direct infection for PRV and HSV-1, resulting in two models of SIE interference for PRV (figure 5.1) and HSV-1 (figure 5.2). While PRV SIE did have significant reduction of intracellularly categorized virion particles to direct infection, HSV-1 did not have any statistical difference between intracellularly categorized virion particles. In the case of PRV, SIE could block attachment or entry of secondary virus, which in turn would cause an overall reduction of entering virion particles. Data collected from live fluorescent microscopy and virion trafficking in chapter 2 seem to learn more towards inhibition of entry/fusion rather than attachment, although more tests are needed to validate those results. Possible steps of inhibition for PRV SIE are summarized in figure 5.1. However, in the case of HSV-1, no statistical difference between intracellularly categorized virions indicate that virions are still entering the cell and not being blocked. This means that some form of post-entry regulation of SIE is occurring. Since regulation of HSV-1 SIE is occurring only a few hours post infection, later steps of genome transcription and translation seem unlikely. If focus was given to modulation of virion trafficking, then inhibition from HSV-1 SIE could be affecting either endosomal release of virions during the endocytic pathway or the release of viral DNA in the nucleus. Figure 5.2 demonstrates some possible places of inhibition for HSV-1 SIE, although more experiments would need to be done to determine the cause of HSV-1 SIE. Other results

determined from chapter 2 that SIE is MOI dependent process that is not affected by cellular receptor occlusion. Comparing analyses between these conditions indicates that early mechanisms of SIE deployed by alphaherpesviruses are a complex network of interactions that affect multiple steps of the viral life cycle.

The work discussed in chapter 3 details our development of a a novel means to compare virion localization through imaging flow cytometry and fluorescent microscopy. This study demonstrated changes to virion distributions can be detected by imaging flow cytometry and fluorescent microscopy. An imaging flow cytometer had adequate viewing capability for population studies that lack the power of the fluorescent microscope. Additionally, fixation minimally affected virion fluorescence of internalized capsids.

Collectively, this data provides a novel means to study SIE of alphaherpesviruses and other viruses. This data ultimately assists in better understanding the complexities surrounding the SIE utilized by alphaherpesvirus. This will contribute to work determining how alphaherpesviruses regulate coinfection that can serve as a foundation for work attempting therapeutic alternatives and the generation of new viral progeny of other herpesviruses.

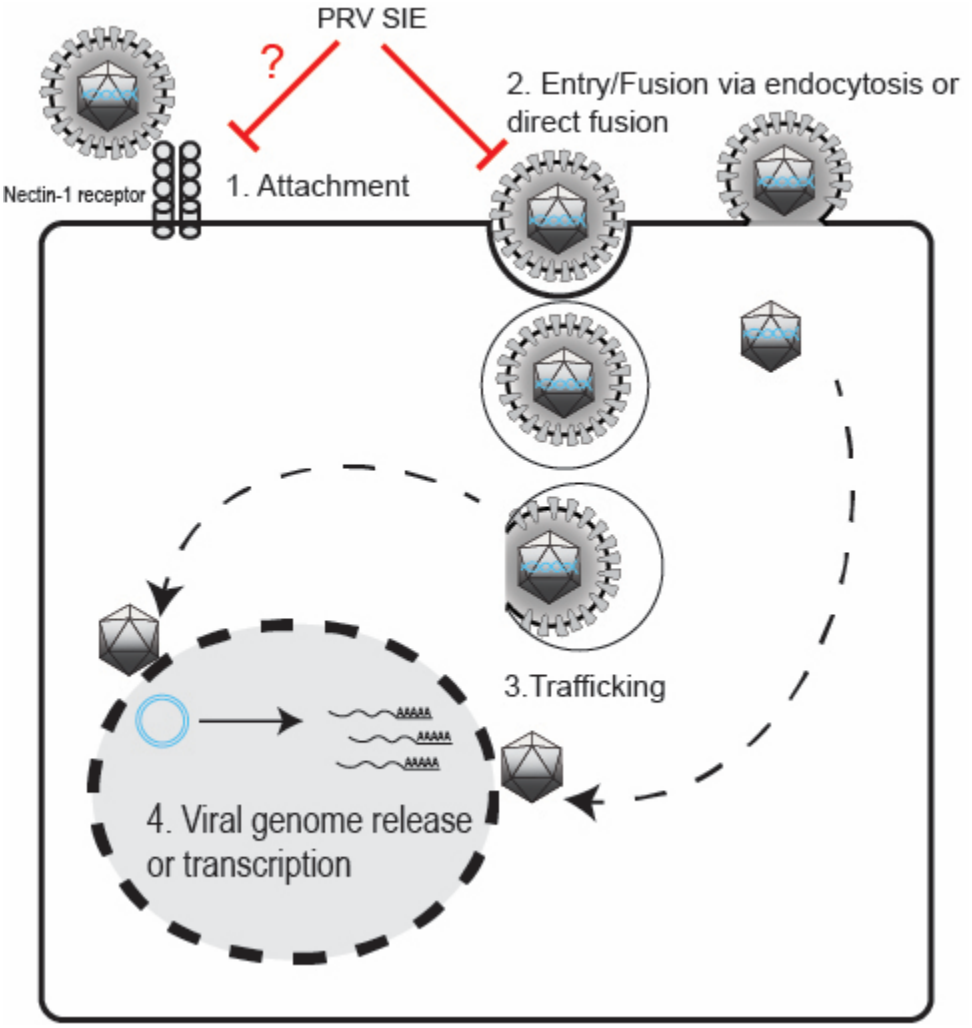

Figure 5.1. Putative model of SIE inhibition of PRV. A schematic representing possible steps affected by PRV SIE. The currently undefined step of viral attachment is possible, while entry/fusion of virion inhibition is confirmed.

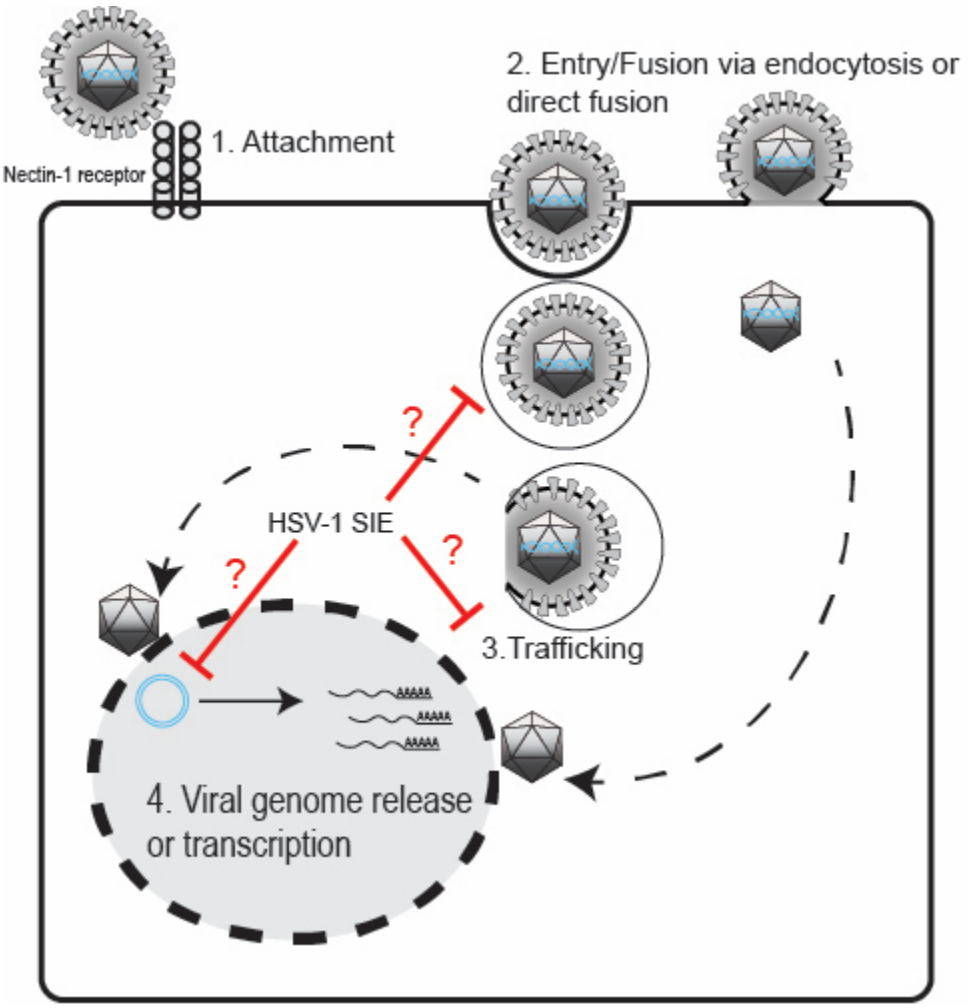

Figure 5.2. Putative model of SIE inhibition of HSV. A schematic representing possible steps affected by HSV SIE. The possible steps of post-entry regulation could include trafficking, endosomal release and DNA release, as shown with the above arrows.

Future Studies

Studies involving superinfection exclusion of continue to be an understudied topic for possible therapeutic development. Currently, a limited number of vaccines have been utilized for some alphaherpesviruses, but none have been implemented for the health sector, not for a lack of targets (Asboe & Pozniak, 2010; Dropulic & Cohen, 2012; Krishnan & Stuart, 2021). Although

some problems may be due to a lack of under stimulation of the immune response due to the type of vaccine, there have been strides for targeted drug intervention for steps of entry and replication for other viruses (Hampson et al., 2021; Laureti et al., 2020). Better understanding of early infection and exclusion of alphaherpesviruses would provide viable targets for the development of prophylactic, antiviral therapy options.

These following experimental goals would facilitate better validation and understanding of early SIE for alphaherpesviruses, improving upon the current model and development of a mechanism:

1. Identify the viral proteins directly responsible for early SIE would need to be determined. A full panel of HSV-1 or PRV mutants lacking early and immediate/early viral proteins would need to be analyzed under conditions of SIE and direct infection. Although experimental data from the dissertation and past data from the lab suggest the involvement of viral proteins, a lack of definitive protein(s) for SIE inhibition prevents a foundation for the development of a mechanism. Theoretically, there is list of total 18 possible viral protein candidates responsible for involvement of early SIE in HSV-1 alone, with 6 for immediate/early proteins and 12 for early proteins. Although there are a few top candidates for each list, nearly all viral proteins have multiple functions and have high synergistic interactions with other proteins for performed responsibilities. As such, although mutants lacking a single viral protein would be important, experiments would also need to be performed with multiple knockouts of viral proteins to eliminate synergistic efforts as well. If experiments with knockouts of the known mutants would fail to elucidate the culprit, then viral proteins with unknown functions would need to be pursued.

2. The possible effect of heterologous SIE would need to be examined with different species of alphaherpesviruses. Studies would need to be done with primary infection of an

alphaherpesvirus like PRV and then subsequently infected with other more medically relevant viruses like HSV-1 and VZV. Since alphaherpesvirus presentation can be differentially expressed with different models, *in vitro* cell cultures models like cell chamber would be necessary. Coupled with protein analysis, these experiments would determine the effect of heterologous SIE would have upon viral progeny of alphaherpesviruses. Experiments would be done in triplicate and with endpoint analysis for early SIE.

Studying early SIE of alphaherpesviruses would provide the means the context to analyze coinfection and the generation of new isolates. With the rise of more virulent strains, studies within this sector would provide importance for prophylactic research or better understanding the spread of alphaherpesviruses.

REFERENCES CITED

REFERENCES CITED

Adams, R. H., & Brown, D. T. (1985). BHK cells expressing Sindbis virus-induced homologous interference allow the translation of nonstructural genes of superinfecting virus. *Journal of Virology*, *54*(2), 351–357. https://doi.org/10.1128/jvi.54.2.351-357.1985

Agelidis, A. M., & Shukla, D. (2015). Cell entry mechanisms of HSV: What we have learned in recent years. *Future Virology*, *10*(10), 1145–1154. https://doi.org/10.2217/fvl.15.85

Akhtar, J., Tiwari, V., Oh, M. J., Kovacs, M., Jani, A., Kovacs, S. K., Valyi-Nagy, T., & Shukla, D. (2008). HVEM and nectin-1 are the major mediators of herpes simplex virus 1 (HSV-1) entry into human conjunctival epithelium. *Investigative Ophthalmology and Visual Science*, *49*(9), 4026–4035. https://doi.org/10.1167/iovs.08-1807

Allen, J. J., Lazerwith, S. E., & Shokat, K. M. (2005). Bio-orthogonal Affinity Purification of Direct Kinase Substrates. *Journal of the American Chemical Society*, *127*(15), 5288–5289. https://doi.org/10.1021/ja050727t

Anna, S., B., Y. M., R., K. P., S., G. R., & L., H.-F. (2014). Varicella-Zoster Virus and Herpes Simplex Virus 1 Can Infect and Replicate in the Same Neurons whether Co- or Superinfected. *Journal of Virology*, *88*(9), 5079–5086. https://doi.org/10.1128/JVI.00252-14

Antinone, S. E., Shubeita, G. T., Coller, K. E., Lee, J. I., Haverlock-Moyns, S., Gross, S. P., & Smith, G. A. (2006). The Herpesvirus Capsid Surface Protein, VP26, and the Majority of the Tegument Proteins Are Dispensable for Capsid Transport toward the Nucleus. *Journal of Virology*, *80*(11), 5494–5498. https://doi.org/10.1128/jvi.00026-06

Arduino, P. G., & Porter, S. R. (2006). Oral and perioral herpes simplex virus type 1 (HSV-1) infection: Review of its management. *Oral Diseases*, *12*(3), 254–270. https://doi.org/10.1111/j.1601-0825.2006.01202.x

Asboe, D., & Pozniak, A. (2010). Antiviral therapy. *Infectious Diseases: Third Edition*, *2*, 1033–1042. https://doi.org/10.1016/B978-0-323-04579-7.00100-3

Banfield, B. W., Kaufman, J. D., Randall, J. A., & Pickard, G. E. (2003). Development of Pseudorabies Virus Strains Expressing Red Fluorescent Proteins: New Tools for Multisynaptic Labeling Applications. *Journal of Virology*, *77*(18), 10106–10112. https://doi.org/10.1128/jvi.77.18.10106-10112.2003

Birkenheuer, C. H., & Baines, J. D. (2019). RNA polymerase II Promoter Proximal Pausing and Release to Elongation are Key Steps Regulating Herpes Simplex Virus 1 Transcription. *Journal of Virology*, *December*. https://doi.org/10.1128/JVI.02035-19

Birkenheuer, C. H., Danko, C. G., & Baines, J. D. (2018). Herpes Simplex Virus 1 Dramatically Alters Loading and Positioning of RNA Polymerase II on Host Genes Early in Infection. *Journal of Virology*, *92*(8), JVI.02184-17. https://doi.org/10.1128/JVI.02184-17

Biryukov, J., & Meyers, C. (2018). Superinfection Exclusion between Two High-Risk Human Papillomavirus Types during a Coinfection. *Journal of Virology*, *92*(8), e01993-17. https://doi.org/10.1128/JVI.01993-17

Biswas, P. S., & Rouse, B. T. (2005). Early events in HSV keratitis - Setting the stage for a blinding disease. *Microbes and Infection*, *7*(4), 799–810. https://doi.org/10.1016/j.micinf.2005.03.003

Bo, Z., Miao, Y., Xi, R., Gao, X., Miao, D., Chen, H., Jung, Y. S., Qian, Y., & Dai, J. (2021). Emergence of a novel pathogenic recombinant virus from Bartha vaccine and variant pseudorabies virus in China. *Transboundary and Emerging Diseases*, *68*(3), 1454–1464. https://doi.org/10.1111/TBED.13813

Bohannon, K. P., Jun, Y., Gross, S. P., & Smith, G. A. (2013). Differential protein partitioning within the herpesvirus tegument and envelope underlies a complex and variable virion architecture. *Proceedings of the National Academy of Sciences of the United States of America*, *110*(17), E1613-20. https://doi.org/10.1073/pnas.1221896110

Bonneau, R. H., Sheridan, J. F., Feng, N., & Glaser, R. (1991). Stress-induced effects on cell-mediated innate and adaptive memory components of the murine immune response to herpes simplex virus infection. *Brain Behavior and Immunity*, *5*(3), 274–295. https://doi.org/10.1016/0889-1591(91)90023-4

Bowden, R., Sakaoka, H., Donnelly, P., & Ward, R. (2004a). High recombination rate in herpes simplex virus type 1 natural populations suggests significant co-infection. *Infection, Genetics and Evolution : Journal of Molecular Epidemiology and Evolutionary Genetics in Infectious Diseases*, *4*(2), 115–123. https://doi.org/10.1016/j.meegid.2004.01.009

Bowden, R., Sakaoka, H., Donnelly, P., & Ward, R. (2004b). High recombination rate in herpes simplex virus type 1 natural populations suggests significant co-infection. *Infection, Genetics and Evolution*, *4*(2), 115–123. https://doi.org/10.1016/j.meegid.2004.01.009

Bowen, C. D., Renner, D. W., Shreve, J. T., Tafuri, Y., Payne, K. M., Dix, R. D., Kinchington, P. R., Gatherer, D., & Szpara, M. L. (2016). Viral forensic genomics reveals the relatedness of classic herpes simplex virus strains KOS, KOS63, and KOS79. *Virology*, *492*, 179–186. https://doi.org/10.1016/j.virol.2016.02.013

Bradshaw, M. J., & Venkatesan, A. (2016). Herpes Simplex Virus-1 Encephalitis in Adults: Pathophysiology, Diagnosis, and Management. In *Neurotherapeutics* (Vol. 13, Issue 3). https://doi.org/10.1007/s13311-016-0433-7

Brandt, C. R. (2005). The role of viral and host genes in corneal infection with herpes simplex virus type 1. *Experimental Eye Research*, *80*(5), 607–621. https://doi.org/10.1016/j.exer.2004.09.007

Bratt, M. A., & Rubin, H. (1968). Specific interference among strains of Newcastle disease virus: III. Mechanisms of interference. *Virology*, *35*(3), 395–407. https://doi.org/https://doi.org/10.1016/0042-6822(68)90218-3

Bray, M., Di Mascio, M., de Kok-Mercado, F., Mollura, D. J., & Jagoda, E. (2010). Radiolabeled antiviral drugs and antibodies as virus-specific imaging probes. *Antiviral Research*, *88*(2), 129–142. https://doi.org/10.1016/j.antiviral.2010.08.005

Breiner, K. M., Schaller, H., & Knolle, P. A. (2001). Endothelial cell–mediated uptake of a hepatitis B virus: A new concept of liver targeting of hepatotropic microorganisms. *Hepatology*, *34*(4), 803–808. https://doi.org/https://doi.org/10.1053/jhep.2001.27810

Brittle, E. E., Reynolds, A. E., & Enquist, L. W. (2004). Two Modes of Pseudorabies Virus Neuroinvasion and Lethality in Mice. *Journal of Virology*, *78*(23), 12951–12963. https://doi.org/10.1128/jvi.78.23.12951-12963.2004

Brunnemann, A.-K., Liermann, K., Deinhardt-Emmer, S., Maschkowitz, G., Pohlmann, A., Sodeik, B., Fickenscher, H., Sauerbrei, A., & Krumbholz, A. (2016). Recombinant herpes simplex virus type 1 strains with targeted mutations relevant for aciclovir susceptibility. *Scientific Reports*, *6*(1), 29903. https://doi.org/10.1038/srep29903

Brunovskis, P., & Velicer, L. F. (1995). The Marek's disease virus (MDV) unique short region: Alphaherpesvirus-homologous, fowlpox virus-homologous, and MDV-specific genes. *Virology*, *206*(1), 324–338. https://doi.org/10.1016/S0042-6822(95)80048-4

Campadelli-fiume, E. G., & Roizman, B. (2022). Part II Basic virology and viral gene effects on host cell functions : alphaherpesviruses.

Campadelli-Fiume, G, Arsenakis, M., Farabegoli, F., & Roizman, B. (1988). Entry of herpes simplex virus 1 in BJ cells that constitutively express viral glycoprotein D is by endocytosis and results in degradation of the virus. *Journal of Virology*, *62*(1), 159–167. https://doi.org/10.1128/jvi.62.1.159-167.1988

Campadelli-Fiume, G, Qi, S., Avitabile, E., Foà-Tomasi, L., Brandimarti, R., & Roizman, B. (1990). Glycoprotein D of herpes simplex virus encodes a domain which precludes penetration of cells expressing the glycoprotein by superinfecting herpes simplex virus. *Journal of Virology*, *64*(12), 6070–6079. http://www.ncbi.nlm.nih.gov/pubmed/2173780

Campadelli-Fiume, Gabriella, Cocchi, F., Menotti, L., & Lopez, M. (2000a). The novel receptors that mediate the entry of herpes simplex viruses and animal alphaherpesviruses into cells.

Reviews in Medical Virology, *10*(5), 305–319. https://doi.org/10.1002/1099-1654(200009/10)10:5<305::AID-RMV286>3.0.CO;2-T

Campadelli-Fiume, Gabriella, Cocchi, F., Menotti, L., & Lopez, M. (2000b). The novel receptors that mediate the entry of herpes simplex viruses and animal alphaherpesviruses into cells. *Reviews in Medical Virology*, *10*(5), 305–319. https://doi.org/https://doi.org/10.1002/1099-1654(200009/10)10:5<305::AID-RMV286>3.0.CO;2-T

Casto, A. M., Huang, M. L. W., Xie, H., Jerome, K. R., Wald, A., Johnston, C. M., & Greninger, A. L. (2020). Herpes simplex virus mistyping due to HSV-1 × HSV-2 interspecies recombination in viral gene encoding glycoprotein B. *Viruses*, *12*(8), 1–8. https://doi.org/10.3390/v12080860

Casto, A. M., Roychoudhury, P., Xie, H., Selke, S., Perchetti, G. A., Wofford, H., Huang, M.-L., Verjans, G. M. G. M., Gottlieb, G. S., Wald, A., Jerome, K. R., Koelle, D. M., Johnston, C., & Greninger, A. L. (2019). Large, Stable, Contemporary Interspecies Recombination Events in Circulating Human Herpes Simplex Viruses. *The Journal of Infectious Diseases*, *Xx Xxxx*, 1–9. https://doi.org/10.1093/infdis/jiz199

Centifanto-Fitzgerald, Y. M., Varnell, E. D., & Kaufman, H. E. (1982). Initial herpes simplex virus type 1 infection prevents ganglionic superinfection by other strains. *Infection and Immunity*, *35*(3), 1125–1132. http://www.ncbi.nlm.nih.gov/pubmed/6279513

Ch'ng, T. H., & Enquist, L. W. (2005). Neuron-to-Cell Spread of Pseudorabies Virus in a Compartmented Neuronal Culture System. *Journal of Virology*, *79*(17), 10875–10889. https://doi.org/10.1128/jvi.79.17.10875-10889.2005

Chen, M., Chen, X., Song, X., Muhammad, A., Jia, R., Zou, Y., Yin, L., Li, L., He, C., Ye, G., Lv, C., Zhang, W., & Yin, Z. (2019). The immune-adjuvant activity and the mechanism of resveratrol on pseudorabies virus vaccine in a mouse model. *International Immunopharmacology*, *76*(July), 105876. https://doi.org/10.1016/j.intimp.2019.105876

Clark Brelje, T., Wessendorf, M. W., & Sorenson, R. L. (2002). Chapter 5 - Multicolor Laser Scanning Confocal Immunofluorescence Microscopy: Practical Application and Limitations. In B. B. T.-M. in C. B. Matsumoto (Ed.), *Cell Biological Applications of Confocal Microscopy* (Vol. 70, pp. 165-249e). Academic Press. https://doi.org/https://doi.org/10.1016/S0091-679X(02)70006-X

Clarke, R. W. (2016). Forces and Structures of the Herpes Simplex Virus (HSV) Entry Mechanism. *ACS Infectious Diseases*, *1*(9). https://doi.org/10.1021/acsinfecdis.5b00059

Clement, C., Tiwari, V., Scanlan, P. M., Valyi-Nagy, T., Yue, B. Y. J. T., & Shukla, D. (2006a). A novel role for phagocytosis-like uptake in herpes simplex virus entry. *Journal of Cell Biology*, *174*(7), 1009–1021. https://doi.org/10.1083/jcb.200509155

Clement, C., Tiwari, V., Scanlan, P. M., Valyi-Nagy, T., Yue, B. Y. J. T., & Shukla, D. (2006b). A novel role for phagocytosis-like uptake in herpes simplex virus entry. *Journal of Cell Biology*, *174*(7), 1009–1021. https://doi.org/10.1083/jcb.200509155

Cliffe, A. R., Arbuckle, J. H., Vogel, J. L., Geden, M. J., Rothbart, S. B., Cusack, C. L., Strahl, B. D., Kristie, T. M., & Deshmukh, M. (2015). Neuronal Stress Pathway Mediating a Histone Methyl/Phospho Switch Is Required for Herpes Simplex Virus Reactivation. *Cell Host and Microbe*, *18*(6). https://doi.org/10.1016/j.chom.2015.11.007

Connolly, S. A., Jackson, J. O., Jardetzky, T. S., & Longnecker, R. (2011). Fusing structure and function: a structural view of the herpesvirus entry machinery. *Nature Reviews Microbiology*, *9*(5), 369–381. https://doi.org/10.1038/nrmicro2548

Connolly, S. A., Whitbeck, J. C., Rux, A. H., Krummenacher, C., Van, S., Littel-Van Den Hurk, D., Cohen, G. H., & Eisenberg, R. J. (2001). *Glycoprotein D Homologs in Herpes Simplex Virus Type 1, Pseudorabies Virus, and Bovine Herpes Virus Type 1 Bind Directly to Human HveC (Nectin-1) with Different Affinities*. https://doi.org/10.1006/viro.2000.0747

Cooper, R. S., & Heldwein, E. E. (2015). Herpesvirus gB: A finely tuned fusion machine. In *Viruses* (Vol. 7, Issue 12, pp. 6552–6569). https://doi.org/10.3390/v7122957

Copeland, R., Balasubramaniam, A., Tiwari, V., Zhang, F., Bridges, A., Linhardt, R. J., Shukla, D., & Liu, J. (2008). Using a 3-O-sulfated heparin octasaccharide to inhibit the entry of herpes simplex virus type 1. *Biochemistry*, *47*(21), 5774–5783. https://doi.org/10.1021/bi800205t

Criddle, A., Thornburg, T., Kochetkova, I., DePartee, M., & Taylor, M. P. (2016). gD-Independent Superinfection Exclusion of Alphaherpesviruses. *Journal of Virology*, *90*(8), 4049–4058. https://doi.org/10.1128/JVI.00089-16

Crump, C. (2018a). Virus assembly and egress of HSV. In *Advances in Experimental Medicine and Biology* (Vol. 1045). https://doi.org/10.1007/978-981-10-7230-7_2

Crump, C. (2018b). Virus Assembly and Egress of HSV. In *Human Herpesviruses: Advances in Experimental Medicine and Biology* (Volume 104). Springer Nature Springer Pte Ltd. https://doi.org/https://doi.org/10.1007/978-981-10-7230-7_2

Crump, C. (2018c). *Virus Assembly and Egress of HSV BT - Human Herpesviruses* (Y. Kawaguchi, Y. Mori, & H. Kimura (eds.); pp. 23–44). Springer Singapore. https://doi.org/10.1007/978-981-10-7230-7_2

Cuddy, S. R., Schinlever, A. R., Dochnal, S., Seegren, P. V., Suzich, J., Kundu, P., Downs, T. K., Farah, M., Desai, B. N., Boutell, C., & Cliffe, A. R. (2020). Neuronal hyperexcitability is a DLK- dependent trigger of herpes simplex virus reactivation that can be induced by IL-

1. *ELife*, *9*, 1–31. https://doi.org/10.7554/eLife.58037

Da Silva Santos, C., Tartour, K., & Cimarelli, A. (2016). A Novel Entry/Uncoating Assay Reveals the Presence of at Least Two Species of Viral Capsids During Synchronized HIV-1 Infection. *PLoS Pathogens*, *12*(9), 1–28. https://doi.org/10.1371/journal.ppat.1005897

Dai, X., & Hong Zhou, Z. (2018). Structure of the herpes simplex virus 1 capsid with associated tegument protein complexes. *Science*, *360*(6384). https://doi.org/10.1126/science.aao7298

Dasika, G. K., & Letchworth, G. J. (2000). Homologous and heterologous interference requires bovine herpesvirus-1 glycoprotein D at the cell surface during virus entry. *Journal of General Virology*, *81*(4), 1041–1049. https://doi.org/10.1099/0022-1317-81-4-1041

Davison, A. J. (2007). Introduction: definition and classification of the human herpesviruses, comparative analysis of the genomes. *Human Herpesviruses: Biology, Therapy, and Immunoprophylaxis*, 10–26.

De Chiara, G., Piacentini, R., Fabiani, M., Mastrodonato, A., Marcocci, M. E., Limongi, D., Napoletani, G., Protto, V., Coluccio, P., Celestino, I., Li Puma, D. D., Grassi, C., & Palamara, A. T. (2019). Recurrent herpes simplex virus-1 infection induces hallmarks of neurodegeneration and cognitive deficits in mice. *PLoS Pathogens*, *15*(3). https://doi.org/10.1371/journal.ppat.1007617

de Oliveira, A. P., Glauser, D. L., Laimbacher, A. S., Strasser, R., Schraner, E. M., Wild, P., Ziegler, U., Breakefield, X. O., Ackermann, M., & Fraefel, C. (2008). Live Visualization of Herpes Simplex Virus Type 1 Compartment Dynamics. *Journal of Virology*, *82*(10), 4974–4990. https://doi.org/10.1128/JVI.02431-07

del Rio, T., Ch'ng, T. H., Flood, E. A., Gross, S. P., & Enquist, L. W. (2005). Heterogeneity of a Fluorescent Tegument Component in Single Pseudorabies Virus Virions and Enveloped Axonal Assemblies. *Journal of Virology*, *79*(7), 3903–3919. https://doi.org/10.1128/jvi.79.7.3903-3919.2005

del Rio, T., Werner, H. C., & Enquist, L. W. (2002). The Pseudorabies Virus VP22 Homologue (UL49) Is Dispensable for Virus Growth In Vitro and Has No Effect on Virulence and Neuronal Spread in Rodents. *Journal of Virology*, *76*(2), 774–782. https://doi.org/10.1128/jvi.76.2.774-782.2002

Delboy, M. G., Roller, D. G., & Nicola, A. V. (2008). Cellular proteasome activity facilitates herpes simplex virus entry at a postpenetration step. *Journal of Virology*, *82*(7), 3381–3390. https://doi.org/10.1128/JVI.02296-07

Deschamps, T., Dogrammatzis, C., Mullick, R., & Kalamvoki, M. (2017a). Cbl E3 Ligase Mediates the Removal of Nectin-1 from the Surface of Herpes Simplex Virus 1-Infected

Cells. *Journal of Virology*, *91*(12). https://doi.org/10.1128/jvi.00393-17

Deschamps, T., Dogrammatzis, C., Mullick, R., & Kalamvoki, M. (2017b). Cbl E3 Ligase Mediates the Removal of Nectin-1 from the Surface of Herpes Simplex Virus 1-Infected Cells. *Journal of Virology*, *91*(12), e00393-17. https://doi.org/10.1128/JVI.00393-17

Doan, M., Vorobjev, I., Rees, P., Filby, A., Wolkenhauer, O., Goldfeld, A. E., Lieberman, J., Barteneva, N., Carpenter, A. E., & Hennig, H. (2018). Diagnostic Potential of Imaging Flow Cytometry. *Trends in Biotechnology*, *36*(7), 649–652. https://doi.org/10.1016/j.tibtech.2017.12.008

Doll, J. R., Thompson, R. L., & Sawtell, N. M. (2019). Infectious herpes simplex virus in the brainstem is correlated with reactivation in the trigeminal ganglia. *Journal of Virology*, *February*. https://doi.org/10.1128/JVI.02209-18

Dropulic, L. K., & Cohen, J. I. (2012). The challenge of developing a herpes simplex virus 2 vaccine. *Expert Review of Vaccines*, *11*(12), 1429–1440. https://doi.org/10.1586/erv.12.129

E., A. S., V., Z. S., & A., S. G. (2010). Resolving the Assembly State of Herpes Simplex Virus during Axon Transport by Live-Cell Imaging . *Journal of Virology*, *84*(24), 13019–13030. https://doi.org/10.1128/JVI.01296-10

Ellenberg, P., Linero, F. N., & Scolaro, L. A. (2007). Superinfection exclusion in BHK-21 cells persistently infected with Junín virus. *Journal of General Virology*, *88*(10), 2730–2739. https://doi.org/https://doi.org/10.1099/vir.0.83041-0

Enquist, L. W. (2002). Exploiting circuit-specific spread of pseudorabies virus in the central nervous system: Insights to pathogenesis and circuit tracers. *Journal of Infectious Diseases*, *186*(SUPPL. 2), 209–214. https://doi.org/10.1086/344278

Enquist, Lynn W., & Card, J. P. (2003). Recent advances in the use of neurotropic viruses for circuit analysis. *Current Opinion in Neurobiology*, *13*(5), 603–606. https://doi.org/10.1016/j.conb.2003.08.001

Escobedo-Bonilla, C. M. (2021). Mini Review: Virus Interference: History, Types and Occurrence in Crustaceans. *Frontiers in Immunology*, *12*(June), 1–10. https://doi.org/10.3389/fimmu.2021.674216

Etienne, L.; Poorval, J.; Dingle, L.; Huang, E.; Grzesik, P.; Desai, P. J. . (2017). Visualization of herpres simplex virus type 1 virions using fluorescent colors. *Journal of Virology Methods*, *176*(5), 139–148. https://doi.org/10.1016/j.physbeh.2017.03.040

Everett, R. D., Freemont, P., Saitoh, H., Dasso, M., Orr, A., Kathoria, M., & Parkinson, J. (1998). The disruption of ND10 during herpes simplex virus infection correlates with the

Vmw110- and proteasome-dependent loss of several PML isoforms. *Journal of Virology*, *72*(8), 6581–6591. https://doi.org/10.1128/JVI.72.8.6581-6591.1998

Everett, R. D., & Maul, G. G. (1994). HSV-1 IE protein Vmw110 causes redistribution of PML. *The EMBO Journal*, *13*(21), 5062–5069. https://pubmed.ncbi.nlm.nih.gov/7957072

Folimonova, S. Y. (2012). Superinfection Exclusion Is an Active Virus-Controlled Function That Requires a Specific Viral Protein. *Journal of Virology*, *86*(10), 5554 LP – 5561. http://jvi.asm.org/content/86/10/5554.abstract

Foster, T. P., Melancon, J. M., & Kousoulas, K. G. (2001). An α-helical domain within the carboxyl terminus of herpes simplex virus type 1 (HSV-1) glycoprotein B (gB) is associated with cell fusion and resistance to heparin inhibition of cell fusion. *Virology*, *287*(1), 18–29. https://doi.org/10.1006/viro.2001.1004

Frank, S. A. (2001). Multiplicity of infection and the evolution of hybrid incompatibility in segmented viruses. *Heredity*, *87*(5), 522–529. https://doi.org/10.1046/j.1365-2540.2001.00911.x

Fujii, H., Harada, S., Yoshikawa, T., Yamada, S., Omura, N., Shibamura, M., Inagaki, T., Kato, H., Fukushi, S., & Saijo, M. (2019). Differences in the likelihood of acyclovir resistance-associated mutations in the thymidine kinase genes of herpes simplex virus 1 and varicella-zoster virus. *Antimicrobial Agents and Chemotherapy*, *63*(5), 1–6. https://doi.org/10.1128/AAC.00017-19

Fuller, A. O., & Spear, P. G. (1987). Anti-glycoprotein D antibodies that permit adsorption but block infection by herpes simplex virus 1 prevent virion-cell fusion at the cell surface (neutralizing antibodies/membrane fusion/glycoproteins/viral penetration) (Vol. 84). http://www.pnas.org/content/pnas/84/15/5454.full.pdf

G., P. V., Jill, M., M., P. C., M., M. I., & D., S. N. (2008). The UL25 Gene Product of Herpes Simplex Virus Type 1 Is Involved in Uncoating of the Viral Genome. *Journal of Virology*, *82*(13), 6654–6666. https://doi.org/10.1128/JVI.00257-08

Gallagher, J. R., Atanasiu, D., Saw, W. T., Paradisgarten, M. J., Whitbeck, J. C., Eisenberg, R. J., & Cohen, G. H. (2014). Functional Fluorescent Protein Insertions in Herpes Simplex Virus gB Report on gB Conformation before and after Execution of Membrane Fusion. *PLoS Pathogens*, *10*(9). https://doi.org/10.1371/journal.ppat.1004373

Geib, T., Sauder, C., Venturelli, S., Hässler, C., Staeheli, P., & Schwemmle, M. (2003). Selective Virus Resistance Conferred by Expression of Borna Disease Virus Nucleocapsid Components. *Journal of Virology*, *77*(7). https://doi.org/10.1128/jvi.77.7.4283-4290.2003

Geraghty, R. J., Jogger, C. R., & Spear, P. G. (2000). Cellular expression of alphaherpesvirus gD interferes with entry of homologous and heterologous alphaherpesviruses by blocking access to a shared gD receptor. *Virology*, *268*(1), 147–158. https://doi.org/10.1006/viro.1999.0157

Group, H. S. (1973). Provisional labels for herpesviruses. *Journal of General Virology*, *20*(3), 417–419. https://doi.org/10.1099/0022-1317-20-3-417

Hamilton, N. (2009). Quantification and its applications in fluorescent microscopy imaging. *Traffic*, *10*(8), 951–961. https://doi.org/10.1111/j.1600-0854.2009.00938.x

Hampson, I. N., Oliver, A. W., & Hampson, L. (2021). Potential effects of human papillomavirus type substitution, superinfection exclusion and latency on the efficacy of the current l1 prophylactic vaccines. *Viruses*, *13*(1), 1–20. https://doi.org/10.3390/v13010022

Harvey, J. W. (2012). *Chapter 6 - Immunohematology* (J. W. B. T.-V. H. Harvey (ed.); pp. 177–190). W.B. Saunders. https://doi.org/https://doi.org/10.1016/B978-1-4377-0173-9.00006-3

Hogue, I. B., Bosse, J. B., Engel, E. A., Scherer, J., Hu, J. R., Del Rio, T., & Enquist, L. W. (2015). Fluorescent Protein approaches in alpha Herpesvirus Research. *Viruses*, *7*(11), 5933–5961. https://doi.org/10.3390/v7112915

Hogue, I. B., Bosse, J. B., Hu, J. R., Thiberge, S. Y., & Enquist, L. W. (2014). Cellular Mechanisms of Alpha Herpesvirus Egress: Live Cell Fluorescence Microscopy of Pseudorabies Virus Exocytosis. *PLoS Pathogens*, *10*(12). https://doi.org/10.1371/journal.ppat.1004535

Huang, I.-C., Li, W., Sui, J., Marasco, W., Choe, H., & Farzan, M. (2008). Influenza A Virus Neuraminidase Limits Viral Superinfection. *Journal of Virology*, *82*(10). https://doi.org/10.1128/jvi.00079-08

Huang, K.-J., Yang, Y.-C., Lin, Y.-S., Huang, J.-H., Liu, H.-S., Yeh, T.-M., Chen, S.-H., Liu, C.-C., & Lei, H.-Y. (2006). The Dual-Specific Binding of Dengue Virus and Target Cells for the Antibody-Dependent Enhancement of Dengue Virus Infection. *The Journal of Immunology*, *176*(5), 2825 LP – 2832. https://doi.org/10.4049/jimmunol.176.5.2825

Huang, W., Xie, P., Xu, M., Li, P., & Zao, G. (2011). The Influence of Stress Factors on the Reactivation of Latent Herpes Simplex Virus Type 1 in Infected Mice. *Cell Biochemistry and Biophysics*, *61*(1), 115–122. https://doi.org/10.1007/s12013-011-9167-7

Huber, M. T., Wisner, T. W., Hegde, N. R., Goldsmith, K. A., Rauch, D. A., Roller, R. J., Krummenacher, C., Eisenberg, R. J., Cohen, G. H., & Johnson, D. C. (2001). Herpes Simplex Virus with Highly Reduced gD Levels Can Efficiently Enter and Spread between

Human Keratinocytes. *Journal of Virology*, *75*(21), 10309–10318. https://doi.org/10.1128/jvi.75.21.10309-10318.2001

Hull, R. (2002). *Matthews' Plant Virology*. Academic Press New York.

Ian B. Hogue, Jolie Jean, Andrew D. Esteves, Nikhila S. Tanneti, Julian Scherer, L. W. E. (2018). Functional Carboxy-Terminal Fluorescent Protein Fusion to Pseudorabies Virus Small Capsid Protein VP26. *Journal of Virolgoy*, *92*(1), 1–12.

Isaacs, A., & Burke, D. C. (1959). Viral interference and interferon. *British Medical Bulletin*, *15*(3), 185–188. https://doi.org/10.1093/oxfordjournals.bmb.a069760

J., N. A., & Sidney, K. (1964). INHIBITORY EFFECT OF HEPARIN ON HERPES SIMPLEX VIRUS. *Journal of Bacteriology*, *87*(5), 1060–1066. https://doi.org/10.1128/jb.87.5.1060-1066.1964

Jarosinski, K. W. (2012). Dual Infection and Superinfection Inhibition of Epithelial Skin Cells by Two Alphaherpesviruses Co-Occur in the Natural Host. *PLoS ONE*, *7*(5), e37428. https://doi.org/10.1371/journal.pone.0037428

Jiang, Y.-C., Feng, H., Lin, Y.-C., & Guo, X.-R. (2016). New strategies against drug resistance to herpes simplex virus. *International Journal of Oral Science*, *8*(1), 1–6. https://doi.org/10.1038/ijos.2016.3

Johnson, R. M., & Spear, P. G. (1989). Herpes simplex virus glycoprotein D mediates interference with herpes simplex virus infection. *Journal of Virology*, *63*(2), 819–827. http://www.ncbi.nlm.nih.gov/pubmed/2536105

Johnston, C., Gottlieb, S. L., & Wald, A. (2016). Status of vaccine research and development of vaccines for herpes simplex virus. *Vaccine*, *34*(26), 2948–2952. https://doi.org/10.1016/j.vaccine.2015.12.076

Jolicoeur, P. (1979). The Fv-1 gene of the mouse and its control of murine leukemia virus replication. In *Current topics in microbiology and immunology* (Vol. 86). https://doi.org/10.1007/978-3-642-67341-2_3

Jones, C., & Perng, G. C. (2010). Towards an understanding of the herpes simplex virus type 1 latency-reactivation cycle. In *Interdisciplinary Perspectives on Infectious Diseases* (Vol. 2010, p. 262415). Hindawi. https://doi.org/10.1155/2010/262415

Jones, D. M., & Padilla-Parra, S. (2016). The β-lactamase assay: Harnessing a FRET biosensor to analyse viral fusion mechanisms. *Sensors (Switzerland)*, *16*(7). https://doi.org/10.3390/s16070950

Joosen, L., Hink, M. A., Gadella, T. W. J., & Goedhart, J. (2014). Effect of fixation procedures on the fluorescence lifetimes of Aequorea victoria derived fluorescent proteins. *Journal of Microscopy*, *256*(3), 166–176. https://doi.org/10.1111/jmi.12168

Karpf, A. R., Lenches, E., Strauss, E. G., Strauss, J. H., & Brown, D. T. (1997a). Superinfection exclusion of alphaviruses in three mosquito cell lines persistently infected with Sindbis virus. *Journal of Virology*, *71*(9), 7119–7123. https://doi.org/10.1128/jvi.71.9.7119-7123.1997

Karpf, A. R., Lenches, E., Strauss, E. G., Strauss, J. H., & Brown, D. T. (1997b). Superinfection exclusion of alphaviruses in three mosquito cell lines persistently infected with Sindbis virus. *Journal of Virology*, *71*(9), 7119–7123. https://doi.org/10.1128/jvi.71.9.7119-7123.1997

Kathie-Anne, W., A., J. M., R., A. W., P., F. K., & J., T. D. L. (2004). Superinfection Exclusion in Duck Hepatitis B Virus Infection Is Mediated by the Large Surface Antigen. *Journal of Virology*, *78*(15), 7925–7937. https://doi.org/10.1128/JVI.78.15.7925-7937.2004

Kidokoro, H., de Vries, L. S., Ogawa, C., Ito, Y., Ohno, A., Groenendaal, F., Saitoh, S., Okumura, A., Ito, Y., & Natsume, J. (2017). Predominant area of brain lesions in neonates with herpes simplex encephalitis. *Journal of Perinatology*, *February*, 1–5. https://doi.org/10.1038/jp.2017.114

Kim, J.-S., Enquist, L. W., & Card, J. P. (1999). Circuit-Specific Coinfection of Neurons in the Rat Central Nervous System with Two Pseudorabies Virus Recombinants. *Journal of Virology*, *73*(11), 9521–9531. https://doi.org/10.1128/jvi.73.11.9521-9531.1999

Kobiler, O., Lipman, Y., Therkelsen, K., Daubechies, I., & Enquist, L. W. (2010). Herpesviruses carrying a Brainbow cassette reveal replication and expression of limited numbers of incoming genomes. *Nat Commun*, *1*(9), 146. https://doi.org/10.1038/ncomms1145

Koelle, D. M., Norberg, P., Fitzgibbon, M. P., Russell, R. M., Greninger, A. L., Huang, M. L., Stensland, L., Jing, L., Magaret, A. S., Diem, K., Selke, S., Xie, H., Celum, C., Lingappa, J. R., Jerome, K. R., Wald, A., & Johnston, C. (2017). Worldwide circulation of HSV-2 × HSV-1 recombinant strains. *Scientific Reports*, *7*(March), 1–12. https://doi.org/10.1038/srep44084

Kollias, C. M., Huneke, R. B., Wigdahl, B., & Jennings, S. R. (2014). Animal models of herpes simplex virus immunity and pathogenesis. In *Journal of NeuroVirology* (Vol. 21, Issue 1, pp. 8–23). https://doi.org/10.1007/s13365-014-0302-2

Kopp, S. J., Ranaivo, H. R., Wilcox, D. R., Karaba, A. H., Wainwright, M. S., & Muller, W. J. (2014). Herpes simplex virus serotype and entry receptor availability alter CNS disease in a mouse model of neonatal HSV. *Pediatric Research*, *76*(6), 528–534.

https://doi.org/10.1038/pr.2014.135

Kotsakis, A., Pomeranz, L. E., Blouin, A., & Blaho, J. A. (2001). Microtubule Reorganization during Herpes Simplex Virus Type 1 Infection Facilitates the Nuclear Localization of VP22, a Major Virion Tegument Protein. *Journal of Virology*, *75*(18), 8697–8711. https://doi.org/10.1128/jvi.75.18.8697-8711.2001

Koyuncu, O. O., Song, R., Greco, T. M., Cristea, I. M., & Enquist, L. W. (2015). The number of alphaherpesvirus particles infecting axons and the axonal protein repertoire determines the outcome of neuronal infection. *MBio*, *6*(2). https://doi.org/10.1128/mBio.00276-15

Kramer, T., & Enquist, L. W. (2013a). Directional spread of alphaherpesviruses in the nervous system. *Viruses*, *5*(2), 678–707. https://doi.org/10.3390/v5020678

Kramer, T., & Enquist, L. W. (2013b). Directional spread of alphaherpesviruses in the nervous system. *Viruses*, *5*(2), 678–707. https://doi.org/10.3390/v5020678

Krishnan, R., & Stuart, P. M. (2021). Developments in Vaccination for Herpes Simplex Virus. *Frontiers in Microbiology*, *12*(December). https://doi.org/10.3389/fmicb.2021.798927

Kukhanova, M. K., Korovina, A. N., & Kochetkov, S. N. (2014). Human herpes simplex virus: life cycle and development of inhibitors. *Biochemistry. Biokhimiia*, *79*(13), 1635–1652. https://doi.org/10.1134/S0006297914130124

L., F. H., A., D. J., A., D. N., J., I. M., Sandra, W., & Rozanne, S.-G. (2022). A Herpesviral Immediate Early Protein Promotes Transcription Elongation of Viral Transcripts. *MBio*, *8*(3), e00745-17. https://doi.org/10.1128/mBio.00745-17

Laureti, M., Paradkar, P. N., Fazakerley, J. K., & Rodriguez-Andres, J. (2020). Superinfection exclusion in mosquitoes and its potential as an arbovirus control strategy. *Viruses*, *12*(11), 1–17. https://doi.org/10.3390/v12111259

Law, G. A., Herr, A. E., Cwick, J. P., & Taylor, M. P. (2018). A new approach to assessing hsv-1 recombination during intercellular spread. *Viruses*, *10*(5), 1–16. https://doi.org/10.3390/v10050220

Lee, S. W. H., Gottlieb, S. L., & Chaiyakunapruk, N. (2022). Healthcare resource utilisation pattern and costs associated with herpes simplex virus diagnosis and management: A systematic review. *BMJ Open*, *12*(1). https://doi.org/10.1136/bmjopen-2021-049618

Lee, Y.-M., Tscherne, D. M., Yun, S.-I., Frolov, I., & Rice, C. M. (2005). Dual Mechanisms of Pestiviral Superinfection Exclusion at Entry and RNA Replication. *Journal of Virology*, *79*(6), 3231–3242. https://doi.org/10.1128/jvi.79.6.3231-3242.2005

Lennette, E. H. (1951). INTERFERENCE BETWEEN ANIMAL VIRUSES. *Annual Review of Microbiology*, *5*(1), 277–294. https://doi.org/10.1146/annurev.mi.05.100151.001425

Lennette, E. H., & Koprowski, H. (1946). INTERFERENCE BETWEEN VIRUSES IN TISSUE CULTURE . *Journal of Experimental Medicine*, *83*(3), 195–219. https://doi.org/10.1084/jem.83.3.195

Linehan, M. M., Richman, S., Krummenacher, C., Eisenberg, R. J., Cohen, G. H., & Iwasaki, A. (2004). In vivo role of nectin-1 in entry of herpes simplex virus type 1 (HSV-1) and HSV-2 through the vaginal mucosa. *Journal of Virology*, *78*(5), 2530–2536. https://doi.org/10.1128/JVI.78.5.2530-2536.2004

Loncoman, C. A., Vaz, P. K., Coppo, M. J., Hartley, C. A., Morera, F. J., Browning, G. F., & Devlin, J. M. (2017). Natural recombination in alphaherpesviruses: Insights into viral evolution through full genome sequencing and sequence analysis. In *Infection, Genetics and Evolution* (Vol. 49, pp. 174–185). Elsevier. https://doi.org/10.1016/j.meegid.2016.12.022

Looker, K. J., Magaret, A. S., May, M. T., Turner, K. M. E., Vickerman, P., Gottlieb, S. L., & Newman, L. M. (2015). Global and regional estimates of prevalent and incident herpes simplex virus type 1 infections in 2012. *PLoS ONE*, *10*(10). https://doi.org/10.1371/journal.pone.0140765

Looker, K. J., Magaret, A. S., Turner, K. M. E., Vickerman, P., Gottlieb, S. L., Newman, L. M., May, M. T., Turner, K. M. E., Vickerman, P., Gottlieb, S. L., & Newman, L. M. (2015). Global estimates of prevalent and incident herpes simplex virus type 2 infections in 2012. *PLoS ONE*, *10*(1). https://doi.org/10.1371/journal.pone.0114989

Loret, S., El Bilali, N., & Lippé, R. (2012). Analysis of herpes simplex virus type I nuclear particles by flow cytometry. *Cytometry Part A*, *81 A*(11), 950–959. https://doi.org/10.1002/cyto.a.22107

Lyman, M. G., Kemp, C. D., Taylor, M. P., & Enquist, L. W. (2009). Comparison of the Pseudorabies Virus Us9 Protein with Homologs from Other Veterinary and Human Alphaherpesviruses. *Journal of Virology*, *83*(14), 6978–6986. https://doi.org/10.1128/JVI.00598-09

Madavaraju, K., Koganti, R., Volety, I., Yadavalli, T., & Shukla, D. (2021). Herpes Simplex Virus Cell Entry Mechanisms: An Update. *Frontiers in Cellular and Infection Microbiology*, *10*(January), 1–18. https://doi.org/10.3389/fcimb.2020.617578

Maroui, M. A., Callé, A., Cohen, C., Streichenberger, N., Texier, P., Takissian, J., Rousseau, A., Poccardi, N., Welsch, J., Corpet, A., Schaeffer, L., Labetoulle, M., & Lomonte, P. (2016). Latency Entry of Herpes Simplex Virus 1 Is Determined by the Interaction of Its Genome with the Nuclear Environment. *PLoS Pathogens*, *12*(9).

https://doi.org/10.1371/journal.ppat.1005834

Maul, G. G., Guldner, H. H., & Spivack, J. G. (1993). Modification of discrete nuclear domains induced by herpes simplex virus type 1 immediate early gene 1 product (ICP0). *The Journal of General Virology*, *74 (Pt 12*, 2679–2690. https://doi.org/10.1099/0022-1317-74-12-2679

McKinney, H. H. (1926). Virus mixtures that may not be detected in young tobacco plants. *Phytopathology*, *16*(89).

Mertz, G. J. (2008). Asymptomatic shedding of herpes simplex virus 1 and 2: Implications for prevention of transmission. *Journal of Infectious Diseases*, *198*(8), 1098–1100. https://doi.org/10.1086/591914

Meurens, F., Schynts, F., Keil, G. M., Muylkens, B., Vanderplasschen, A., Gallego, P., & Thiry, E. (2004). Superinfection prevents recombination of the alphaherpesvirus bovine herpesvirus 1. *Journal of Virology*, *78*(8), 3872–3879. https://doi.org/10.1128/JVI.78.8.3872-3879.2004

Michel, N., Allespach, I., Venzke, S., Fackler, O. T., & Keppler, O. T. (2005). The nef protein of human immunodeficiency virus establishes superinfection immunity by a dual strategy to downregulate cell-surface CCR5 and CD4. *Current Biology*, *15*(8). https://doi.org/10.1016/j.cub.2005.02.058

Miller, J. L., Weed, D. J., Lee, B. H., Pritchard, S. M., & Nicola, A. V. (2019). Low-pH Endocytic Entry of the Porcine Alphaherpesvirus Pseudorabies Virus. *Journal of Virology*, *93*(2). https://doi.org/10.1128/jvi.01849-18

Mitterreiter, J. G., Titulaer, M. J., Van Nierop, G. P., Van Kampen, J. J. A., Aron, G. I., Osterhaus, A. D. M. E., Verjans, G. M. G. M., & Ouwendijk, W. J. D. (2016). Prevalence of intrathecal acyclovir resistant virus in herpes simplex encephalitis patients. *PLoS ONE*, *11*(5). https://doi.org/10.1371/journal.pone.0155531

Muylkens, B., Farnir, F., Meurens, F., Schynts, F., Vanderplasschen, A., Georges, M., & Thiry, E. (2009). Coinfection with Two Closely Related Alphaherpesviruses Results in a Highly Diversified Recombination Mosaic Displaying Negative Genetic Interference. *Journal of Virology*, *83*(7), 3127–3137. https://doi.org/10.1128/jvi.02474-08

Nagel, C. H., Döhner, K., Binz, A., Bauerfeind, R., & Sodeik, B. (2012). Improper Tagging of the Non-Essential Small Capsid Protein VP26 Impairs Nuclear Capsid Egress of Herpes Simplex Virus. *PLoS ONE*, *7*(8). https://doi.org/10.1371/journal.pone.0044177

Naghavi, M. H., & Walsh, D. (2017). Microtubule Regulation and Function during Virus Infection. *Journal of Virology*, *91*(16). https://doi.org/10.1128/jvi.00538-17

Nethe, M., Berkhout, B., & van der Kuyl, A. C. (2005). Retroviral superinfection resistance. In *Retrovirology* (Vol. 2). https://doi.org/10.1186/1742-4690-2-52

Neumaier, F., Zlatopolskiy, B. D., & Neumaier, B. (2020). Nuclear medicine in times of covid-19: How radiopharmaceuticals could help to fight the current and future pandemics. *Pharmaceutics*, *12*(12), 1–26. https://doi.org/10.3390/pharmaceutics12121247

Nichols, J. E., Mock, D. J., & Roberts, N. J. (1993). Use of FITC-labeled influenza virus and flow cytometry to assess binding and internalization of virus by monocytes-macrophages and lymphocytes. *Archives of Virology*, *130*(3), 441–455. https://doi.org/10.1007/BF01309672

Nicola, A. V., & Straus, S. E. (2004). Cellular and Viral Requirements for Rapid Endocytic Entry of Herpes Simplex Virus. *Journal of Virology*, *78*(14), 7508–7517.

https://doi.org/10.1128/jvi.78.14.7508-7517.2004

Nicola, A. V, Hou, J., Major, E. O., & Straus, S. E. (2005). Herpes simplex virus type 1 enters human epidermal keratinocytes, but not neurons, via a pH-dependent endocytic pathway. *Journal of Virology*, *79*(12), 7609–7616. https://doi.org/10.1128/JVI.79.12.7609-7616.2005

Nishi, K., & Saigo, K. (2007). Cellular internalization of green fluorescent protein fused with herpes simplex virus protein VP22 via a lipid raft-mediated endocytic pathway independent of caveolae and Rho family GTPases but dependent on dynamin and Arf6. *Journal of Biological Chemistry*, *282*(37), 27503–27517. https://doi.org/10.1074/jbc.M703810200

Nowak, M. A., & May, R. M. (1994). Superinfection and the evolution of parasite virulence. *Proceedings of the Royal Society of London. Series B: Biological Sciences*, *255*(1342), 81–89. https://doi.org/10.1098/rspb.1994.0012

Osorio, F. A., & Rock, D. L. (1992). A murine model of pseudorabies virus latency. *Microbial Pathogenesis*, *12*(1), 39–46. https://doi.org/10.1016/0882-4010(92)90064-U

Owen, D. J., Crump, C. M., & Graham, S. C. (2015). Tegument assembly and secondary envelopment of alphaherpesviruses. In *Viruses* (Vol. 7, Issue 9, pp. 5084–5114). https://doi.org/10.3390/v7092861

Pomeranz, L. E., Reynolds, A. E., & Hengartner, C. J. (2005). Molecular Biology of Pseudorabies Virus: Impact on Neurovirology and Veterinary Medicine. *Microbiology and Molecular Biology Reviews*, *69*(3), 462–500. https://doi.org/10.1128/mmbr.69.3.462-500.2005

Rahn, E., Petermann, P., Hsu, M. J., Rixon, F. J., & Knebel-Mörsdorf, D. (2011). Entry pathways of herpes simplex virus type 1 into human keratinocytes are dynamin- and cholesterol-

dependent. *PLoS ONE*, *6*(10). https://doi.org/10.1371/journal.pone.0025464

Remeijer, L., Maertzdorf, J., Buitenwerf, J., Osterhaus, A. D. M. E., & Verjans, G. M. G. M. (2002). Corneal herpes simplex virus type 1 superinfection in patients with recrudescent herpetic keratitis. *Investigative Ophthalmology and Visual Science*, *43*(2), 358–363.

Ren, C. Z., Hu, W. Y., Zhang, J. W., Wei, Y. Y., Yu, M. L., & Hu, T. J. (2021). Establishment of inflammatory model induced by Pseudorabies virus infection in mice. *Journal of Veterinary Science*, *22*(2), 1–13. https://doi.org/10.4142/JVS.2021.22.E20

Renner, D. W., & Szpara, M. L. (2017). The Impacts of Genome-wide Analyses on our Understanding of Human Herpesvirus Diversity and Evolution. *Journal of Virology*, *92*(1), JVI.00908-17. https://doi.org/10.1128/JVI.00908-17

Roizman, B., & Furlong, D. (1974). *The Replication of Herpesviruses BT - Reproduction: DNA Animal Viruses* (H. Fraenkel-Conrat & R. R. Wagner (eds.); pp. 229–403). Springer US.

https://doi.org/10.1007/978-1-4684-2703-5_4

Roizman, B., & Whitley, R. J. (2013). An inquiry into the molecular basis of HSV latency and reactivation. *Annual Review of Microbiology*, *67*, 355–374. https://doi.org/10.1146/annurev-micro-092412-155654

Rooney, B. V., Crucian, B. E., Pierson, D. L., Laudenslager, M. L., & Mehta, S. K. (2019). Herpes virus reactivation in astronauts during spaceflight and its application on earth. In *Frontiers in Microbiology* (Vol. 10, Issue feburay). https://doi.org/10.3389/fmicb.2019.00016

Rutkowski, A. J., Erhard, F., L'Hernault, A., Bonfert, T., Schilhabel, M., Crump, C., Rosenstiel, P., Efstathiou, S., Zimmer, R., Friedel, C. C., & Dölken, L. (2015). Widespread disruption of host transcription termination in HSV-1 infection. *Nature Communications*, *6*. https://doi.org/10.1038/ncomms8126

Rux, A. H., Lou, H., Lambris, J. D., Friedman, H. M., Eisenberg, R. J., & Cohen, G. H. (2002). Kinetic analysis of glycoprotein C of herpes simplex virus types 1 and 2 binding to heparin, heparan sulfate, and complement component C3b. *Virology*, *294*(2), 324–332. https://doi.org/10.1006/viro.2001.1326

Sanfilippo, C. M., Chirimuuta, F. N. W., & Blaho, J. A. (2004). Herpes Simplex Virus Type 1 Immediate-Early Gene Expression Is Required for the Induction of Apoptosis in Human Epithelial HEp-2 Cells. *Journal of Virology*, *78*(1), 224–239. https://doi.org/10.1128/JVI.78.1.224-239.2004

Sawitzky, D., Hampl, H., & Habermehl, K. O. (1990). Comparison of heparin-sensitive

attachment of pseudorabies virus (PRV) and herpes simplex virus type 1 and identification of heparin-binding PRV glycoproteins. *Journal of General Virology*, *71*(5), 1221–1225. https://doi.org/10.1099/0022-1317-71-5-1221

Schlesinger, R. W. (1959). Interference between animal viruses. *The Viruses*, *3*, 157–194.

Schmid, D. S. (2019). Mixing It Up: New Insights Into Interspecies Recombination Between Herpes Simplex Virus Type 1 and 2. *The Journal of Infectious Diseases*, *18*(Xx), 1–2. https://doi.org/10.1093/infdis/jiz200

Schneider-Schaulies, J., Schnorr, J. J., Brinckmann, U., Dunster, L. M., Baczko, K., Liebert, U. G., Schneider-Schaulies, S., & ter Meulen, V. (1995). Receptor usage and differential downregulation of CD46 by measles virus wild-type and vaccine strains. *Proceedings of the National Academy of Sciences of the United States of America*, *92*(9), 3943–3947. https://doi.org/10.1073/pnas.92.9.3943

Schneider, S. M., Pritchard, S. M., Wudiri, G. A., Trammell, C. E., & Nicola, A. V. (2019). Early steps in herpes simplex virus infection blocked by a proteasome inhibitor. *MBio*, *10*(3), 1–14. https://doi.org/10.1128/mBio.00732-19

Scholtes, L., & Baines, J. D. (2009). Effects of major capsid proteins, capsid assembly, and DNA cleavage/packaging on the pUL17/pUL25 complex of herpes simplex virus 1. *Journal of Virology*, *83*(24), 12725–12737. https://doi.org/10.1128/JVI.01658-09

Seffer, M. T., Cottam, D., Forni, L. G., & Kielstein, J. T. (2021). Heparin 2.0: A New Approach to the Infection Crisis. *Blood Purification*, *50*(1), 28–34. https://doi.org/10.1159/000508647

Shearer, W. T., Rosenwasser, L. J., Bochner, B. S., Allen, T. M., Altfeld, M., & Boston, P. (2003). *Molecular mechanisms in allergy and clinical immunology HIV-1 superinfection*. 829–835. https://doi.org/10.1067/mai.2003.1821

Shukla, S. Y., Singh, Y. K., & Shukla, D. (2009). Role of nectin-1, HVEM, and PILR- in HSV-2 entry into human retinal pigment epithelial cells. *Investigative Ophthalmology and Visual Science*, *50*(6), 2878–2887. https://doi.org/10.1167/iovs.08-2981

Simon, K. O., Cardamone, J. J. J., Whitaker-Dowling, P. A., Youngner, J. S., & Widnell, C. C. (1990). Cellular mechanisms in the superinfection exclusion of vesicular stomatitis virus. *Virology*, *177*(1), 375–379. https://doi.org/10.1016/0042-6822(90)90494-c

Singh, I. R., Suomalainen, M., Varadarajan, S., Garoff, H., & Helenius, A. (1997). Multiple Mechanisms for the Inhibition of Entry and Uncoating of Superinfecting Semliki Forest Virus. *Virology*, *231*(1), 59–71. https://doi.org/https://doi.org/10.1006/viro.1997.8492

Sloutskin, A., Yee, M. B., Kinchington, P. R., & Goldstein, R. S. (2014). Varicella-Zoster Virus and Herpes Simplex Virus 1 Can Infect and Replicate in the Same Neurons whether Co- or

Superinfected. *Journal of Virology*, *88*(9), 5079–5086. https://doi.org/10.1128/JVI.00252-14

Smith, G. (2012). Herpesvirus Transport to the Nervous System and Back Again. *Annual Review of Microbiology*, *66*(1), 153–176. https://doi.org/10.1146/annurev-micro-092611-150051

Smith, G. A., & Enquist, L. W. (2000). A self-recombining bacterial artificial chromosome and its application for analysis of herpesvirus pathogenesis. *Proceedings of the National Academy of Sciences of the United States of America*, *97*(9), 4873–4878. https://doi.org/10.1073/pnas.080502497

Song, R., Koyuncu, O. O., Greco, T. M., Diner, B. A., Cristea, I. M., & Enquist, L. W. (2016). Two modes of the axonal interferon response limit alphaherpesvirus neuroinvasion. *MBio*, *7*(1). https://doi.org/10.1128/mBio.02145-15

Spear, P. G. (2004). Herpes simplex virus: Receptors and ligands for cell entry. *Cellular Microbiology*, *6*(5), 401–410. https://doi.org/10.1111/j.1462-5822.2004.00389.x

Spear, P. G., Eisenberg, R. J., & Cohen, G. H. (2000). Three Classes of Cell Surface Receptors for Alphaherpesvirus Entry. *Virology*, *275*(1), 1–8. https://doi.org/https://doi.org/10.1006/viro.2000.0529

Steck, F. T., & Rubin, H. (1966). The mechanism of interference between an avian leukosis virus and rous sarcoma virus: I. Establishment of interference. *Virology*, *29*(4), 628–641. https://doi.org/https://doi.org/10.1016/0042-6822(66)90287-X

Stevenson, M., Meier, C., Mann, A. M., Chapman, N., & Wasiak, A. (1988). Envelope glycoprotein of HIV induces interference and cytolysis resistance in CD4+ cells: Mechanism for persistence in AIDS. *Cell*, *53*(3), 483–496. https://doi.org/https://doi.org/10.1016/0092-8674(88)90168-7

Stiles, K. M., & Krummenacher, C. (2010). Glycoprotein D actively induces rapid internalization of two nectin-1 isoforms during herpes simplex virus entry. *Virology*, *399*(1), 109–119. https://doi.org/10.1016/j.virol.2009.12.034

Sugimoto, K., Uema, M., Sagara, H., Tanaka, M., Sata, T., Hashimoto, Y., & Kawaguchi, Y. (2008). Simultaneous Tracking of Capsid, Tegument, and Envelope Protein Localization in Living Cells Infected with Triply Fluorescent Herpes Simplex Virus 1. *Journal of Virology*, *82*(11), 5198–5211. https://doi.org/10.1128/JVI.02681-07

Suzich, J. B., & Cliffe, A. R. (2018). Strength in diversity: Understanding the pathways to herpes simplex virus reactivation. In *Virology* (Vol. 522). https://doi.org/10.1016/j.virol.2018.07.011

Szpara, M. L., Gatherer, D., Ochoa, A., Greenbaum, B., Dolan, A., Bowden, R. J., Enquist, L. W., Legendre, M., & Davison, A. J. (2014). Evolution and diversity in human herpes simplex virus genomes. *Journal of Virology*, *88*(2), 1209–1227. https://doi.org/10.1128/JVI.01987-13

Szpara, M. L., Tafuri, Y. R., Parsons, L., Shamim, S. R., Verstrepen, K. J., Legendre, M., & Enquist, L. W. (2011). A wide extent of inter-strain diversity in virulent and vaccine strains of Alphaherpesviruses. *PLoS Pathogens*, *7*(10), 14–17. https://doi.org/10.1371/journal.ppat.1002282

Tatiana, G., Gabriella, C.-F., & Laura, M. (2004). Entry of Herpes Simplex Virus Mediated by Chimeric Forms of Nectin1 Retargeted to Endosomes or to Lipid Rafts Occurs through Acidic Endosomes. *Journal of Virology*, *78*(22), 12268–12276. https://doi.org/10.1128/JVI.78.22.12268-12276.2004

Taylor, M. P., Kobiler, O., & Enquist, L. W. (2012). Alphaherpesvirus axon-to-cell spread involves limited virion transmission. *Proceedings of the National Academy of Sciences*, *109*(42), 17046–17051. https://doi.org/10.1073/pnas.1212926109

Taylor, Matthew P., & Enquist, L. W. (2015). Axonal spread of neuroinvasive viral infections. *Trends in Microbiology*, *23*(5), 283–288. https://doi.org/10.1016/j.tim.2015.01.002

Tebaldi, G., Pritchard, S. M., & Nicola, A. V. (2020). Herpes Simplex Virus Entry by a Nonconventional Endocytic Pathway. *Journal of Virology*, *94*(24). https://doi.org/10.1128/jvi.01910-20

Thellman, N. M., & Triezenberg, S. J. (2017). Herpes simplex virus establishment, maintenance, and reactivation: In vitro modeling of latency. In *Pathogens* (Vol. 6, Issue 3). https://doi.org/10.3390/pathogens6030028

Thier, K., Petermann, P., Rahn, E., Rothamel, D., Bloch, W., & Knebel-Mörsdorf, D. (2017). Mechanical barriers restrict invasion of herpes simplex virus 1 into human oral mucosa. *Journal of Virology*, *September*, JVI.01295-17. https://doi.org/10.1128/JVI.01295-17

Till, G., Christian, S., Sascha, V., Christel, H., Peter, S., & Martin, S. (2003). Selective Virus Resistance Conferred by Expression of Borna Disease Virus Nucleocapsid Components. *Journal of Virology*, *77*(7), 4283–4290. https://doi.org/10.1128/JVI.77.7.4283-4290.2003

Tsatsos, M., MacGregor, C., Athanasiadis, I., Moschos, M. M., Hossain, P., & Anderson, D. (2016). Herpes simplex virus keratitis: an update of the pathogenesis and current treatment with oral and topical antiviral agents. In *Clinical and Experimental Ophthalmology* (Vol. 44, Issue 9, pp. 824–837). https://doi.org/10.1111/ceo.12785

Tscherne, D. M., Evans, M. J., von Hahn, T., Jones, C. T., Stamataki, Z., McKeating, J. A.,

Lindenbach, B. D., & Rice, C. M. (2007). Superinfection Exclusion in Cells Infected with Hepatitis C Virus. *Journal of Virology*, *81*(8), 3693–3703. https://doi.org/10.1128/jvi.01748-06

Tscherne, D. M., Manicassamy, B., & García-Sastre, A. (2010). An enzymatic virus-like particle assay for sensitive detection of virus entry. *Journal of Virological Methods*, *163*(2), 336–343. https://doi.org/10.1016/J.JVIROMET.2009.10.020

Vallbracht, M., Brun, D., Tassinari, M., Vaney, M., & Pehau-arnaudet, G. (2018). Structure-Function Dissection of Pseudorabies Virus Glycoprotein B Fusion Loops. *Journal of Virology*, *92*(1), 1–26.

van der Pol, E., de Rond, L., Coumans, F. A. W., Gool, E. L., Böing, A. N., Sturk, A., Nieuwland, R., & van Leeuwen, T. G. (2018). Absolute sizing and label-free identification of extracellular vesicles by flow cytometry. *Nanomedicine: Nanotechnology, Biology, and Medicine*, *14*(3), 801–810. https://doi.org/10.1016/j.nano.2017.12.012

van Iwaarden, J. F., van Strijp, J. A., Ebskamp, M. J., Welmers, A. C., Verhoef, J., & van Golde, L. M. (1991). Surfactant protein A is opsonin in phagocytosis of herpes simplex virus type 1 by rat alveolar macrophages. *American Journal of Physiology-Lung Cellular and Molecular Physiology*, *261*(2), L204–L209. https://doi.org/10.1152/ajplung.1991.261.2.L204

van Velzen, M., Missotten, T., van Loenen, F. B., Meesters, R. J. W., Luider, T. M., Baarsma, G. S., Osterhaus, A. D. M. E., & Verjans, G. M. G. M. (2013). Acyclovir-resistant herpes simplex virus type 1 in intra-ocular fluid samples of herpetic uveitis patients. *Journal of Clinical Virology*, *57*(3), 215–221. https://doi.org/10.1016/j.jcv.2013.03.014

Vlasak, J., Hoang, V. M., Christanti, S., Peluso, R., Li, F., & Culp, T. D. (2016). Use of flow cytometry for characterization of human cytomegalovirus vaccine particles. *Vaccine*, *34*(20), 2321–2328. https://doi.org/10.1016/j.vaccine.2016.03.067

Volker, L., Sandra, H., Ulrike, H., Francois, P., & Ralf, B. (2003). Viral and Cellular Determinants of Hepatitis C Virus RNA Replication in Cell Culture. *Journal of Virology*, *77*(5), 3007–3019. https://doi.org/10.1128/JVI.77.5.3007-3019.2003

Walters, K., Joyce, M. A., Addison, W. R., Fischer, K. P., Tyrrell, D. L. J., & Irol, J. V. (2004). Superinfection Exclusion in Duck Hepatitis B Virus Infection Is Mediated by the Large Surface Antigen. *Journal of Virology*, *78*(15), 7925–7937. https://doi.org/10.1128/jvi.78.15.7925-7937.2004

Wang, S., Hirose, S., & Ghiasi, H. (2019). The Absence of Lymphotoxin-α, a Herpesvirus Entry Mediator (HVEM) Ligand, Affects Herpes Simplex Virus 1 Infection In Vivo Differently than the Absence of Other HVEM Cellular Ligands. *Journal of Virology*, *93*(16), 1–15. https://doi.org/10.1128/jvi.00707-19

Whitley, R. J., Kimberlin, D. W., & Roizman, B. (1998). Herpes Simplex Viruses. *Oxford University Press*, *26*(3), 541–553.

Whitley, R. J., & Roizman, B. (2001). Herpes simplex virus infections. *Lancet*, *357*(9267), 1513–1518. https://doi.org/10.1016/S0140-6736(00)04638-9

Wojaczynski, G. J., Engel, E. A., Steren, K. E., Enquist, L. W., & Patrick Card, J. (2015). The neuroinvasive profiles of H129 (herpes simplex virus type 1) recombinants with putative anterograde-only transneuronal spread properties. *Brain Structure and Function*, *220*(3), 1395–1420. https://doi.org/10.1007/s00429-014-0733-9

Yedowitz, J. C., Kotsakis, A., Schlegel, E. F. M., & Blaho, J. A. (2005). Nuclear Localizations of the Herpes Simplex Virus Type 1 Tegument Proteins VP13/14, vhs, and VP16 Precede VP22-Dependent Microtubule Reorganization and VP22 Nuclear Import. *Journal of Virology*, *79*(8), 4730–4743. https://doi.org/10.1128/jvi.79.8.4730-4743.2005

Yuan, S., Wang, J., Zhu, D., Wang, N., Gao, Q., Chen, W., Tang, H., Wang, J., Zhang, X., Liu, H., Rao, Z., & Wang, X. (2018). Cryo-EM structure of a herpesvirus capsid at 3.1 Å. *Science*, *360*(6384). https://doi.org/10.1126/science.aao7283

Zhang, X. F., Zhang, S., Guo, Q., Sun, R., Wei, T., & Qu, F. (2018). A new mechanistic model for viral cross protection and superinfection exclusion. *Frontiers in Plant Science*,

9(January), 1–9. https://doi.org/10.3389/fpls.2018.00040

Zhou, Z. H., Chen, D. H., Jakana, J., Rixon, F. J., & Chiu, W. (1999). Visualization of tegument-capsid interactions and DNA in intact herpes simplex virus type 1 virions. *Journal of Virology*, *73*(4), 3210–3218. https://doi.org/10.1128/JVI.73.4.3210-3218.1999

Zou, G., Zhang, B., Lim, P.-Y., Yuan, Z., Bernard, K. A., & Shi, P.-Y. (2009). Exclusion of West Nile Virus Superinfection through RNA Replication. *Journal of Virology*, *83*(22), 11765–11776. https://doi.org/10.1128/jvi.01205-09

APPENDICES

APPENDIX A

CO-AUTHORED PUBLICATIONS

viruses

Published: 25 April 2018 doi: 10.3390/v1005220

viruses

MDPI

Article

A New Approach to Assessing HSV-1 Recombination during Intercellular Spread

Gabrielle A. Law, Alix E. Herr, James P. Cwick and Matthew P. Taylor *

Department of Microbiology & Immunology, Montana State University, Bozeman, MT 59717, USA; gabriellealaw@gmail.com (G.A.L.); alixeherr@gmail.com (A.E.H.); jpcwick@gmail.com (J.P.C.)
* Correspondence: mptaylor@montana.edu; Tel.: +1-406-994-7467

Received: 9 March 2018; Accepted: 20 April 2018; Published: 25 April 2018

Abstract: The neuroinvasive Herpes simplex virus type 1 (HSV-1) utilizes intergenomic recombination in order to diversify viral populations. Research efforts to assess HSV-1 recombination are often complicated by the use of attenuating mutations, which differentiate viral progeny but unduly influence the replication and spread. In this work, we generated viruses with markers that allowed for classification of viral progeny with limited attenuation of viral replication. We isolated viruses, harboring either a cyan (C) or yellow (Y) fluorescent protein (FP) expression cassette inserted in two different locations within the viral genome, in order to visually quantify the recombinant progeny based on plaque fluorescence. We found that the FP marked genomes had a limited negative affect on the viral replication and production of progeny virions. A co-infection of the two viruses resulted in recombinant progeny that was dependent on the multiplicity of infection and independent of the time post infection, at a rate that was similar to previous reports. The sequential passage of mixed viral populations revealed a limited change in the distribution of the parental and recombinant progeny. Interestingly, the neuroinvasive spread within neuronal cultures and an in vivo mouse model, revealed large, random shifts in the parental and recombinant distributions in viral populations. In conclusion, our approach highlights the utility of FP expressing viruses in order to provide new insights into mechanisms of HSV-1 recombination.

Keywords: alphaherpesvirus; HSV-1; recombination; fluorescent protein; cell–cell spread; neuroinvasion; neuron culture; intravitreal injection

1. Introduction

Herpes Simplex virus type 1 (HSV-1) is a persistent and pervasive human pathogen with global relevance [1,2]. Infections of HSV-1 typically manifest in the mucosal or epithelial surfaces. Occasionally, infections can manifest on the corneal surfaces of the eye. Invariably, all HSV-1 infections will spread into peripheral neurons. Once infected, the peripheral neurons remain persistently infected with HSV-1 for the lifespan of the host, spreading the virus either back to sites of primary infection or into neurons of the central nervous system, where it can cause severe encephalitis [3,4].

Recombination is a primary driver of the genomic diversity and evolution of HSV-1. In order for recombination to occur, cells within the host tissues must become infected by multiple virions. The viral genomes are then able to exchange DNA during replication, in order to generate the recombinant genomes, which are packaged into progeny virions. There is substantial evidence to indicate that HSV-1 recombination occurs at significant rates during infection and replication [5–7]. The next generation sequencing of HSV-1 from patients demonstrates that the diversity of viral genomes correlates with geographical clades [8,9]. Interestingly, all of the analyzed genomes show evidence of extensive recombination, which is suggestive of high rates of co-infection in human populations [10]. Recombination can lead to a generation of strains that are more pathogenic and/or resistant to current

anti-viral therapies. In fact, this inter-viral recombination is continuing to drive the alphaherpesvirus evolution. Chimeric genomes, resulting from recombination between HSV-1 and HSV type 2 (HSV-2), are circulating within patient populations [11]. The recombination between the wild-type and the attenuated vaccine strain of Varicella Zoster virus (VZV), a related alphaherpesvirus, has resulted in the generation of a new clade of VZV [12]. Knowing the frequency of recombination, as well as the factors which influence it, is an important part of understanding and treating the viral disease, and developing effective vaccines.

The mechanisms of inter-genomic recombination have been extensively studied for HSV-1 [13–15]. Recombination requires nuclear genome replication and occurs early during the replication of the HSV-1 double-stranded DNA genomes [16,17]. Despite all of this information, there have been issues regarding the definitive rates of HSV-1 recombination between in vitro and in vivo experimental models. It is clear that high rates of recombination occur in vivo, and that they can promote the development of novel, pathogenic isolates [18,19]. Many of these studies utilize viruses that are harboring mutations that facilitate the identification of parental and progeny genomes. While these mutations are useful for quantifying recombination, they often attenuate the virus to the point where its ability to replicate is considerably diminished, when compared to wild-type viruses. These attenuations inherently bias recombination experiments, so as to favor the replication of the non-mutant, non-marker bearing virus. To truly understand the rates and consequences of recombination, we will need to develop a system that does not utilize such strongly attenuated viruses to facilitate the easy, rapid detection of recombinant viral progeny following co-infection.

In the following study, we set out to engineer and characterize viruses with markers that did not significantly alter the kinetics of the infection, but would still allow for the accurate discrimination of parental and recombinant progeny. We did this by constructing fluorescent protein (FP), which expressed mutants that had limited attenuation compared with the wild-type HSV-1. Genetic cassettes bearing the FP markers were inserted at distant locations within the HSV-1 genome, at sites that were characterized as having a minimal effect on viral replication and fitness [20]. Following the characterization of viral replication and competition against wild-type HSV-1, we set out to analyze two major factors that contributed to intergenomic recombination: the rates of co-infection and intercellular viral transmission. To model the effect of the intercellular spread on recombination, we employed a combination of a sequential viral passage, a compartmentalized neuronal cell culture system, and an in vivo mouse model of the neuroinvasive viral spread.

2. Materials and Methods

2.1. Cells and Virus

Vero cells, a kind gift of the Enquist lab, were maintained in Dulbecco's Modified Eagle's Medium (DMEM), which contained 10% (*v*/*v*) fetal bovine serum and 1% penicillin/streptromycin. All of the steps of the viral isolation, analysis, and production were completed in Vero cells. All of the infections were performed with the HSV-1 strain 17, which was derived from a sequence verified isolate, provided by the Enquist lab. The viruses that were developed for the recombination expressing yellow fluorescent protein (YFP) with a nuclear localization sequence (NLS) (HSV-1 OK12, first described in [21] and referred to here in the manuscript as HSV-1 YFP_{UL}) and cyan fluorescent protein (CFP)-NLS (HSV-1 MT002 referred to as HSV-1 CFP_{US} in the manuscript), which were both derived from the HSV-1 strain 17.

2.2. Construction of FP-Expressing Viruses

HSV-1 YFP_{UL} was a previously described virus, which contained a genetic cassette that was inserted between the viral genes U_L37/U_L38, which allowed for a cytomegalovirus (CMV) driven expression of a nuclear localization sequence that was tagged eYFP [21]. HSV-1 CFP_{US} was a novel recombinant strain, which was isolated for this work with a similar genetic cassette inserted between

the viral genes U_S1/U_S2, however, this cassette encoded a nuclear localization sequence, which tagged Turquoise2. Both of the sites in the viral genome that were chosen for the insertion of this genetic cassette had been previously shown to tolerate genetic inserts without a reduction of viral titer [20].

The insertion of the Turquoise2 expression cassette required construction of a plasmid that contained a fluorophore expression cassette similar to HSV-1 OK12, which was flanked by homology arms that would promote the recombination into the U_S1/U_S2 region of the HSV-1 genome. Approximately 500 bp of the homologous sequence flanking the 5′ and 3′ of the Us 1/2 insertion site, was PCR amplified from purified HSV-1 strain 17 DNA. The Turquoise2 CMV driven expression cassette was PCR amplified from the plasmid vector, pMT06 [22]. All of the PCR amplification was done with a Q5 DNA polymerase mix (Qiagen, Hilden, Germany). The PCR products were visualized and isolated from a 1% agarose Tris-Acetate EDTA (TAE) gel followed by purification using gel extraction (Qiagen). All of the PCR products contained 15 bp of the homologous overlapping sequence in order to facilitate In-Fusion cloning (ClonTech, Mountain View, CA, USA) into a plasmid backbone, which contained ampicillin resistance. The generation of the final construct was achieved with a 3-way ligation reaction, followed by the transformation and isolation of resistant bacterial colonies. The positive recombinant clones were identified with a colony PCR. The resulting isolated and purified plasmid was verified by Sanger sequencing.

To isolate HSV-1 viruses with insertions in the U_S1/U_S2 locus, purified plasmids were linearized with an XmnI/XbaI double digest. The linearized plasmid was co-transfected with the purified HSV-1 strain 17 DNA into Vero cells. The resulting progeny plaques were screened for the Turquoise2 expression, followed by three subsequent rounds of plaque isolation in order to obtain high quality, stable, and pure isolates. All of the viral stocks were verified by fluorescence microscopy for maintenance of the FP expression. A minimum of 100 plaques were imaged to ensure a greater than 99% homogeneity of expression in the population of the viruses that were used for infections.

2.3. Microscopy

All of the fluorescent imaging was performed on a TiEclipse inverted fluorescence microscope (Nikon Instruments, Melville, NY, USA), which employed a motorized objective turret, motorized X–Y stage, and mechanical shutters for transmitted and fluorescent illumination. The fluorescence illumination was supplied by a SpectraX illuminator (Lumencor, Beaverton, OR, USA), which contained six high-intensity, band-pass restricted LED illuminators that were oriented for a single path of illumination. The excitation sources were paired with specific multi-pass dichroic mirrors and emission filters, including the CFP/YFP/RFP filter pairs (Chroma Technology Corp., Bellows Falls, VT, USA). To quantify the FP expression and frequency of phenotypes in the progeny viral populations, a multi-image tile was acquired from the viral plaque assays. For each image area, three channels were captured, which acquired a transmitted light, CFP, and YFP. The scoring of plaques was based on the FP expression as described below.

2.4. Quantification of Recombination

To assess the recombination frequency occurring during HSV-1 replication and spread, Vero cell monolayers were co-inoculated with equal amounts of HSV-1 CFP_{US} and YFP_{UL} at the indicated multiplicity of infection (MOI). Following a one-hour inoculation at 37 °C, the monolayer was washed with phosphate-buffered saline. The cells and supernatant that contained the progeny virions were harvested by scraping at the times the post-infection was indicated in each experiment. The infected samples were then subjected to one freeze–thaw cycle, ultra-sonicated, and titer evaluated by the plaque assay. The resulting plaques were imaged for the FP expression of individual plaques. The plaques that fluoresced only a single color were denoted as a parent genome and those that fluoresced two colors or those with no detectable fluorescence, were counted as a recombinant progeny.

The influence of the multi-cycle replication on HSV recombination was determined by passaging virion progeny from cells co-infected with the two FP-expressing viruses. The progeny from a Vero cell

monolayer co-inoculated at an MOI of 10, of HSV-1 CFP_{US} and YFP_{UL}, was harvest as described above. The progeny was plated at limiting dilutions onto cell monolayers in order to determine the viral titer and to quantify the marker expression in the plaques. This progeny, termed inoculum, was then used to infect the Vero cells at an MOI of 10. The resulting progeny of this first, and subsequently second and third, rounds of passage (a total of three sequential rounds of infection and amplification) was analyzed for viral titer and fluorescent examination in order to quantify the distribution of the plaque phenotypes. The statistical analysis of the resulting plaque phenotype distributions was performed in GraphPad Prism 7.0 software (GraphPad Software, La Jolla, CA, USA).

2.5. Compartmentalized Neuronal Cultures

Neuronal cultures were constructed with a trichamber design, as previously described [23,24]. Briefly, primary mouse superior cervical ganglions (SCG) were dissected from embryos, which were harvested at day 13.5 to 14.5 from pregnant C57Bl/6 mice. Plastic tissue culture dishes were coated with poly-ornithine (Sigma-Aldrich, St. Louis, MO, USA), followed by murine laminin (ThermoFisher Scientific, San Francisco, CA, USA), before culturing. Parallel groves were etched into the surface of culture dishes and covered by 1% methylcellulose in 1× DMEM. Autoclaved vacuum grease was applied to one side of CAMP320 Teflon three compartment rings (Tyler Research, Edmonton, Alberta, CA, USA). The Teflon rings were then placed on the tissue culture dishes so that the parallel groves were perpendicular to, and extended across all of the compartments. The dissociated SCG neurons were plated into one of the side compartments, which was labeled the cell body compartment. The SCG cultures were maintained in a neuronal media comprising of Neurobasal Media, which was augmented with 1% penicillin/streptomycin-glutamine, B27 supplement, and 50 ng/mL Neuronal Growth Factor 2.5S (ThermoFisher Scientific), until axons had penetrated and grown into the far axon compartment, which took approximately 17–25 days.

A monolayer of ~5×10^5 Vero cells in 1% FBS supplemented neuronal media was plated in the far axon compartment one day prior to infecting the compartmentalized neuronal cultures. Before infecting the cell body compartment with the virus, the media in the middle compartment was replaced with 1% methylcellulose supplemented neuronal media. The compartmentalized SCG cultures were infected with 1×10^6 pfu of each parent virus in conditioned neuronal media at the cell body compartment. Following the one-hour incubation, the inoculum was replaced with the original volume of media in the compartment. The cell body and axon compartments were both harvested after 48 h, followed by an evaluation of the viral titer and progeny marker expression, as described above.

2.6. Intravitreal Inoculation and Tissue Harvesting

The murine eye model was used to understand the influence of the HSV spread in neurons on diversity through recombination. We adapted the inoculation and tissue harvesting from the extensive work of J. Patrick Card [25,26]. Briefly, the murine eye model utilized the nervous system connections with defined retrograde and anterograde circuits in mice, in order to analyze the neuroinvasive spread. Primary inoculum was contained within the mouse's eye, resulting in replication within the retinal cells. The virus spread to the brain occurs along synaptic connections with both the optic and oculomotor nerve fiber tracts.

All of the procedures with mice were submitted and approved through Montana State University's Institutional Animal Care and Use Committee and conformed to the best practices, as defined by AALAC and the Office of Laboratory Animal Welfare guidelines. For all of the experiments, we used male mice between 8 and 12 weeks of age. The mice were anesthetized with isoflurane and ~1×10^6 pfu (approximately 2 µL) of an equal inoculum of HSV-1 CFP_{US} and YFP_{UL} was injected intra-vitreally into the right eye. The infected mice were sacrificed after 72 h, using a pentobarbital solution (fatal plus) followed by cardiac perfusion with saline. Each skull was manually removed and the brain and infected eye were harvested and placed in Hank's Balanced Saline Solution (HBSS) prior to processing. Each brain was dissected to isolate sub-regions, which reflected the different

routes of spread. Briefly, each brain was placed in an adult mouse brain matrix (Zivic Instruments, Pittsburgh, PA, USA). First, two parallel slices were made at positions 6 and 12. Then, each brain was sliced in half to separate the left and right hemisphere. These slices allowed for the isolation of the two halves of the midbrain and the hindbrain. Based on the eye of injection, the midbrain sections were identified as being on the same side (ipsilateral) or the opposing side (contralateral). To obtain viral titers from the dissected tissue, we adapted a protocol from previously published methods [27]. Briefly, the dissected tissue sections were diluted in equivalent amounts of HBSS and snap-frozen in either liquid nitrogen or dry ice/ethanol, prior to storage at −80 °C. Following the rapid thawing, the tissues were homogenized by extensive trituration with a wide bore Pasteur pipet. The homogenized samples were ultra-sonicated and centrifuged at 1000 rpm in order to pellet large debris. The clarified supernatant was the source of the material that was used to assess the viral titer and quantification of progeny plaque phenotypes.

3. Results

3.1. Adapting Two-Color Fluorescent Protein Expression to Monitor Recombination

To assess intergenomic viral recombination, we sought to develop a FP based marker transfer assay. We isolated two viruses that contained genetic cassettes expressing fluorescent proteins inserted at distant sites in the viral genome (Figure 1). These cassettes were inserted into the HSV-1 strain 17 genome, at sites that had been previously found to tolerate genetic insertions with limited impact on viral replication and spread [20]. The first virus contained an insert between the viral genes $U_L37/38$ that drove the expression of a nuclear localized YFP (referred to as HSV-1 YFP_{UL}). The second virus contained an insert between the viral genes $U_S1/2$ that expressed a nuclear localized CFP (referred to as HSV-1 CFP_{US}). The genetic distance between the insertion sites allowed for many potential recombination events to be visualized, based on changes in the FP expression. Co-infection with HSV-1 CFP_{US} and YFP_{UL} could result in four distinct viral progeny phenotypes, based on the FP expression in the viral plaques. The viral plaques that expressed either the YFP or CFP fluorescence were classified as progeny of parental genomes. Viral plaques that exhibited either a dual FP expression or no FP expression were classified as a progeny resulting from intergenomic recombination between the parental genomes (Figure 1A).

An important part of our analysis was the capability to rapidly and correctly identify plaque phenotypes. Plaques that expressed both of the FP's could result from either recombination or from a mixture of multiple viruses amplifying in the same region of the cell monolayer. The distribution of the FP expression in the plaque could be used to discriminate the dual FP expressing viruses from the plaques that were initiated by multiple viruses (Supplemental Figure S1). We only observed mixed plaque phenotypes in approximately 1.5% of the population of the plaques, and all had revealed non-homogenous FP expression, which was often "sectored". The frequency of mixed plaques was in line with prior observations that used mixtures of three HSV recombinants, each expressing a fluorophore in the same cassette. When assessing the distribution of plaques, we also observed that approximately 2% of plaques contained more than one fluorescent protein (an unpublished observation from [21]). Since these fluorescent protein cassettes were inserted in the same position, the only way to express the multiple fluorophores was from multiple viral genomes initiating the plaque. Importantly, the rate of the mixed plaque formation correlated with the concentration of the virus that was present in the diluted sample, plated onto cells for visualization. These parallel observations confirmed that the mixed plaques occurred infrequently and that the majority of the plaques were initiated by a single genome. Based on this interpretation, we continued to characterize the FP expressing viruses.

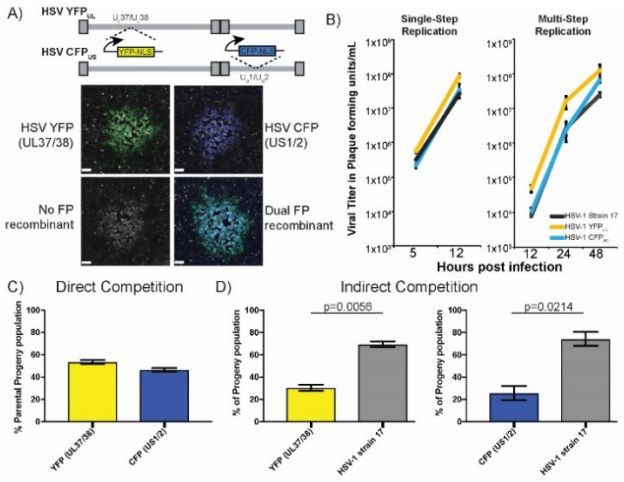

Figure 1. Characterization of the genetically tagged Herpes simplex virus (HSV) genomes. (**A**) Schematic representation of the fluorescent protein expression cassette location on the HSV-1 genome. Boxes represent large terminal and internal repeat sequences. Expression cassettes for yellow fluorescent protein (YFP)- and cyan fluorescent protein (CFP)-NLS proteins have been inserted in the UL36/37 and US1/2 loci, respectively. The genetic insertions result in different fluorescent expression phenotypes of the resulting viral plaques (images in panels below, scale bar = 100 µm). Parental infections result in YFP and CFP positive plaques. Upon co-infection, the genomes can recombine, producing progeny containing both of the genetic cassettes. Those plaques will either express both of the fluorescent proteins (Dual FPs) or the lack fluorescent protein expression (No-FP); (**B**) single step replication plots of parent viral isolates; HSV YFP_{UL}, HSV CFP_{US}, and HSV-1 strain 17. The proportion of the viral progenies were plotted following the (**C**) direct competition assay between parent viruses and the (**D**) indirect competition assay against HSV-1 strain 17. The indicated FP expressing HSV virus or HSV-1 strain 17 were co-infected at an MOI of 10 for each virus. The total infected cells were harvested at 8 hpi. The harvested virus was plated at a limiting dilution on the cell monolayers and plaques and was scored based on the fluorescent protein expression. A statistical *t*-test comparison of the direct and indirect competition assays revealed significant differences between the wild-type and FP expressing viruses.

To assess HSV recombination, the parental viruses, HSV-1 CFP_{US} and YFP_{UL}, needed to have similar capabilities of viral replication, or fitness, to each other. Ideally, these viruses would also maintain replication and spread capabilities that were comparable to the wild-type HSV-1. Initially, we compared the capacity of these viruses to replicate under conditions of single-step and multi-step replication (Figure 1B). The cells were inoculated with each virus at the indicated MOI's, and were subsequently harvested at the indicated times, post-infection. The viral titer was assessed to measure the extent of the viral replication. We observed that the resulting viral growth kinetics were comparable for the three viruses and those viruses maintained the expression cassette during both the single and multi-step replication experiments. Viral fitness was further evaluated by looking at direct and indirect competition during mixed infections. The competition assays assess the fitness as a function of the viral ability to produce progeny when competing for resources. If two viruses have a similar fitness, they should have produced similar amounts of progeny. Direct competition was assessed by infecting cells

with equal amounts of HSV-1 CFP_{US} and YFP_{UL}. The resulting viral progeny were evenly distributed between the YFP and CFP expression, indicative of close to equal fitness between the two viruses (Figure 1C). Indirect competition was assessed by co-inoculating either HSV-1 CFP_{US} and YFP_{UL} with the parental HSV-1 strain 17. Under these conditions, there was an apparent reduction in both the CFP and YFP plaques, compared with the non-fluorescent plaques (Figure 1D). The resulting progeny were 70% non-fluorescent expressing, indicative of a moderately greater fitness of the wild-type virus, compared with the FP cassette containing viruses. Notably, both CFP_{US} and YFP_{UL} had the same apparent reduction in the amount of progeny when in competition with strain 17, which confirmed their equivalent relative fitness. Despite the reduced fitness of both viruses, these viruses demonstrated a significant improvement in fitness, with respect to previous studies on recombination. Importantly, the FP expressing viruses had an equivalent, if not slightly greater, capacity to replicate, compared with the wild-type viruses (Figure 1B). The direct and indirect comparison of fitness were not previously evaluated for the marked viruses that were used in prior recombination studies. The results indicated that a minimal impact was incurred on viral replication by insertion of either of the FP expression cassettes, which favored the continued experimentation with these new tools, in order to analyze the viral recombination.

3.2. Evaluation of Intergenomic Recombination

Since there was little effect on the replication and progeny production of HSV-1 CFP_{US} and YFP_{UL}, we proceeded to analyze the production of recombinant progeny during viral replication. To evaluate whether the amount of recombinant progeny that was produced was influenced by the time of the replication, we harvested cells over the course of a single replication cycle and assessed the progeny phenotypes by fluorescent microscopy. A balanced inoculum, which consisted of both HSV-1 CFP_{US} and YFP_{UL} at MOI 10 was used to infect cells. The cells were harvested at the indicated times, post co-infection, and the resulting plaque forming units were analyzed for FP expression. No recombinant progeny was detectable at 0 or 3 h post co-infection, which coincided with the eclipse phase of HSV-1 replication. The recombinant plaque phenotypes were detectable starting at 6 h post-infection, comprising 20% of the total analyzed plaque population (Figure 2A). This percentage of the recombinant plaques remained constant for the remainder of the collected time points. In addition to the recombinant progeny, all of the phenotypes remained at a relatively similar proportion of the population through the entire viral replication cycle. Our observations indicated that the production of recombinant progeny appeared to be constant throughout the course of viral replication. Importantly, we observed equivalent amounts of both recombinant phenotypes, which supported the argument that the FP-cassettes were not causing skewing of the recombinant progeny.

The ability to generate recombinant progeny was most likely influenced by the extent of cellular co-infection. The level of co-infection was positively correlated to the inoculating dose that was used during the experimental infections. We determined the influence of the inoculating dose on recombination by manipulating the MOI of the HSV-1 CFP_{US} and YFP_{UL} that were used to initially co-infect the cells. The cells were co-infected at the indicated MOI of infection, which was allowed to proceed for eight hours before the cells were harvested and the viral titer was quantified. The expression of the FP's was assessed through the plaque assay and microscopy (Figure 2B). We observed that recombinant progeny increased as a function of the MOI of infection. At an MOI of 50, there appeared to be saturation, as the frequency of recombinant progeny only slightly increased. We also observed that at a low MOI of 0.1, there were significant amounts of recombinant progeny that were produced, making up approximately 7.6% of the total plaque population. Based upon the distribution of the recombinant progeny that was produced across the range of MOI's, we chose to represent the data with a semi-log plot visualization, which revealed a near linear correlation between the recombinant progeny production, as a function of the inoculating dose. When taken together, the data supported the conclusion that the FP expression cassettes could be used to monitor recombination during HSV-1

co-infection. Further, our results were concordant with the previous reports on recombination rates and the timing of recombinant production during HSV-1 replication [13–15].

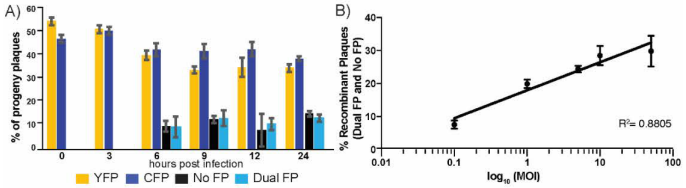

Figure 2. Effects of time and MOI on recombinant progeny output. (**A**) The effect of time during replication was assessed by counting the distribution of the fluorescent plaques during a time course of viral infection. Cells were infected at an MOI of 10 and subsequently harvested at 0, 3, 6, 9, 12, and 24 h post-infection. Infected cell lysates were plated at a limiting dilution and the resulting progenies were scored for the number of fluorescent plaques from each of the four genome types; (**B**) the effect of MOI on the total recombinant progeny production was assessed by differential inoculation. Vero cells were inoculated at an MOI of 0.1, 1, 5, 10, or 50 of the HSV YFP and HSV CFP viruses and the viral progeny was harvest at 8 hpi. As MOI increases, the frequency of the recombinant progeny increases with logarithmic progression. When the data are expressed as a plot of % recombinant progeny versus the $\log_{10}$ value of the MOI, the resulting linear slope is achieved with a logarithmic regression. Presented is a representative experiment involving replicates of three at each MOI that was evaluated, with standard deviation plotted between replicates.

3.3. Stable Distribution of Recombinant Progeny during Sequential Passage

Next, we wanted to understand whether the resulting recombinant progenies were influenced by intercellular spread. To address this question, we utilized sequential rounds of viral infection in immortalized epithelial cells, in order to understand changes in the viral populations. After the initial recombination events produced diverse populations, the viral population dynamics over several replication cycles were assessed by a serial passage of progeny. Following an initial co-infection with HSV-1 CFP_{US} and YFP_{UL}, the progeny virus was sequentially passaged for three subsequent rounds of infection (Figure 3).

The viral populations that were sampled at each passage were assessed for the distribution of the FP expressing plaques. The initial population (inoculum) contained about 28% recombinant progeny, equally split between the dual FP-expressing and dark recombinants. At passage 1, the population contained approximately 32% recombinant progeny, with a slightly higher proportion of dark recombinants (16%) than the dual FP recombinants (15%). The total number of recombinants as a proportion of the population appeared to equilibrate at around 35%, by passage 2. Between the four plaque phenotypes, only the non-FP expressing population exhibited a slight, statistically significant, increase in the portion of the total viral population. The three other plaque phenotypes had equivalent slight decreases that were within the inter-sampling error between the replicates. Importantly, even after three serial passages, no single phenotype overtook a substantial proportion of the population. Parallel experiments using an MOI of 1 also produced similar results. These observations indicated that continued co-infection between the 4 possible genome configurations does not lead to dominance by any one viral genome, supporting our conclusion that the FP expression cassettes have limited effects on viral replication. Additionally, the apparent reductions of fitness that were observed during the indirect competition for the FP expressing viruses only resulted in a modest enrichment in the no-FP recombinant populations. This enrichment in no-FP recombinants was not detectable until the 2nd and 3rd passage of the population. These findings supported our conclusion that the FP cassettes

were not skewing the resulting recombinant progeny populations and had a minimal effect on the replication and dissemination of these viruses.

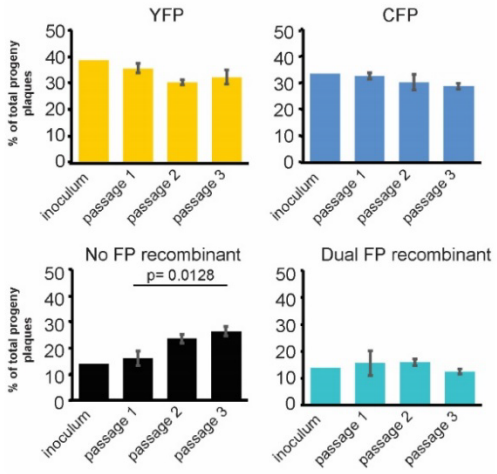

Figure 3. Recombinant progeny after multiple cycles of infection. A mixed population of HSV-1 viruses were generated following co-infection (inoculum) and progeny viruses were sequentially passaged three times. The inoculum and each subsequent passage were analyzed for content of the individual FP expression. Each plaque phenotype is plotted as a percent of the total plaque distribution. Data represents the average of the triplicate samples, with error bars as the standard deviation between replicates. Significant changes were only observed in the No-FP populations, as evaluated by one-way ANOVA.

3.4. Recombination during Transneuronal Spread

We were very interested to understand whether neuronal infection and spread had any impact on the recombinant progeny production. To address this concept, the recombination assay was implemented in a compartmentalized neuronal chamber, in order to determine the influence of neuronal replication and spread on the recombinant progeny production. The compartmentalized neuronal cultures were a model for neuronal infection and axonal spread of HSV-1 [23,24]. As depicted in the model diagram, the culture generated three distinct compartments, which separated the neuron cell bodies from the axon terminals, which allowed for the controlled inoculation of cell bodies and discrimination from the resulting axonal spread (Figure 4A). The Vero cells were plated on the exposed axons, to act as detector cells that received and amplified the infectious progeny. A balanced inoculum of HSV-1 CFP_{US} and YFP_{UL} was used to co-infect the neuronal cell bodies. The infection was allowed to progress for 48 h, at which point neuronal replication, axonal spread, and amplification in the detector cell layer had reached a maximum [21,24]. The progeny populations were plated at a limiting dilution and the plaque phenotypes were analyzed by fluorescent microscopy. Across a total of eight neuronal cultures, we consistently observed higher numbers of recombinant progeny in the neuronal cell body compartment compared with the axon compartment. On average, 38.6 $\pm$ 4.9 percent of the viral progeny in neuronal cell body compartments were recombinant. In the far axon compartments, where the infectious virions were transported and subsequently amplify in the detector cell layer, 29.3 $\pm$ 8.7

percent of viral progeny were recombinant (Figure 4B). Interestingly, there was a larger variance in phenotype distribution between replicates and the statistically significant shift in both CFP and No-FP populations in samples from the axon compartment. This variance was not related to differences in the total viral titer. One complication in interpreting these differences was the recombination that could have occurred during amplification of virus in the layer of detector Vero cells. However, this effect was likely minimal, based on the previous reports of limited viral co-infection following the axon-to-cell spread of the HSV-1 in this neuronal model [21]. We could conclude that the diverse viral populations that were generated in the cell body compartment transmitted the infection via the axonal spread to the epithelial cells, with only small changes in the composition and diversity of the viral population.

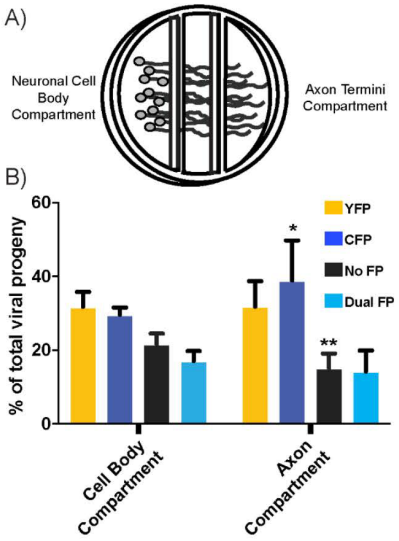

Figure 4. Effect of transneuronal spread on populations of recombinant viruses. (**A**) A schematic representation of the compartmentalized neuronal culture system. Briefly, a Teflon ring is attached to the culture surface. Dissociated superior cervical ganglions (SCG) neurons are plated in the left cell body compartment. Those cell bodies extend axon projections under the two internal walls, resulting in isolated axon termini in the Axon Compartment. Prior to infection, detector cells (not depicted in diagram) are plated in the axon compartment to amplify infectious progeny that transmit via axon-to-cell spread; (**B**) after 48 h of the cell body compartment inoculation, both compartments were harvested and plated at limiting dilution. The plaques developing from the viral progeny were analyzed for the distribution of FP expression in the cell body and axon compartments. * denotes $p < 0.05$, ** denotes $p < 0.005$ as identified through pairwise *t*-test comparison.

3.5. Recombinant Progeny Production during Transneuronal Spread In Vivo

To observe the effect of trans-neuronal spread on recombination in vivo, we adapted our HSV-1 recombination assay to a mouse-eye model of neuroinvasive spread. When HSV-1 invades the central nervous system, infectious virions were transmitted between neurons at or near neuronal synapses. An effective method of modelling the central nervous system (CNS) invasion by HSV-1, was to use a murine model of the intravitreal viral inoculation. In this system, we were able to control the levels of

primary co-infection and monitor the recombination rates as the virus spread from the eye into the CNS [26,28]. This system had the added benefit that all of the tissue was accessible, allowing the direct assessment of the viral populations at different stages of the spread in the mouse brain. The primary infection occurred within the cells of the ciliary body and in the retinal ganglion cell layers after the intravitreal injection into the right eye of the mouse. Following primary infection, progeny virions were transported within innervating nerve tracts. From the retinal ganglia cells the infection was transmitted via the optic nerve into the regions of the midbrain contralateral to the site of the injection. Similarly, from cells of the ciliary body the infection spread via the oculomotor nerve to the ipsilateral sites in the midbrain. Subsequently, the infection underwent one to two more synaptic transmissions before it reached neurons in the hindbrain (Figure 5A) [26,29].

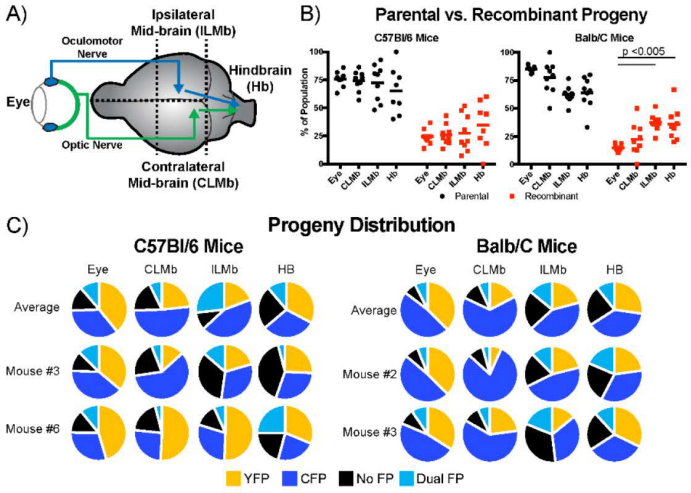

Figure 5. Effect of neuroinvasive spread on populations of viruses in vivo. (**A**) A schematic of the murine eye model for neuroinvasive spread; (**B**) frequency of parental progeny and recombinant progeny obtained from the eye, contralateral midbrain (CLMb), ipsilateral midbrain (ILMb), and hindbrain (Hb). Data presented are the summation of the two experiments for both C57Bl/6 and Balb/C mice. Each experiment contained between four and five mice; (**C**) distribution of FP distributions from the eye, CLMb, ILMb, and Hb are plotted. The top row shows the average distribution of plaques for the our sites in both C57Bl/6 and Balb/C mice. The lower rows are two example distributions from independent mice from each experimental group. Significant differences indicated were identified by two-way ANOVA analysis.

The analysis of the recombinant viral populations following neuroinvasive spread was done on tissue that was extracted from the eye, the ipsilateral and contralateral midbrain, and the hind brain. To understand whether the host's genetic background had influenced the potential outcomes, we compared infections in both Balb/c and C57Bl/6 inbred lines of mice, which exhibited differing susceptibilities to HSV-1 infection [30]. In both lines of mice, the primary replication in the eye exhibited distributions that roughly paralleled our results from the cultured cells, with between 20–25% of the viral progeny being the product of a recombination event. We observed more recombinant progeny as the virus spread deeper into the brain, which indicated a positive correlation between the number of

the spread events and the relative proportion of the recombinant progeny in the population (Figure 5B). The amount of variability that was observed between the animals with respect to the diversity of viral populations also increased with trans-neuronal transmission events. There appeared to be more variation between the viral populations in the C57Bl/6 and Balb/c mice, as well as more differences in the production of the recombinant progeny. In the Balb/c mice, the eye and the contralateral midbrain (CMb) populations had a similar frequency of recombinant progeny. However, the frequency of recombinant progeny was significantly different in the ipsilateral midbrain and hindbrain sites (ILMb and Hb, respectively). There was an increased variability in the parental and recombinant genotypes between the individual mice and between the sites of the infection in the same mouse (Figure 5C). On average, the viral populations in the C57Bl/6 mice favored the expansion of the no-FP viral populations, especially in the hindbrain. In contrast, the Balb/C mice supported higher levels of the CFP_{US} virus. Curiously, the variation in the distribution of the viral populations at different sites in the same animal were very large. From these distributions, we concluded that the changes to the viral populations were greater than what was expected from the sequential passage or the single transneuronal spread experiments. Importantly, for this method, there was no apparent selective advantage that was driving the outgrowth of the viruses that lacked the FP expression cassettes. The sum of our observations supported our rationale for using limited attenuated viruses in order to track recombination in the various models of the intercellular spread.

4. Discussion

We set out to analyze the recombination during HSV-1 infection using viruses that contained the FP expression cassettes, which would have little detrimental effect on viral fitness. Using two viruses that maintained high levels of relative fitness, we found that the extensive recombination between genomes produced upwards of 30% of the viral progeny expressing recombinant phenotypes. The mixed populations of the viruses that were generated by recombination, revealed a limited change during the sequential passage and during one round of transneuronal spread. Interestingly, distributions of viral populations changed dramatically during neuroinvasive spread in an animal model of infection. We concluded that the FP expressing viruses were a new way to monitor recombination mediated change in mixed viral populations. Further studies could employ pairs of viruses that harbor the FP cassette at differing genomic sites or that contained it on different genomic backgrounds. Additionally, an analysis of the selection pressure effects could take advantage of closely paired FP genetic markers.

One of the biggest goals of our research was the development of marked viral genomes with limited attenuation on the viral replication or spread. The added benefit of using FP expression was the simple and rapid discrimination between parental and recombinant viral progeny. While the measurement of the viral replication did not reveal any differences between the FP expressing viruses, the indirect competition of the two viruses against the parental HSV-1 strain 17 did reveal reductions in competitive fitness. It is worth noting that the differences in the replication were amplified because of the nature of the analysis; each gain of one virus came at the detriment to the other. In fact, the sequential passaging of the mixed viral populations suggested there was only a small fitness advantage that was afforded to the genomes that lacked the FP expression cassettes. It was also not surprising, given that the added genome content of about 3 kb of DNA per genetic cassette, that each of the FP expressing viruses would influence the replication and virion assembly [20,31]. Furthermore, the evaluation of the mixed viral populations in the neuronal models of the infection did not reflect any strong pressure against the maintenance of the genetic cassettes. Together these data indicated that the insertion of the FP expression cassette had limited influence on viral replication and was not unfavorably skewing the results of our experiments in order to analyze recombination.

The overall extent of recombination that was observed and the independence of the recombinant progeny from the time during the viral replication were completely in line with prior observations [32–34]. Additionally, the dependence of the recombinant output on the MOI was also in line with prior observations and expectations. Interestingly, the frequency of recombinant progeny

as a function of the MOI resulted in a surprisingly close linear response when it was modeled as a logarithmic function. At the lower end of the MOI range we observed a surprisingly high rate of recombinant progeny production. The extent of the recombinant production at an MOI of 0.1 was in line with the expected extent of the co-infection, based on the Poisson-based distributions of co-infection. In contrast was the apparent saturation of recombinant progeny production at the highest amounts of viral inoculum. The saturation could be best explained by the apparent limitation on the number of viral genomes that could replicate in a cell [35,36]. As the MOI exceeded the carrying capacity of the cell for viral genomes, so too would the capability to produce the recombinant progeny be limited. Together, the variables of the co-infection and limitations on the viral genome replication were both influencing the rate of the recombination in our experiments.

An unfortunate limitation of our approach was the inability to calculate an absolute rate of recombination, during HSV-1 replication. Calculating the rate of recombination would have required some assumptions that were not supported by prior research. Firstly, we would need to know the absolute distance between the two genetic markers. However, the ability of the HSV-1 genomes to change the relative orientation between the U_L and U_S regions leads to four different genome isomers [37]. The resulting genetic distance between our two genetic cassettes then ranged from as little as 50 kb to upwards of 110 kb. The second assumption was that recombination occurred at an even rate across the viral genome. However, prior research suggested that so called "hot-spots" for recombination correlate with small and large repetitive DNA elements scattered throughout the HSV-1 genome [19]. The largest limitation was in the assessment of the recombinant progeny. The assay that we developed only detected recombination upon the exchange of the expression cassette; we were unable to detect the recombination reactions outside of the two cassettes or as the result of a double cross-over event between the cassettes. It was even more complicated when analyzing the sequential passage and neuroinvasive spread data. After the initial co-infection produced the recombinant progeny, that progeny underwent co-infection and recombination with the myriad combinations of the viral genomes. The high rate of the recombinant progeny that was produced from the first cycle of the co-infection would then have influenced the reversion of the genomes back to the parental phenotypes at an equivalent rate to the production of new recombinant phenotypes. Despite an inability to calculate an absolute rate of recombination, there were many advantages to the approach we took that could continue to provide insights into HSV-1 recombination.

The strategy of the fluorescent marker transfer to analyze HSV-1 recombination already highlighted one outstanding issue in the field. By combining our fluorescent markers with an in vivo model of the neuroinvasive spread, we were able to observe the same larger apparent rates of recombination that others had reported for in vivo infections [5,19,38,39]. The difference was that our FP expressing viruses were comparably fit, with an equal capacity to infect and replicate. A comparison of the phenotype distributions during the neuronal infection and spread did not reveal major changes that would unduly skew the interpretation of the recombinant progeny. The relative similarity was likely why we saw that the initial production of the recombinant progeny at the sites of injection in mice mirrored our results from cultured cells. The resulting distributions of FP phenotypes diverged from our cultured experiments as the mixed viral populations spread into the brain. After undergoing multiple cycles of neuronal replication and transneuronal spread there was a great divergence between the individual samples, which became most amplified in the hindbrain. The apparent enrichment of No-FP viruses in the C57Bl/6 mice potentially mirrored the enrichment that we observed during the sequential passage. In contrast, the enrichment of the CFP_{US} virus in the Balb/C mice may have reflected some gain in the neuronal infection, replication, or spread, which was moderately indicated in the compartmentalized neuronal cultures. Intriguingly, multiple animals supported the recombinant plaque populations that exceeded 50% of the total virion population. This enrichment in recombinant progeny was most likely due to the stochastic selection processes that were enforced on the population of viruses that were transmitted between neurons. Limitations on the extent of the co-infection and on transneuronal spread of viruses were observed in a number of in vitro and in vivo systems [21,40].

With this assay, it was now possible to identify the effect and potential mechanisms of such stochastic selection on viral evolution.

There is great potential for the strategy of genetically tagged genomes in order to produce new findings in the HSV-1 recombination. Despite the limitation that one pair of markers cannot elucidate the true rate of recombination, a strategy employing multiple different pairs of FP cassette containing genomes would be able to overcome many of the limitations and assumptions. Similarly, we can pair the fluorescent cassettes with the attenuating mutations to evaluate how recombination drives viral evolution in different infection models. The pair of viruses we have developed can already be exploited as an easy read-out for recombinant progeny, in order to evaluate the effect of gene disruption or chemical inhibition on viral and cellular pathways, which are hypothesized for their importance in HSV-1 recombination. In summary, we have established a strong foundation for the continued development of viral genomes harboring FP expression cassettes, in order to analyze HSV-1 recombination.

Supplementary Materials: Supplementary materials can be found at http://www.mdpi.com/1999-4915/10/5/220/s1.

Author Contributions: Gabrielle A. Law and Matthew P. Taylor conceived and designed the experiments; Gabrielle A. Law, Alix E. Herr, and James P. Cwick performed the experiments; Gabrielle A. Law and Matthew P. Taylor analyzed the data; Gabrielle A. Law, Alix E. Herr, and Matthew P. Taylor wrote the paper.

Acknowledgments: We thank J. Patrick Card for his guidance and training in intravitreal inoculation. We also would like to thank Kyle Hain and Irina Kochetkova for their insight and constructive criticism on the manuscript. Funding of Gabrielle Law, Alix E. Herr, James P. Cwick and Matthew P. Taylor was provided by the National Institutes of Health Career Development Award [K22106948-01A1] and IDeA Program grant GM110732 [8P20GM103500-10]. Further support for Alix E. Herr and Matthew P. Taylor was provided by the Montana Agricultural Experiment Station. Gabrielle Law also received funding from an INBRE undergraduate research program at MSU, supported by the National Institute of General Medical Sciences of the National Institutes of Health [P20GM103474].

Conflicts of Interest: The authors declare no conflict of interest.

References

1. Smith, J.S.; Robinson, N.J. Age-specific prevalence of infection with herpes simplex virus types 2 and 1: A global review. *J. Infect. Dis.* **2002**, *186* (Suppl. 1), S3–S28. [CrossRef] [PubMed]
2. Whitley, R.J.; Roizman, B. Herpes simplex virus infections. *Lancet* **2001**, *357*, 1513–1518. [CrossRef]
3. Granerod, J.; Ambrose, H.E.; Davies, N. Causes of encephalitis and differences in their clinical presentations in England: A multicentre, population-based prospective study. *Lancet* **2010**, *10*, 835–844. [CrossRef]
4. Tsatsos, M.; MacGregor, C.; Athanasiadis, I.; Moschos, M.M.; Hossain, P.; Anderson, D. Herpes simplex virus keratitis: An update of the pathogenesis and current treatment with oral and topical antiviral agents. *Clin. Exp. Ophthalmol.* **2016**, *44*, 824–837. [CrossRef] [PubMed]
5. Loncoman, C.A.; Vaz, P.K.; Coppo, M.J.; Hartley, C.A.; Morera, F.J.; Browning, G.F.; Devlin, J.M. Natural recombination in alphaherpesviruses: Insights into viral evolution through full genome sequencing and sequence analysis. *Infect. Genet. Evol.* **2017**, *49*, 174–185. [CrossRef] [PubMed]
6. Thiry, E.; Meurens, F.O.; Muylkens, B.T.; McVoy, M.; Gogev, S.; Thiry, J.; Vanderplasschen, A.; Epstein, A.; Keil, G.N.; Schynts, F.D.R. Recombination in alphaherpesviruses. *Rev. Med. Virol.* **2005**, *15*, 89–103. [CrossRef] [PubMed]
7. Burrel, S.; Boutolleau, D.; Ryu, D.; Agut, H.; Merkel, K.; Leendertz, F.H.; Calvignac-Spencer, S. Ancient Recombination Events between Human Herpes Simplex Viruses. *Mol. Biol. Evol.* **2017**, *34*, 1713–1721. [CrossRef] [PubMed]
8. Szpara, M.L.; Gatherer, D.; Ochoa, A.; Greenbaum, B.; Dolan, A.; Bowden, R.J.; Enquist, L.W.; Legendre, M.; Davison, A.J. Evolution and diversity in human herpes simplex virus genomes. *J. Virol.* **2014**, *88*, 1209–1227. [CrossRef] [PubMed]
9. Kolb, A.W.; Ané, C.; Brandt, C.R. Using HSV-1 Genome Phylogenetics to Track Past Human Migrations. *PLoS ONE* **2013**, *8*, e76267. [CrossRef] [PubMed]

10. Bowden, R.; Sakaoka, H.; Donnelly, P.; Ward, R. High recombination rate in herpes simplex virus type 1 natural populations suggests significant co-infection. *Infect. Genet. Evol.* **2004**, *4*, 115–123. [CrossRef] [PubMed]
11. Koelle, D.M.; Koelle, D.M.; Norberg, P.; Norberg, P.; Fitzgibbon, M.P.; Fitzgibbon, M.P.; Russell, R.M.; Greninger, A.L.; Huang, M.-L.; Stensland, L.; et al. Worldwide circulation of HSV-2 × HSV-1 recombinant strains. *Sci. Rep.* **2017**, *7*, 44084. [CrossRef] [PubMed]
12. Norberg, P.; Depledge, D.P.; Kundu, S.; Atkinson, C.; Brown, J.; Haque, T.; Hussaini, Y.; MacMahon, E.; Molyneaux, P.; Papaevangelou, V.; et al. Recombination of Globally Circulating Varicella Zoster Virus. *J. Virol.* **2015**, *89*, 7133–7146. [CrossRef] [PubMed]
13. Esparza, J.; Benyesh-Melnick, B.; Schaffer, P.A. Intertypic complementation and recombination between temperature-sensitive mutants of herpes simplex virus types 1 and 2. *Virology* **1976**, *70*, 372–384. [CrossRef]
14. Dasgupta, U.B.; Summers, W.C. Genetic recombination of Herpes simplex virus, the role of the host cell and UV-irradiation of the virus. *Mol. Genet. Genom.* **1980**, *178*, 617–623. [CrossRef]
15. Wildy, P. Recombination with Herpes Simplex Virus. *Microbiology* **1955**, *13*, 346–360. [CrossRef] [PubMed]
16. Wilkinson, D.; Weller, S. The Role of DNA Recombination in Herpes Simplex Virus DNA Replication. *IUBMB Life* **2003**, *55*, 451–458. [CrossRef] [PubMed]
17. Dutch, R.E.; Bianchi, V.; Lehman, I.R. Herpes simplex virus type 1 DNA replication is specifically required for high-frequency homologous recombination between repeated sequences. *J. Virol.* **1995**, *69*, 3084–3089. [PubMed]
18. Kolb, A.W.; Lee, K.; Larsen, I.; Craven, M.; Brandt, C.R. Quantitative Trait Locus Based Virulence Determinant Mapping of the HSV-1 Genome in Murine Ocular Infection: Genes Involved in Viral Regulatory and Innate Immune Networks Contribute to Virulence. *PLoS Pathog.* **2016**, *12*, e1005499. [CrossRef] [PubMed]
19. Lee, K.; Kolb, A.W.; Sverchkov, Y.; Cuellar, J.A.; Craven, M.; Brandt, C.R. Recombination Analysis of Herpes Simplex Virus Type 1 Reveals a Bias towards GC Content and the Inverted Repeat Regions. *J. Virol.* **2015**, *89*, 7214–7223. [CrossRef] [PubMed]
20. Morimoto, T.; Arii, J.; Akashi, H.; Kawaguchi, Y. Identification of multiple sites suitable for insertion of foreign genes in herpes simplex virus genomes. *Microbiol. Immunol.* **2008**, *53*, 155–161. [CrossRef] [PubMed]
21. Taylor, M.P.; Kobiler, O.; Enquist, L.W. Alphaherpesvirus axon-to-cell spread involves limited virion transmission. *Proc. Natl. Acad. Sci. USA* **2012**, *109*, 17046–17051. [CrossRef] [PubMed]
22. Criddle, A.; Thornburg, T.; Kochetkova, I.; DePartee, M.; Taylor, M.P. gD-Independent Superinfection Exclusion of Alphaherpesviruses. *J. Virol.* **2016**, *90*, 4049–4058. [CrossRef] [PubMed]
23. Ch'ng, T.H.; Enquist, L.W. An in vitro system to study trans-neuronal spread of pseudorabies virus infection. *Vet. Microbiol.* **2006**, *113*, 193–197. [CrossRef] [PubMed]
24. Curanovic, D.; Ch'ng, T.H.; Szpara, M.; Enquist, L. Compartmented neuron cultures for directional infection by alpha herpesviruses. *Curr. Protoc. Cell Biol.* **2009**. [CrossRef]
25. Card, J.P.; Enquist, L.W. Use and Visualization of Neuroanatomical Viral Transneuronal Tracers. In *Visualization Techniques*; Humana Press: Totowa, NJ, USA, 2012; pp. 225–268.
26. Card, J.P.; Enquist, L.W. Transneuronal circuit analysis with pseudorabies viruses. *Curr. Protoc. Neurosci.* **2001**, *68*, 1–5.
27. Rosato, P.C.; Leib, D.A. Neuronal Interferon Signaling Is Required for Protection against Herpes Simplex Virus Replication and Pathogenesis. *PLoS Pathog.* **2015**, *11*, e1005028. [CrossRef] [PubMed]
28. Card, J.P.; Whealy, M.E.; Robbins, A.K.; Moore, R.Y.; Enquist, L.W. Two alpha-herpesvirus strains are transported differentially in the rodent visual system. *Neuron* **1991**, *6*, 957–969. [CrossRef]
29. Pickard, G.E.; Smeraski, C.A.; Tomlinson, C.C.; Banfield, B.W.; Kaufman, J.; Wilcox, C.L.; Enquist, L.W.; Sollars, P.J. Intravitreal injection of the attenuated pseudorabies virus PRV Bartha results in infection of the hamster suprachiasmatic nucleus only by retrograde transsynaptic transport via autonomic circuits. *J. Neurosci.* **2002**, *22*, 2701–2710. [CrossRef] [PubMed]
30. Lopez, C. Genetics of natural resistance to herpesvirus infections in mice. *Nature* **1975**, *258*, 152–153. [CrossRef] [PubMed]
31. Hogue, I.; Bosse, J.; Engel, E.; Scherer, J.; Hu, J.-R.; del Rio, T.; Enquist, L. Fluorescent Protein Approaches in Alpha Herpesvirus Research. *Viruses* **2015**, *7*, 5933–5961. [CrossRef] [PubMed]
32. Dangler, C.A.; Deaver, R.E.; Kolodziej, C.M. Genetic recombination between two strains of Aujeszky's disease virus at reduced multiplicity of infection. *J. Gen. Virol.* **1994**, *75 Pt 2*, 295–299. [CrossRef] [PubMed]

viruses

Published: 25 April 2018 doi: 10.3390/v1005220

33. Yao, X.D.; Elias, P. Recombination during early herpes simplex virus type 1 infection is mediated by cellular proteins. *J. Biol. Chem.* **2001**, *276*, 2905–2913. [CrossRef] [PubMed]
34. Muylkens, B.; Farnir, F.; Meurens, F.; Schynts, F.; Vanderplasschen, A.; Georges, M.; Thiry, E. Coinfection with Two Closely Related Alphaherpesviruses Results in a Highly Diversified Recombination Mosaic Displaying Negative Genetic Interference. *J. Virol.* **2009**, *83*, 3127–3137. [CrossRef] [PubMed]
35. Kobiler, O.; Brodersen, P.; Taylor, M.P.; Ludmir, E.B.; Enquist, L.W. Herpesvirus replication compartments originate with single incoming viral genomes. *MBio* **2011**, *2*, e00278-11. [CrossRef] [PubMed]
36. Kobiler, O.; Lipman, Y.; Therkelsen, K.; Daubechies, I.; Enquist, L.W. Herpesviruses carrying a Brainbow cassette reveal replication and expression of limited numbers of incoming genomes. *Nat. Commun.* **2010**, *1*, 146–148. [CrossRef] [PubMed]
37. Roizman, B.; Jacob, R.J.; Knipe, D.M.; Morse, L.S.; Ruyechan, W.T. On the Structure, Functional Equivalence, and Replication of the Four Arrangements of Herpes Simplex Virus DNA. *Cold Spring Harb. Symp. Quant. Biol.* **1979**, *43*, 809–826. [CrossRef] [PubMed]
38. Glazenburg, K.L.; Moormann, R.J.; Kimman, T.G.; Gielkens, A.L.; Peeters, B.P. In vivo recombination of pseudorabies virus strains in mice. *Virus Res.* **1994**, *34*, 115–126. [CrossRef]
39. Javier, R.T.; Sedarati, F.; Stevens, J.G. Two avirulent herpes simplex viruses generate lethal recombinants in vivo. *Science* **1986**, *234*, 746–748.
40. Herr, A.E.; Hain, K.S.; Taylor, M.P. Limitations on the Multiplicity of Cellular Infection during Human Alphaherpesvirus Disease. *Curr. Clin. Microbiol. Rep.* **2017**, *4*, 167–174. [CrossRef]